A

Dissertation Report

On

Design, Fabrication and Performance analysis of Heat Recovery Unit in Solar Thermal Energy Conversion System Used in Jaggery Making Process

Submitted in Partial Fulfilment of the Requirements for the Award of Degree of

Master of Technology

In

Energy Engineering

By

VIKASH GORA

2013PME5246

Under the supervision of

Dr. M. Mohan Jagadeesh Kumar
Associate Professor
Department of Mechanical Engineering
GVP College of Engineering (A),
Vizag, India

Dr. G. D. Agarwal
Associate professor
Department of Mechanical Engineering
M.N.I.T. Jaipur, India

DEPARTMENT OF MECHANICAL ENGINEERING

MALAVIYA NATIONAL INSTITUTE OF TECHNOLOGY, JAIPUR

JUNE 2017

DEPARTMENT OF MECHANICAL ENGINEERING
JAIPUR (RAJASTHAN)-302017
MALAVIYA NATIONAL INSTITUTE OF TECHNOLOGY

CERTIFICATE

This is certified that the dissertation report entitled **"Design, Fabrication and Performance analysis of Heat Recovery Unit in Solar Thermal Energy Conversion System Used in Jaggery Making Process"** prepared by **Vikash Gora** (ID-2013PME5246), in the partial fulfilment of the award of the Degree of **Master of Technology** in **Energy Engineering** of Malaviya National Institute of Technology, Jaipur is a record of bonafide research work carried out by him under my supervision and is hereby approved for submission. The contents of this dissertation work, in full or in parts, have not been submitted to any other Institute or University for the award of any degree or diploma.

Date:
Place:

Dr. M. Mohan Jagadeesh Kumar
Associate Professor
Department of Mechanical Engineering
GVP College of Engineering (A),
Vizag, India

Date:
Place:

Dr. G. D. Agrawal
Associate Professor
Department of Mechanical Engineering
M.N.I.T., Jaipur, India

DEPARTMENT OF MECHANICAL ENGINEERING
MALAVIYA NATIONAL INSTITUTE OF TECHNOLOGY
JAIPUR (RAJASTHAN)-302017

DECLARATION

I **Vikash Gora** hereby declare that the dissertation entitled **"Design, Fabrication and Performance analysis of Heat Recovery Unit in Solar Thermal Energy Conversion System Used in Jaggery Making Process"** being submitted by me in partial fulfilment of the degree of **M. Tech (Energy Engineering)** is a research work carried out by me under the supervision of **Dr. M. Mohan Jagadeesh Kumar** and **Dr. G. D. Agrawal,** and the contents of this dissertation work, in full or in parts, have not been submitted to any other Institute or University for the award of any degree or diploma. I also certify that no part of this dissertation work has been copied or borrowed from anyone else. In case any type of plagiarism is found out, I will be solely and completely responsible for it.

Date: Vikash Gora

Place: M. Tech. (Energy Engineering)

2013PME5246

ACKNOWLEDGEMENT

I feel immense pleasure in conveying my heartiest thanks and profound gratitude to my supervisors **Dr. M. Mohan Jagadeesh Kumar** and **Dr. G. D. Agrawal,** who provided me with their generous guidance, valuable help and endless encouragement by taking personal interest and attention. No words can fully convey my feelings of respect and regard for them.

I would like to express my sincere and profound gratitude to **Mr. Rishabh Choudhary, Mr. Satyender Kumar, Mr. Pushpendra Kumar Sharma** (Ph.D. Scholar), **Mr. Karan Yadav** and all the member of the Department of Mechanical Engineering, M.N.I.T., Jaipur, who were abundantly helpful and offered invaluable assistance, support and guidance with their experience and knowledge, throughout my dissertation work.

I also express my deepest gratitude to all my **family members** for their blessings and affection, without which I would not be able to endure hard time and carry on. Lastly, but not least I thank one and all who have helped me directly or indirectly in completion of the report.

(Vikash Gora)

ABSTRACT

Jaggery traditionally called as Gur in India, is prepared by using sugarcane juice and bagasse as raw materials. Dry Bagasse is used to produce required amount of heat by combustion in an open earthen furnace. Heat produced is used to boil the sugarcane juice up to its striking point temperature to prepare jaggery. The energy loss due to inefficient combustion process, the energy loss through exhaust gases, conduction, convection and radiation energy losses from the furnace wall makes the conventional open earthen pan furnace as quite inefficient unit. Bagasse can be saved either by making the process more efficient or using by alternative sources of energy to produce heat required for the jaggery making process. Bagasse can be used as raw material for paper and pulp industry and can also be used as a raw material to produce the industrial process heat, thereby generating additional money to the farmers.

In the present work, a modified process is proposed to substitute conventional jaggery making process. Solar energy is proposed to use as a source of heat energy in place of bagasse to boil the sugarcane juice. A part of the proposed modified process is being implemented, a heat recovery unit comprising a heat exchanger and a solar collector is initially designed, fabricated and tested. An algorithm was developed to design and optimise the geometric parameters of shell and tube heat exchangers different configurations. Based on this algorithm, a user defined program was made in M.S. Excel for different tube arrangements (staggered and aligned). Based on the output of the program staggered tube arrangement is chosen to manufacture. Heat exchanger integrated with a solar collector is being fabricated and tested to find its thermal performance.

It was observed from the experimental results that temperature of liquid in the storage tank is steadily increasing and reaching to its maximum value by the evening time. The Evacuated Tube Solar Collector during its one day of operation is found to be achieving a maximum temperature of liquid (water) nearly 85℃ from 60℃ . The heated liquid from the ETSC was used to preheat the secondary liquid in the Shell and Tube Heat Exchanger. It was observed that the effectiveness of STHE is reaching to a maximum value of 0.74

when hot fluid (flowing through the tube) mass flow rate is 60 kg/h and cold fluid (flowing through the shell) mass flow rate is 300 kg/h. Similarly it was reaching to an average maximum value of 0.6508 when the mass flow rate of cold fluid is 60 kg/h and mass flow rate of hot fluid is changing from 120 to 300 kg/h. Hence, it was concluded that the heat transfer coefficients and hence the effectiveness of the STHE will be maximum when either hot or cold fluid is set to be flowing at lower mass flow rate keeping the mass flow rate of other fluid at higher values.

Table of Contents

ACKNOWLEDGEMENT ..... **iii**

ABSTRACT ..... **iv**

Table of Contents ..... **vi**

List of Figures ..... **x**

List of Tables ..... **xiii**

Nomenclature ..... **xv**

List of Abbreviations ..... **xviii**

Chapter 1 INTRODUCTION **1**

1.1 Conventional jaggery making process 8

1.1.1 Juice Extraction: 8

1.1.2 Settling: 9

1.1.3 Boiling: 9

1.1.4 Cooling and moulding: 11

1.1.5 Storage: 11

1.2 Purpose of thermally efficient conventional jaggery making process 11

1.3 Heat recovery unit 12

1.3.1 Solar Energy 13

1.3.2 Radiation at the Earth's Surface 13

1.3.3 Solar Thermal Systems 14

1.3.4 Concentrating Collectors 15

1.3.5 Non-concentrating Collectors 15

1.3.6 Heat exchanger 18

1.4 Need of the study 21

1.5 Objectives 21

1.6 Organisation of thesis 21

Chapter 2 LITERATURE REVIEW 23

2.1 Difficulties with the conventional jaggery making process: 23
2.2 Possible solutions 24
2.3 Past research work on jaggery making process 26
2.4 Flat plate collector 29
2.5 Evacuated tube solar collector 31
2.6 Shell and tube heat exchanger 34
2.7 Summary of literature review 35

Chapter 3 DESIGN AND FABRICATION OF HEAT EXCHANGER 37

3.1 Data reduction 37
3.2 Heat exchanger design 46
3.3 Fabrication of heat exchanger 48
3.4 Challenges faced during fabrication process 54

Chapter 4 DEVELOPMENT OF EXPERIMENTAL SETUP 55

4.1 Description of the experimental setup 55
4.1.1 Evacuated tube solar collector 56
4.1.2 Shell and tube heat exchanger 58
4.1.3 Pump, tank and connecting pipe specification 59
4.2 Experimental procedure 61
4.3 Instrumentation 62
4.3.1 Thermocouple 62
4.3.2 Weather station 63
4.3.3 Temperature scanners 64
4.4 Problems faced during experimentation 65

Chapter 5 DATA COLLECTION AND ANALYSIS 66

5.1 Experimental results of evacuated tube solar collector 66
5.2 Performance analysis of evacuated tube solar collector 68
5.3 Experimental results of shell and tube heat exchanger 69
5.3.1 Experiment on 28th April 2017: 70

5.3.2 Experiment on 29th April 2017: 72
5.3.3 Experiment on 30th April 2017: 73
5.3.4 Experiment on 1st May 2017: 75
5.3.5 Experiment on 3rd May 2017: 77
5.3.6 Experiment on 4th May 2017: 79
5.3.7 Experiment on 5th May 2017: 81
5.3.8 Experiment on 6th May 2017: 83
5.3.9 Experiment on 7th May 2017: 85
5.3.10 Experiment on 8th May 2017: 87
5.3.11 Experiment on 9th May 2017: 89
5.3.12 Experiment on 10th May 2017: 91
5.3.13 Experiment on 11th May 2017: 93
5.3.14 Experiment on 12th May 2017: 95
5.3.15 Experiment on 13th May 2017: 97
5.3.16 Experiment on 14th May 2017: 99
5.3.17 Experiment on 3rd June 2017: 101
5.3.18 Experiment on 4th June 2017: 103
5.3.19 Experiment on 5th June 2017: 105
5.3.20 Experiment on 6th June 2017: 107
5.3.21 Experiment on 7th June 2017: 109
5.3.22 Experiment on 8th June 2017: 111
5.3.23 Experiment on 9th June 2017: 113
5.3.24 Experiment on 10th June 2017: 115
5.3.25 Experiment on 11th June 2017: 117
5.4 Performance analysis of shell and tube heat exchanger 119
5.5 Comparison between experimental and calculated fluid temperatures 121

Chapter 6 CONCLUSIONS 124

6.1 Scope for future work 125

References 126

Appendix-A.1 Costing of the experimental setup 130

Appendix-A.2 Calibration of the temperature sensors 132

List of Figures

S. No.	Name	Page No.
1.1	Process flow chart of jaggery making process	8
1.2	Block diagram of conventional jaggery making process	10
1.3	Heat recovery unit	13
1.4	Classification of solar water heater	14
1.5	Flat plate collector	16
1.6	Working of water in glass ETSC (a)without a reflector and (b) with a reflector	18
1.7	Classification of heat exchanger	19
1.8	Shell and tube heat exchanger	20
2.1	Modified jaggery making process	25
2.2	Modified jaggery making process indicating the work done in the report by red rectangle	36
3.1	Different types of tube arrangements (a) aligned and (b) staggered	38
3.2	Heat exchanger isometric view by keeping the shell part partially transparent	47
3.3	Marking of the plates	48
3.4	Centre punch	48
3.5	Drilling of the plates	49
3.6	Plates after drilling	49
3.7	After grinding or finishing of the plates	49
3.8	Grinder	49
3.9	After separating all the plates	50
3.10	Baffle plate after cutting	50
3.11	Inserting the baffle plates inside the shell	50
3.12	After welding one baffle plate	50
3.13	After welding both the baffle plates	51
3.14	Inserting the main plate	51
3.15	After welding of the main plate	51
3.16	After inserting the Copper (*Cu*) tubes	51
3.17	After gas tungsten arc welding of the Copper (*Cu*) tubes	52
3.18	Outside view of the header	52
3.19	Inside view of the header	52
3.20	Inlet or outlet of the shell	52
3.21	Putting insulation and cover	53
3.22	Front view of the heat exchanger	53
3.23	Top view of the heat exchanger	53

4.1	Block diagram of experimental procedure (a) Heating of primary fluid with the help Evacuated Tube Solar Collector and (b) Exchange of this heat to the secondary fluid with the help of Shell and Tube Heat Exchanger	56
4.2	Schematic view of Evacuated Tube Solar Collector showing location of temperature sensors	57
4.3	An evacuated tube with inlet and outlet temperature sensors	58
4.4	Schematic diagram of the experimental setup of the heat exchanger	59
4.5	Experimental setup	60
4.6	Calibration of the temperature sensors using Fluke 4586A super-daq precision temperature scanner	63
4.7	MNIT weather station	64
4.8	Temperature scanners (a) multispan ms 1208 and (b) masibus 8208	65
4.9	Leakage form tubes	65
5.1	Evacuated tube solar collector (a) Variation of different parameters w.r.t. time (b) notations used	68
5.2	Variation of different heat exchanger parameters with time based on the experimental results of 28th April 2017	71
5.3	Variation of different heat exchanger parameters with time based on the experimental results of 29th April 2017	73
5.4	Variation of different heat exchanger parameters with time based on the experimental results of 30th April 2017	75
5.5	Variation of different heat exchanger parameters with time based on the experimental results of 01st May 2017	77
5.6	Variation of different heat exchanger parameters with time based on the experimental results of 03rd May 2017	79
5.7	Variation of different heat exchanger parameters with time based on the experimental results of 04th May 2017	81
5.8	Variation of different heat exchanger parameters with time based on the experimental results of 05th May 2017	83
5.9	Variation of different heat exchanger parameters with time based on the experimental results of 06th May 2017	85
5.10	Variation of different heat exchanger parameters with time based on the experimental results of 07th May 2017	87
5.11	Variation of different heat exchanger parameters with time based on the experimental results of 08th May 2017	89
5.12	Variation of different heat exchanger parameters with time based on the experimental results of 09th May 2017	91
5.13	Variation of different heat exchanger parameters with time based on the experimental results of 10th May 2017	93
5.14	Variation of different heat exchanger parameters with time based on the experimental results of 11th May 2017	95
5.15	Variation of different heat exchanger parameters with time based on the experimental results of 12th May 2017	97

5.16	Variation of different heat exchanger parameters with time based on the experimental results of 13th May 2017	99
5.17	Variation of different heat exchanger parameters with time based on the experimental results of 14th May 2017	101
5.18	Variation of different heat exchanger parameters with time based on the experimental results of 03rd June 2017	103
5.19	Variation of different heat exchanger parameters with time based on the experimental results of 04th June 2017	105
5.20	Variation of different heat exchanger parameters with time based on the experimental results of 05th June 2017	107
5.21	Variation of different heat exchanger parameters with time based on the experimental results of 06th June 2017	109
5.22	Variation of different heat exchanger parameters with time based on the experimental results of 07th June 2017	111
5.23	Variation of different heat exchanger parameters with time based on the experimental results of 08th June 2017	113
5.24	Variation of different heat exchanger parameters with time based on the experimental results of 09th June 2017	115
5.25	Variation of different heat exchanger parameters with time based on the experimental results of 10th June 2017	117
5.26	Variation of different heat exchanger parameters with time based on the experimental results of 11th June 2017	119
5.27	Variation of heat exchanger effectiveness w.r.t. fluid flow rate	121
5.28	Comparison between experimental and calculated fluid temperatures of 07th June 2017	123

List of Tables

S. No.	Name	Page No.
1.1	Area, production and yield of sugarcane in major growing countries	2
1.2	Area, production and yield of sugarcane in major growing states of India	3
1.3	Area, production and yield of sugarcane in India	4
1.4	Utilisation of sugarcane for different purposes in India	5
1.5	Per capita consumption of sugar, gur and khandsari	6
1.6	Nutritive value of jaggery, Khandsari and sugar per 100 gm	7
3.1	The Property Values of water in saturated state	40
3.2	Values of constants C and n_1	40
3.3	Input to program: Heat Exchanger design input data	45
3.4	Output from the program: Calculated parameters	46
4.1	Geographical and weather data of Jaipur	55
4.2	Specification of Evacuated Tube Solar Collector	56
4.3	Notation of temperature sensors used in Evacuated Tube Solar Collector	57
4.4	Heat exchanger specification	58
4.5	Specification of pump, tank and connecting pipes	59
4.6	Specification of the temperature scanners	64
5.1	Variation of different parameters of Evacuated Tube Solar Collector on 4th June 2017	67
5.2	Fluid temperatures and performance parameters of heat exchanger on 28th April 2017	70
5.3	Fluid temperatures and performance parameters of heat exchanger on 29th April 2017	72
5.4	Fluid temperatures and performance parameters of heat exchanger on 30th April 2017	74
5.5	Fluid temperatures and performance parameters of heat exchanger on 01st May 2017	76
5.6	Fluid temperatures and performance parameters of heat exchanger on 03rd May 2017	78
5.7	Fluid temperatures and performance parameters of heat exchanger on 04th May 2017	80
5.8	Fluid temperatures and performance parameters of heat exchanger on 05th May 2017	82
5.9	Fluid temperatures and performance parameters of heat exchanger on 06th May 2017	84

5.10	Fluid temperatures and performance parameters of heat exchanger on 07th May 2017	86
5.11	Fluid temperatures and performance parameters of heat exchanger on 08th May 2017	88
5.12	Fluid temperatures and performance parameters of heat exchanger on 09th May 2017	90
5.13	Fluid temperatures and performance parameters of heat exchanger on 10th May 2017	92
5.14	Fluid temperatures and performance parameters of heat exchanger on 11th May 2017	94
5.15	Fluid temperatures and performance parameters of heat exchanger on 12th May 2017	96
5.16	Fluid temperatures and performance parameters of heat exchanger on 13th May 2017	98
5.17	Fluid temperatures and performance parameters of heat exchanger on 14th May 2017	100
5.18	Fluid temperatures and performance parameters of heat exchanger on 03rd June 2017	102
5.19	Fluid temperatures and performance parameters of heat exchanger on 04th June 2017	104
5.20	Fluid temperatures and performance parameters of heat exchanger on 05th June 2017	106
5.21	Fluid temperatures and performance parameters of heat exchanger on 06th June 2017	108
5.22	Fluid temperatures and performance parameters of heat exchanger on 07th June 2017	110
5.23	Fluid temperatures and performance parameters of heat exchanger on 08th May 2015	112
5.24	Fluid temperatures and performance parameters of heat exchanger on 09th June 2017	114
5.25	Fluid temperatures and performance parameters of heat exchanger on 10th June 2017	116
5.26	Fluid temperatures and performance parameters of heat exchanger on 11th June 2017	118
5.27	Heat exchanger effectiveness and Reynold's number with fluid flow rate	120
5.28	Comparison between experimental and calculated fluid temperatures on 07th June 2017	122
A.1.1	Representing costing of all the items used in the experimental setup.	128
A.2.1	Calibration of temperature sensors form 1 to 19	130
A.2.2	Calibration of temperature sensors from 20 to 30	130

Nomenclature

Symbols:

Notation	Description	Unit
a_s	Shell side pass area	m^2
A	Heat exchanger surface area	m^2
A_{ab}	Evacuated tube solar collector absorber area	m^2
A_b	Baffle cross-sectional area	m^2
A_{gc}	Evacuated tube solar collector gross area	m^2
A_{ap}	Evacuated tube solar collector aperture area	m^2
A_s	Shell cross-sectional area	m^2
B	Baffle spacing (Pitch)	m
C	Tube pitch pass coefficient	Unit less
C_p	Specific Heat	$Jkg^{-1}K^{-1}$
d_e	Equivalent shell diameter or Shell hydraulic diameter	m
d_i	Tube internal diameter	m
d_o	Tube outer diameter	m
D_s	Shell inside diameter	m
f_t	Darcy's friction factor	Unit less
F	Correction factor for Temperature difference	Unit less
FR	Collector heat removal factor	Unit less
h	Convective heat transfer coefficient	$Wm^{-2}K^{-1}$
k	Thermal conductivity	$Wm^{-1}K^{-1}$
L	Tube length	m
$LMTD$	Logarithmic mean temperature difference	K
$\dot{m}$	Mass flow rate	$kgsec^{-1}$
$\dot{m}_{sf}$	Shell side fluid mass flow rate	$kgsec^{-1}$
$\dot{m}_{tf}$	Tube side fluid mass flow rate	$kgsec^{-1}$
n	Number of tube passes	Unit less
n_1	Numerical constant	Unit less
N_t	Number of tubes	Unit less
P	Efficiency of shell and tube heat exchanger	Unit less
Pr	Prandtl number	Unit less

$\dot{Q}$	Heat transfer rate	W
$\dot{Q}_{sf}$	Shell side heat transfer rate	W
$\dot{Q}_{tf}$	Tube side heat transfer rate	W
$\dot{Q}_u$	Useful solar energy	W
R	Correction coefficient	Unit less
Re	Reynolds number	Unit less
R_f	Fouling resistance	m^2K/W
S	Solar radiation on absorber	W/m^2
S_d	Diagonal tube spacing (pitch)	m
S_l	Longitudinal tube spacing (pitch)	m
S_t	Transverse tube spacing (pitch)	m
t_1, t_2	Initial and final time of measurement	℃
T	Temperature	℃
T_1, T_2	Initial and final average temperature of the system respectively during the period of measurement, averaged from two thermocouple reading located at inlet and outlet	℃
T_{ci}	Cold fluid inlet temperature	℃
T_{co}	Cold fluid outlet temperature	℃
T_{hi}	Hot fluid inlet temperature	℃
T_{ho}	Hot fluid outlet temperature	℃
T_i , T_o	In flow and out flow temperature through the opening of the tube	℃
$\overline{T}$	Average temperature of the tank during measurement period	℃
T_a	Average ambient temperature during measurement period	℃
U	Overall heat transfer coefficient	$Wm^{-2}K^{-1}$
v	Fluid velocity	$m\,sec^{-1}$
Δh	Heat transfer difference	$Wm^{-2}K^{-1}$
V_c	Volume of cold fluid	Litre
V_{hx}	Volume of heat exchanger	Litre
v_s	Shell side fluid velocity	$m\,sec^{-1}$
V_t	Total volume of liquid to be heated	Litre

Greek symbols:

Notation	Description	Unit
α	Thermal absorption	Unit less
β	Coefficient of volumetric expansion	Unit less
γ	Inclination angle	Degree (°)
δ	delta	Unit less
ε	Thermal Emissivity	Unit less
μ	Dynamic Viscosity	Pasec
ρ	Density	kgm^{-3}
η	Thermal efficiency of Evacuated Tube Solar Collector	Unit less

Subscripts:

Notation	Description
c	Cold stream
h	Hot stream
i	Inlet
o	Outlet
s	Shell side
t	Tube side
hx	Heat exchanger

List of Abbreviations

ETC	Evacuated Tube Collector
ETSC	Evacuated Tube Solar Collector
GTAW	Gas Tungsten Arc Welding
PSO	Particle Swamp Optimisation
SDS	Sodium Dodecyl Sulfate
STHE	Shell and Tube Heat Exchanger
SWCNT	Single Walled Carbon Nanotube
UpETsc	U-pipe Evacuated Tube Solar Collector
WGETsc	Water in Glass Evacuated Tube Solar Collector

Chapter 1 INTRODUCTION

Jaggery is a traditional sweetener, mostly used in Asia, Africa and some countries of America. It is known by different names in the different parts of the world such as Gur in India, Jaggery in Myanmar (Burma) and African countries, Panela in Mexico and South America, Naam Taan Oi in Thailand, Hakuru in Sri Lanka and Desi in Pakistan. It is made from sugarcane juice, palm sap, sorghum and dates without removing molasses and crystals. Sugarcane, a cash crop, is the most important crop for the production of sugar, jaggery and khandsari **(Status Paper on Sugarcane, 2016-17)**.

In the world, India is the second largest cultivator and producer of sugarcane after Brazil as shown in Table 1.1. Brazil used an average of 78.54 lakh hectare of area and produced 6162.97 lakh tonnes of sugarcane having yield of 78.47 tonnes per hectare in 2006-10. Whereas for the same period India on an average used 45.99 lakh hectare of area and produced 3124.42 lakh tonnes having yield of 67.93 tonnes per hectare. Colombia has the highest yield average of 98.04 tonnes per hectare for the same period which means a drastic improvement is possible in the yield average and should be made in India.

In India, the area for the cultivation of sugarcane has increased from 11.76 lakh hectare to 48.86 lakh hectare, yield has increased from 30.90 tonnes per hectare to 70.09tonnes per hectare and production of sugarcane has increased from 363.54 lakh hectares to 3423.82 lakh hectares from 1930-31 to 2010-11 respectively as shown in Table 1.2. Therefore, we can say that the area, yield and production of sugarcane have shown an upward trend.

Table 1.3 represents area, production and yield of major sugarcane growing states of India for the years 2008-09 to 2010-11. Uttar Pradesh is the highest producer and cultivator of sugarcane among Indian states. Andhra Pradesh, Gujarat, Karnataka, Maharashtra, Tamil Nadu, Bihar and Uttarakhand are other major sugarcane cultivators and producers.

Table 1.1: Area, production and yield of sugarcane in major growing countries (2006-10) (Status Paper on Sugarcane, 2016-17)

Country	Area (Lakh hectare)						Production (Lakh tonnes)						Yield (Tonnes/hectare)					
	2006	2007	2008	2009	2010	Average	2006	2007	2008	2009	2010	Average	2006	2007	2008	2009	2010	Average
Argentina	3.2	3.2	3.6	3.5	3.5	3.4	264.5	239.6	269.6	255.8	250.0	255.9	84.0	74.9	74.9	74.1	71.4	75.7
Australia	4.2	4.1	3.8	3.9	4.1	4.0	371.3	364.0	326.2	302.8	314.6	335.8	89.5	89.1	85.7	77.4	77.7	83.9
Brazil	63.6	70.8	81.4	86.2	90.8	78.5	4774.1	5497.1	6453.0	6916.1	7174.6	6163.0	75.1	77.6	79.3	80.3	79.0	78.5
China	13.9	16.0	17.5	17.1	17.0	16.3	933.1	1137.3	1249.2	1162.5	1114.5	1119.3	67.2	71.2	71.2	68.1	65.8	68.7
Colombia	4.1	4.1	3.8	3.8	3.8	3.9	384.5	385.0	385.0	385.0	385.0	384.9	93.8	93.9	100.4	101.5	101.3	98.0
India	42.0	51.5	50.6	44.2	41.7	46.0	2811.7	3555.2	3481.9	2850.3	2923.0	3124.4	66.9	69.0	68.9	64.5	70.1	67.9
Mexico	6.8	6.9	6.7	7.1	7.0	6.9	506.8	520.9	511.1	494.9	504.2	507.6	74.5	75.4	76.4	69.7	71.6	73.5
Pakistan	9.1	10.3	12.4	10.3	9.4	10.3	446.7	547.4	639.2	500.5	493.7	525.5	49.2	53.2	51.5	48.6	52.4	51.0
Philippines	3.9	3.8	4.0	4.0	3.6	3.9	315.5	320.0	340.0	325.0	340.0	328.1	80.4	83.6	85.4	80.5	93.7	84.6
Thailand	9.4	9.9	10.3	9.3	9.8	9.7	476.6	643.7	735.0	668.2	688.1	642.3	50.6	65.3	71.4	71.7	70.4	66.0
Others	47.3	47.6	48.2	48.8	46.0	47.6	2939.1	2951.0	2950.8	3009.2	2757.3	2921.5	62.2	62.0	61.2	61.7	60.0	61.4
World	207.4	228.1	242.3	238.2	236.6	230.5	14223.8	16161.1	17341.0	16870.3	16945.1	16308.2	68.6	70.8	71.6	70.8	71.6	70.7

Table 1.2: Area, production and yield of sugarcane in India (Status Paper on Sugarcane, 2016-17)

Year	Cultivation Area (Lakh hectare)	Production (Lakh tonnes)	Yield (tonnes/hectare)
1930-31	11.76	363.54	30.90
1940-41	16.17	519.78	32.10
1950-51	17.07	548.23	32.10
1960-61	24.15	1100.01	45.50
1970-71	26.15	1263.68	48.30
1980-81	26.67	1542.48	57.80
1990-91	36.86	2410.45	65.40
2000-01	43.16	2959.56	68.60
2001-02	44.11	2972.08	67.40
2002-03	45.20	2873.83	63.60
2003-04	39.38	2338.62	59.40
2004-05	36.62	2370.88	64.80
2005-06	42.01	2811.72	66.90
2006-07	51.51	3555.20	69.00
2007-08	50.55	3481.88	68.90
2008-09	44.15	2850.29	64.60
2009-10	41.75	2923.02	70.05
2010-11	48.85	3423.82	70.09
Average*	44.41	2960.13	66.65

Average* indicates the average was taken for the year 2001-02 to 2010-11.

Table 1.3: Area, production and yield of sugarcane in major growing states of India (Status Paper on Sugarcane, 2016-17)

S. No.	State	Area (Lakh hectare)			Production (Lakh tonnes)			Yield (tonnes/hectare)		
		2008-09	2009-10	2010-11	2008-09	2009-10	2010-11	2008-09	2009-10	2010-11
1	Andhra Pradesh	2.00	1.58	1.92	153.8	117.1	149.6	76.90	74.11	77.92
2	Gujarat	2.20	1.54	1.90	155.1	124	137.6	73.03	80.52	72.42
3	Karnataka	2.80	3.37	4.23	233.3	304.4	396.6	88.65	90.33	93.76
4	Madhya Pradesh	0.71	0.60	0.65	29.8	25.4	26.7	42.40	42.33	41.08
5	Maharashtra	7.70	7.56	9.65	606.5	641.6	818.9	81.29	84.87	84.86
6	Tamil Nadu	3.10	2.93	3.16	328	297.5	342.5	108.15	101.54	108.39
7	Bihar	1.10	1.16	2.48	49.6	50.3	127.6	32.44	43.36	51.45
8	Haryana	0.90	0.74	0.85	51.3	53.4	60.4	63.29	72.16	71.06
9	Punjab	0.81	0.60	0.70	46.7	37	41.7	60.27	61.67	59.57
10	Uttar Pradesh	20.80	19.77	21.25	1090.5	1171.4	1205.5	57.12	59.25	56.73
11	Uttarakhand	1.10	0.96	1.07	55.9	58.4	65	62.02	60.83	60.75
12	West Bengal	0.20	0.14	0.15	16.4	10	11.3	74.71	71.43	75.33
	Others	0.78	0.78	0.84	33.4	32.6	40.4	64.60	70.00	70.10

The utilisation of sugarcane for different purposes for the year 2000-01 to 2010-11 has been shown in Table 1.4. There is quite variation in the utilisation of sugarcane for different purposes so by taking the average, it can be concluded that 64.87% of the sugarcane was used for the production of white sugar, 11.82% of the sugarcane was used for seed, feed and chewing and rest was used for the production of Gur and Khandsari. On an average 23.05% of the sugarcane was used for the production of Gur and Khandsari for 2000-01 to 2010-11.

Table 1.4: Utilisation of sugarcane for different purposes in India (Status Paper on Sugarcane, 2016-17)

Year	Production of Sugarcane (Lakh tonnes)	Cane used for (Lakh tonnes)			Percentage of sugarcane production utilised for		
		Production of white sugar	Seed, feed & chewing, etc.	Gur and Khandsari	Production of white sugar	Seed, feed & chewing, etc.	Gur and Khandsari
2000-01	2959.56	1766.60	339.30	853.66	59.70	11.50	28.80
2001-02	2972.08	1803.46	347.24	821.38	60.70	11.70	27.60
2002-03	2873.83	1943.65	335.24	594.94	67.60	11.70	20.70
2003-04	2338.62	1325.11	278.30	735.21	56.70	11.90	31.40
2004-05	2370.88	1247.72	282.13	841.03	52.60	11.90	35.50
2005-06	2811.72	1886.72	334.59	590.41	67.10	11.90	21.00
2006-07	3555.20	2792.95	423.07	339.18	78.60	11.90	9.50
2007-08	3481.88	2499.06	405.25	501.26	71.80	11.60	16.60
2008-09	2850.29	1449.83	338.33	1062.13	50.90	11.90	37.20
2009-10	2923.02	1855.48	347.84	719.70	63.50	11.90	24.60
2010-11	3423.82	2398.07	407.43	618.32	70.00	11.90	18.10
Average*	2960.13	1920.21	349.94	682.36	64.87	11.82	23.05

Average* indicates the average was taken for the year 2001-02 to 2010-11.

Per capita consumption of sugar, gur and khandsari in India is given in Table 1.5. It was found that the consumption of sugar was increased by ten times from last four decades and at the same time the consumption of gur and khandsari is almost same and constant. The consumption of gur and khandsari is likely to be increased in the near future due to the awareness of medical illness with high consumption of sugar among the people and makes them shift towards the substitutes of sugar like gur and khandsari.

Table 1.5: Per capita consumption of sugar, gur and khandsari (Status Paper on Sugarcane, 2016-17)

Year	Population in Million (As on 1st March)	Consumption (lakh tonnes)		Per capita consumption (kg/annum)		Total per capita consumption of sugar, gur & khandsari (kg/annum)
		Sugar	Gur & Khandsari	Sugar	Gur & Khandsari	
1960-61	439	21.13	66.87	4.8	15.2	20.0
1970-71	546	40.25	74.37	7.4	13.6	21.0
1980-81	684	49.80	85.22	7.3	12.5	19.8
1990-91	846	107.15	90.71	12.7	10.7	23.4
2000-01	1029	162.00	86.09	15.7	8.4	24.1
2001-02	1043	167.81	83.11	16.1	8.0	24.1
2002-03	1060	183.84	56.94	17.3	5.4	22.7
2003-04	1077	172.85	71.46	16.0	6.6	22.6
2004-05	1093	185.00	81.75	16.9	7.5	24.4
2005-06	1106	189.45	57.39	17.1	5.2	22.3
2006-07	1122	201.60	33.38	18.0	3.0	21.0
2007-08	1138	220.00	50.93	19.3	4.5	23.8
2008-09	1154	230.00	107.92	19.9	9.3	29.2
2009-10	1170	210.00	73.12	17.9	6.2	24.1
2010-11	1186	207.36	59.94	17.5	5.1	22.6
Average*	1115	197	68	17.65	6.06	23.71

Average* indicates the average was taken for the year 2001-02 to 2010-11.

With the enhancement in the per capita income and improvement in the standard of living, demand has been shifted from jaggery and khandsari to sugar **(Status Paper on Sugarcane, 2016-17)** as shown in Table 1.5. The consumption of sugar has increased in the urban areas whereas rural areas still consume Gur and Khandsari **(Status Paper on Sugarcane, 2016-17)**. In 1960-61, per capita consumption of sugar was 4.8 kg per annum and of Gur and Khandsari was 15.2 kg per annum has shifted to 17.5 kg per annum and 5.1 kg per annum respectively. Therefore, it can be concluded that in the coming decades, the consumption of Gur and Khandari is going to show a downward trend.

India is largest sugar consumer in the world. Indian sugar industry is the country's second largest agriculture-based organised industry after textile industry. Cultivation of sugarcane has less risk and it assures some return to farmers even in adverse climatic conditions or market situations. As per a survey report of 2010-11, sugar and jaggery based industries are providing huge amount of employment either directly or through its ancillary units to the rural people. Around 50 million Indian farmers and their families are directly

involved in the cultivation of sugarcane and around 0.5 million unskilled and skilled labours are involved in Indian sugar factories and sugar-related industries **(Status Paper on Sugarcane, 2016-17)**.

A comparison of the nutritional value of the Jaggery, Khandsari and Sugar is shown in Table 1.6. Jaggery contains 65-85% sucrose, 10-15% reducing sugars, 0.4% proteins, 0.1% fats, 3-10 gm moisture and 0.6-1% minerals in which Calcium is 8 mg, Phosphorus is 4 mg and Iron is 11 mg whereas sugar contains 99.5% sucrose, 0.05% minerals and 0.2-0.4 gm moisture. Khandsari is produced by two different methods one is Sulphur process and other is a non-sulphur process. The nutritional value of the khandsari produced by both processes are same; there is difference in moisture content and energy content. Khandsari contains 97.5% sucrose, 0.05% minerals in which Calcium is 100 mg. So, it can be concluded that the jaggery is more nutritional than khandsari and sugar.

Table 1.6: Nutritive value of jaggery, Khandsari and sugar per 100 gm (Rao et al., 2006)

Particulars	**Jaggery**	**Khandsari**		**Sugar**
		Sulphur Process	**Non-sulphur process**	
Sucrose	65-85	97.5	96	99.5
Reducing sugar	10-15	-	-	-
Proteins	0.4	-	-	-
Fats	0.1	-	-	-
Total Minerals	0.6-1	0.05	0.2	0.05
Calcum, mg	8	100	100	-
Phosphorus, mg	4	-	-	-
Iron, mg	11	-	-	-
Moisture, g	3-10	0.3	0.5	0.2-0.4
Energy, Kcal	383	395	388	398

Sugar can`t be digested without Calcium and Potassium, and as it does not contain both the minerals, therefore, it takes both of them from the body. Therefore, because of the presence of all these nutritional values, Jaggery is also known as medicinal sugar. Jaggery purifies blood, prevents rheumatic afflictions and bile disorders. There are many other health benefits of jaggery **(Rao et al., 2006)**.

1.1 Conventional jaggery making process

Figure 1.1 shows the process flow of conventional jaggery making process. In the conventional jaggery making process, 12-15 workers are engaged in different activities at any point of time. It is a batch process. In one batch 250-300 kg of jaggery is being produced. Around 4-5 jaggery making batches are carried out throughout the day i.e. producing 1-1.25 tonnes of jaggery every day **(Shiralkar et al., 2014)**.

The conventional jaggery making process consists of the following steps:

1.1.1 Juice Extraction:

Juice extraction is the first stage of the jaggery making process as shown in Figure 1.1. Sugarcane juice is extracted by crushing sugarcane in a cane crusher. Bagasse comes as a byproduct of the crushing process as shown in Figure 1.2. Bagasse is then laid down in open area for solar or sun drying. Later, this dried bagasse is used as fuel for the boiling furnace as illustrated in Figure 1.2.

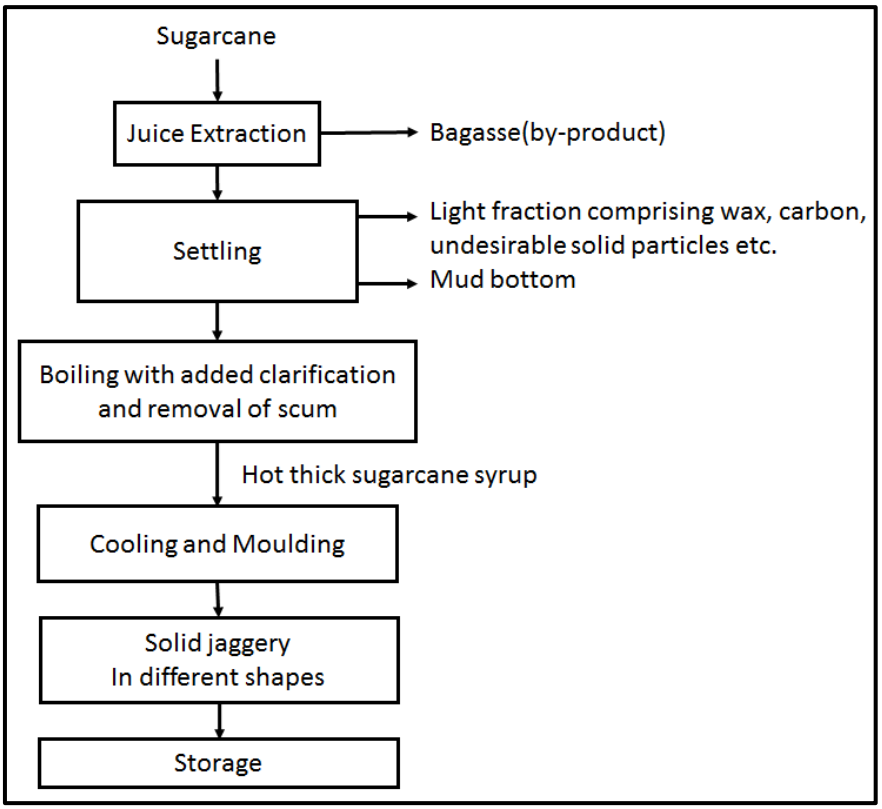

Figure 1.1: Process flow chart of jaggery making process (Rao et al., 2006).

Mostly three roller cane crushers (horizontal or vertical) are used as a sugar cane crusher by the farmers. Horizontal three roller cane crushers are preferred over vertical three roller cane crushers as its juice extraction efficiency is higher and is around 55-60%. The juice extraction efficiency can be increased to 77-80% in sugar mills with the help of multiple crushing and hot water. In general, farmers do not prefer mixing of hot water due to

i. An additional amount of heat energy is required to prepare the hot water.
ii. Latent heat is required to evaporate hot water from the sugar cane juice.

As both the above two points, increases the production cost of jaggery which is not proportionate to the amount of jaggery produced therefore farmers don't use the hot water to increase the juice extraction efficiency.

1.1.2 Settling:

The extracted sugarcane juice is collected in a masonry settling tank where it rests for some time for the separation of light and heavy particles from sugarcane juice as shown in Figure 1.1. So the light particles can be removed from the upside of the settling tank, and mud and other heavy particles can be removed from the bottom. From the middle part of the settling tank, the juice is transferred to the boiling pan which is being filled up to 1/3rd of its total capacity.

1.1.3 Boiling:

The clear juice is then heated using bagasse (byproduct during juice extraction) as the fuel in the open earthen pan furnace as shown in Figure 1.2. The entire boiling process can be divided into three stages **(Jakkamputi and Mandapati, 2016)**:

a) **Sensible heating up to 100°C:** It is the first stage of boiling process. During this process, sensible heat i.e. the amount of energy required to heat the sugarcane juice from room temperature to its boiling temperature, is supplied. The heat energy supplied in this process is around 6.08% of the total heat energy required to make the jaggery from sugarcane juice.

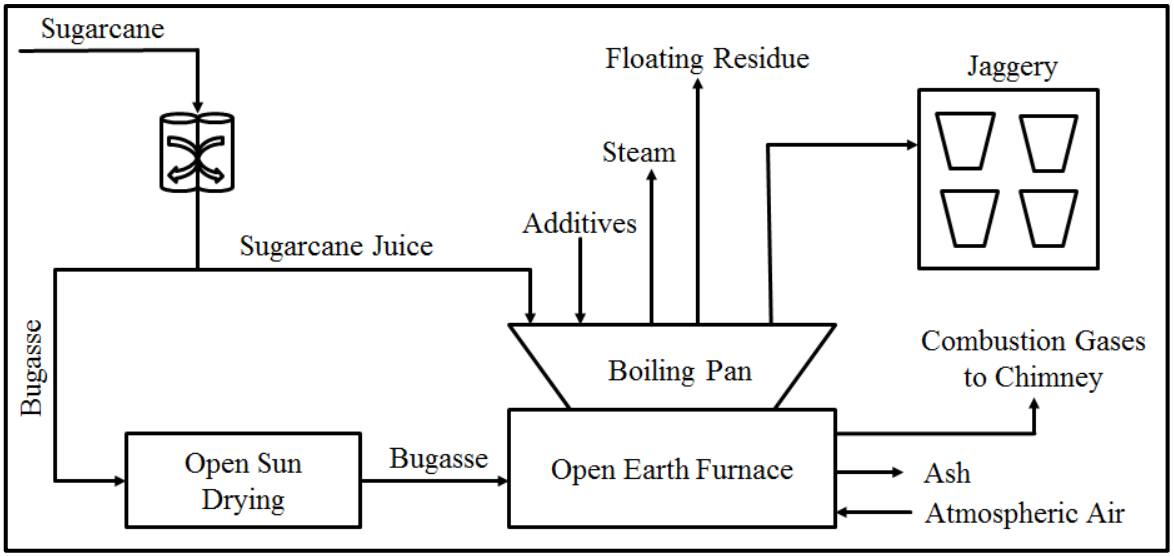

Figure 1.2: Block diagram of conventional jaggery making process (Jakkamputi and Mandapati, 2016)

b) Latent heating at 100°C: It is the second stage of boiling process. During this process, latent heat i.e. the heat energy required to evaporate the water in the sugarcane juice at 100°C is supplied to the sugarcane juice. It requires the major amount of total energy and is around 39.22% of the total energy supplied.

c) Sensible heating up to striking point (118°C): It is the last stage in the boiling process. During this process, sensible heat required to increase the sugarcane temperature from 100°C to its striking point (the moment when the sugarcane juice becomes semisolid and non-sticky to the boiling pan) is supplied. It is around 0.1% of the total energy supplied.

Additives/Clarificants are also added during the boiling process to improve the quality of jaggery, its storability and its acceptability. Earlier natural additives were used like mucilage of bhindi, chkani, kateshevari, etc. **(Rao et al., 2006)**. But now a days emphasis is given on chemical additives. The common chemical additives added are Lime (Calcium Oxide-CaO), Hydros, super phosphate, phosphoric acid, chemiflocks and alum **(Rao et al., 2006; Shiralkar et al., 2014)**.

Lime is the most common additive to clarify the boiling sugarcane juice. When lime (Calcium Oxide) is mixed with water, it converts into Calcium hydroxide. As Calcium is a complexing agent therefore it forms scum which needs to be removed time to time from the

boiling sugarcane juice. Addition of Lime increases the pH of boiling sugarcane juice and improves consistency of the jaggery by increasing crystallisation of sucrose. But the excess addition of lime darkens the colour of the jaggery. The amount of lime addition depends upon quality of lime, quality of sugarcane juice and impurities. Hydros, a bleaching agent, decolourises the boiling juice.

The addition of these additives or clarificants results in the formation of scum which needs to be removed time to time. Generally, this scum needs to be removed at three different stages. And if not removed then degrades the quality of the jaggery. Therefore, multiple effect evaporation concept performed under closed conditions practised in chemical industries, can`t be adopted for sugarcane juice heating **(Shiralkar et al., 2014)**.

1.1.4 Cooling and moulding:

After the boiling process, the hot syrup is then transferred to wooden or aluminium moulds or earthen pots to solidify. The end point of boiling is checked by taking a small quantity of the hot syrup and cooling it in cold water and finally shaping it with a finger. A small quantity of the mustard oil or ground nut oil is sprinkled to prevent excess frothing and also to make hot syrup easily flowing during transfer from one container to the other container. The shape and size of moulds or pots vary according to the required shape and size of the jaggery.

1.1.5 Storage:

Storage is not a direct stage of jaggery making process but as both jaggery and khandsari are prone to moisture in the air. And a lot of jaggery and khandsari is wasted by not properly storing it. Therefore, before the end use it is being given as the last stage of jaggery making process.

1.2 Purpose of thermally efficient conventional jaggery making process

(Solomon, 2011) has pointed out many reasons to increase the thermal efficiency of jaggery making process, which are as follows:

i. Valuable products can be made from the waste material of sugarcane byproducts like pulp and paper, different types of panel or insulating boards, biogas, bioelectricity, ethanol, alcohol and so on.
ii. More employment opportunities can be provided by a sugarcane byproducts based industry.
iii. Economic status of sugarcane growers and workers can be improved by paying higher prices of sugarcane crop.
iv. Pollution load can be minimised by utilising sugarcane byproducts (bagasse and molasses).
v. General economy of the sugar industry can be improved by setting up byproduct based industry.
vi. Sugarcane byproducts can also be utilised for the combustion process in different industries.
vii. As the international trade of sugar has been decreased due to higher production cost of sugar in the country **(Status Paper on Sugarcane, 2016-17)**. So, it seems a profitable venture.

1.3 Heat recovery unit

The proposed heat recovery unit consists of a solar collector and a heat exchanger. The primary fluid (Water, Glycerine, Isobutene, etc.) flow through the solar collector and absorbs solar energy. The high-temperature primary fluid from the collector flows through the heat exchanger where it transfers heat to the sugarcane juice. So, the whole process can be broken into two separate processes:

1) Heating of the primary fluid with the help of solar collector (FPC or ETSC) Figure 1.3 (a).
2) Transfer of this heat energy to the secondary fluid (sugarcane juice) with the help of a heat exchanger Figure 1.3 (b).

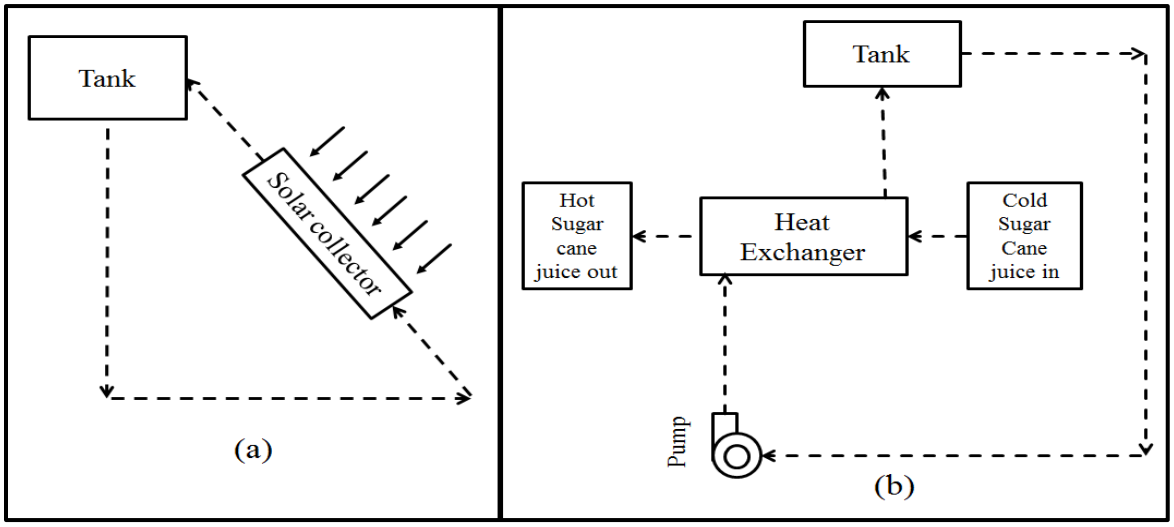

Figure 1.3: Heat recovery unit (a) Heating of primary fluid with the help of FPC or ETSC and (b) Circuit where primary fluid is moving and interacting with sugarcane juice

The block diagram of the solar collector (FPC or ETSC) interacting with the solar radiation is shown in Figure 1.3 (a). The flow diagram of a circuit where primary fluid is moving and exchanging heat energy with sugarcane juice is shown in Figure. 1.3 (b).

1.3.1 Solar Energy

A tiny fraction of the solar radiation incident on the earth, can satisfy the world's total energy requirement. This great potential of the solar energy has made researchers look for technologies to utilise this vast, inexhaustible energy resource.

The standard value of solar constant (solar constant is the energy from the sun, per unit time received by a unit area of the surface perpendicular to the radiation, in space at the earth's mean distance from the sun) is 1353 W/m^2 **(Garg et al., 2013)**.

1.3.2 Radiation at the Earth's Surface

The X-rays and other very short-wave radiations of the solar spectrum are absorbed highly in the ionosphere by nitrogen, oxygen and other atmospheric components. The ozone layer absorbs most of the UV rays. The wavelength longer than about 3.0 μm is absorbed by CO_2 and H_2O i.e. only very little energy beyond 3.0 μm reaches the ground. Thus, from

the application of solar energy, only radiation of wavelength between 0.3 and 3.0 μm need to be considered.

This solar radiation is transmitted through the atmosphere and undergoes many variations due to scattering and absorption. A portion of solar radiation and some scattered radiation reaches the ground as diffuse radiation. There will always be some diffuse radiation, even at the time of very clear sky. The amount of depletion of solar radiation depends upon the amount of dust particles, water vapour, ozone content, atmospheric pressure, cloudiness, etc., and on solar altitude.

Areas lying on the earth between 35° N to 35° S latitudes receive maximum solar radiation **(Garg et al., 2013)**. India is among countries who are blessed to have sufficient amount of solar radiation. It is located north of the equator between 8°4' to 37°6' latitude **(Wikipedia oganization, 2017)**.

1.3.3 Solar Thermal Systems

Various solar energy collection and conversion systems like water heaters, air heaters, solar air-conditioning and water distillation systems, green houses, solar stills, solar cookers, solar dryers and solar furnaces, etc., have been developed. Solar thermal systems have been found to be economically most attractive in actual applications. In all such systems, a solar collector is the most important element.

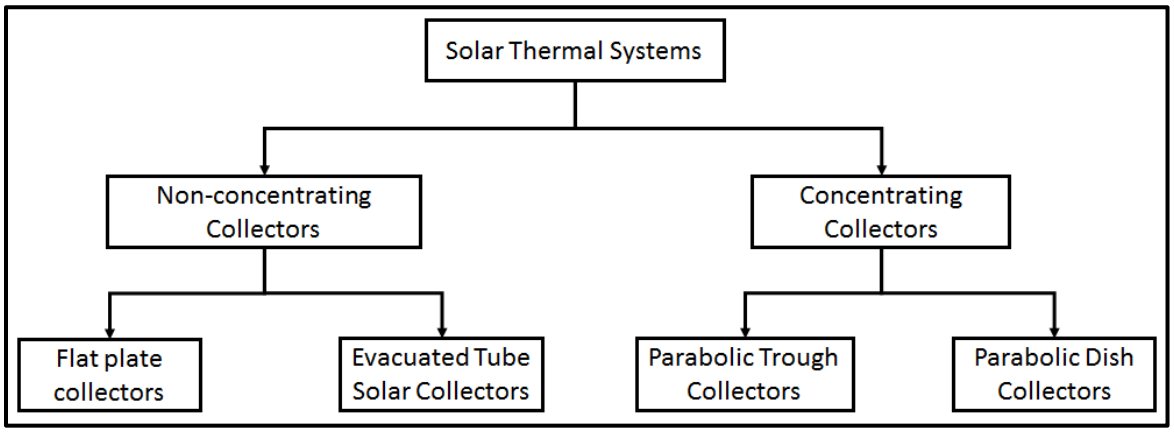

Figure 1.4: Classification of solar water heater

A solar collector is a special kind of heat exchanger that transforms solar radiation into heat energy. Several designs of the solar collectors have been developed. They can be broadly classified as concentrating collectors and non-concentrating collectors as shown in Figure 1.4 in case of water heaters.

1.3.4 Concentrating Collectors

Parabolic dish collectors and parabolic trough collectors are examples of concentrating collectors. These collectors consist of a device to concentrate the solar radiation on a small absorbing surface. Thus, they are capable of delivering very high amount heat energy to the fluid thus, increasing the temperature of the fluid very high which is not possible with non-concentrating collectors. The losses from the collector are lower due to small area of the absorbing surface. They require a tracking mechanism to follow the sun's movement so that the radiation is directed to the absorbing surface. During diffused radiation, these collectors are not effective.

1.3.5 Non-concentrating Collectors

These collectors are designed for application requiring energy at low to moderate temperatures (up to about 100 °C). These devices are mechanically simpler and use both direct and diffuse radiation. Flat plate collectors and evacuated tube collectors are some examples of non-concentrating collectors. These collectors mainly consist of an absorber surface on which the solar radiations fall. Thus, they are capable of delivering a temperature below 100 °C. The losses from the collector are more as compared to the concentrating collectors, due to large area of the absorbing surface. They don`t require any tracking mechanism. These collectors are more effective even during diffused radiation.

A. Flat Plate Collector

A flat-plate collector is installed at a fixed position facing the sun at an optimum inclination to the horizontal depending on the latitude of the location. Water heating is its major application which can be used for different purposes like domestic use (cleaning of utensils, clothes and bathing), industrial use (colouring, heating of secondary fluid), etc.

As shown in Figure 1.5, a flat plate collector consists of five components as follows:

i. **Cover plate:** Its work is to entrap short-wave solar radiation falling on it by transmitting and converting them into long wave radiations. For the long wave radiations, it works as an opaque surface. Glazing is done on it, to increase its efficiency. Toughened glass and transparent plastic covers are used as cover plate.

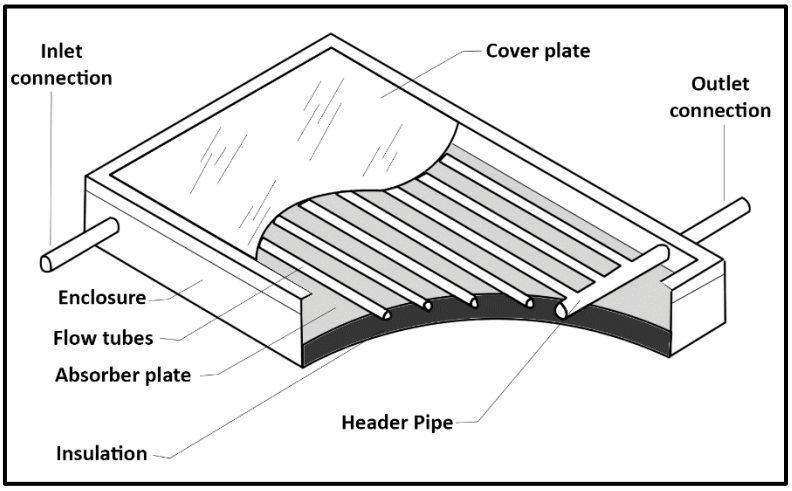

Figure 1.5: Flat plate collector

ii. **Absorber plate:** Its work is to absorb all the solar radiation falling on it and transmitting it to the tubes. It is mainly made up of Copper (Cu). Selective coating of black chrome, nickel black, copper oxide, etc., is being done on it to increase its efficiency.

iii. **Flow tubes:** Its work is to transmit the energy taken from absorber plate to the fluid flowing through it. It is also made up of Copper (Cu). These are connected to the storage tank where hot water is being kept, through header pipes.

iv. **Insulation:** Its work is to stop transmission of the heat energy through the bottom and side surfaces. Mainly made up of glass wool, rockwool and so on.

v. **Enclosure:** Its work is to support the above-mentioned components and is made up of iron sheet, wood.

B. Evacuated Tube Solar Collector

Evacuated tube solar collectors are very efficient and can achieve very high temperatures. They are well-suited to commercial and industrial heating applications and can be an effective alternative to flat-plate collectors for domestic space heating, especially in areas where it is often cloudy.

It contains several rows of glass tubes connected to a header pipe. Each tube has the air removed from it (evacuated) to eliminate heat loss through convection and conduction. Inside the glass tube, a flat or curved aluminium or copper fin is attached to a metal pipe. The fin is covered with a selective coating that transfers heat to the fluid that is circulating through the pipe. There are two main types of evacuated tube collectors:

1) **Heat pipe evacuated tube collectors:** Heat pipe evacuated tube collectors contain a copper heat pipe, which is attached to an absorber plate, inside a vacuum sealed solar tube. The heat pipe is hollow and the space inside is also evacuated. Inside the heat pipe is a small quantity of liquid, such as alcohol or purified water plus special additives. The vacuum enables the liquid to boil at lower temperatures than it would at normal atmospheric pressure. When sunlight falls the surface of the absorber, the liquid in the heat tube quickly turns to hot vapour and rises to the top of the pipe. Water or glycol flows through a manifold and picks up the heat. The fluid in the heat pipe condenses and flows back down the tube. This process continues, as long as the sun shines.

   Since there is a "dry" connection between the absorber and the header, installation is much easier than with U-pipe direct flow collectors. Individual tubes can also be exchanged without emptying the entire system of its fluid and should one tube break, there is little impact on the complete system.

   Heat pipe collectors must be mounted with a minimum tilt angle of around 25° for the internal fluid of the heat pipe to return to the hot absorber.

2) **Direct-flow evacuated-tube collectors:** There are different arrangements of direct flow evacuated tube collector:
   a. U-pipe water in glass evacuated tube collector: It consists of two pipes inside the evacuated tube that run down and back in the U-shape. One pipe is for inlet fluid and the other for outlet fluid. Since the fluid flows in and out of each tube, the tubes are non-replaceable. They are cheap compared to flat plate collectors.

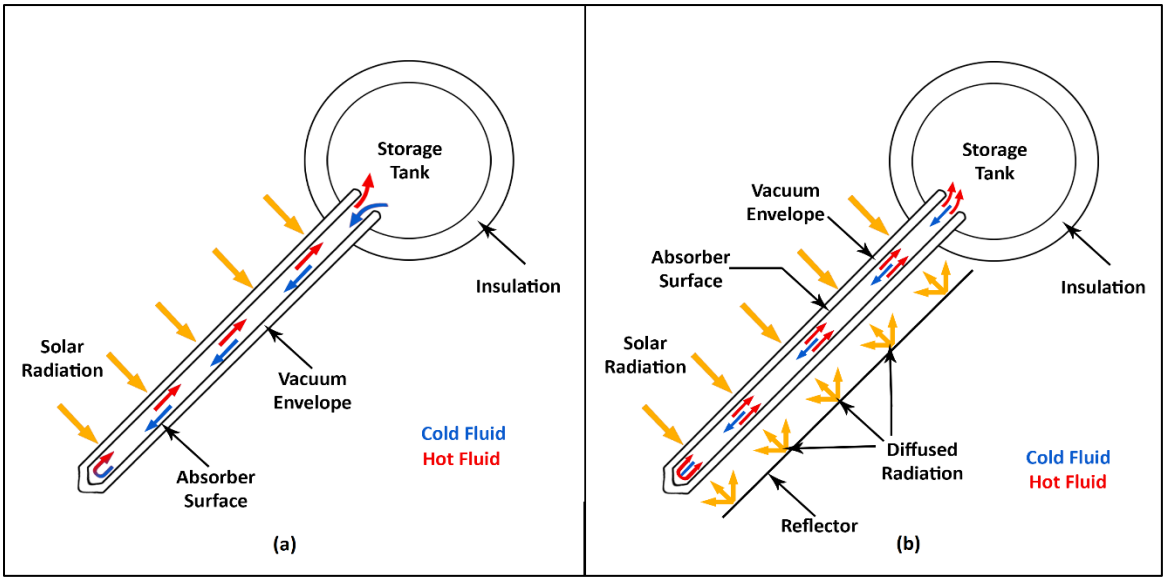

Figure 1.6: Working of water in glass ETSC (a) without a reflector and (b) with a reflector.

b. Water in glass evacuated tube collector: Water is kept directly inside the evacuated tubes. Convection phenomenon takes place for heating of water as shown in Figure 1.6. Since these tubes are directly connected with the storage tank, therefore installation is much easier than with U-pipe direct flow collectors. But individual tubes can`t be replaced without emptying the entire system of its fluid. If one tube breaks, the entire system is going to be empty. It is easy to use and is cheap compared to flat plate collector. Mainly it is used for domestic water heating purposes.

1.3.6 Heat exchanger

Heat exchanger is a device used to transfer heat between two fluids; a hot fluid and a cold fluid. The aim may either to add heat to cold fluid or to remove heat from the hot fluid. Different kinds of heat exchangers have been developed. They can be classified depending upon their application as shown in Figure 1.7. They find various applications in automobile radiators, condensers and evaporators of refrigeration and air conditioning units, boilers, condensers, super heaters, air preheaters and economisers of power plants, etc. The heat exchangers are classified as follows **(Kumar, 2015)**:

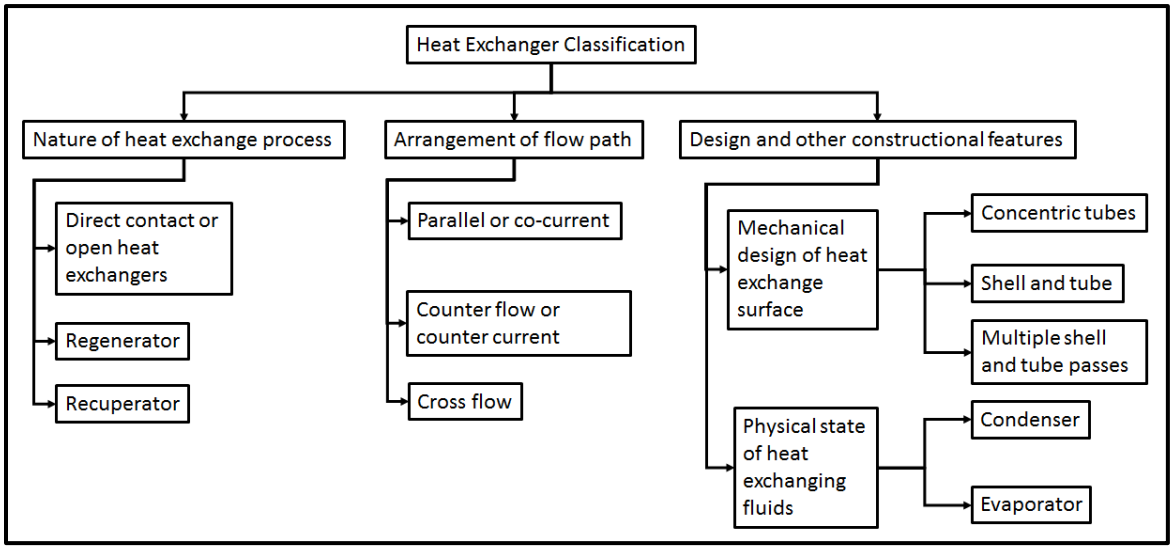

Figure 1.7: Classification of Heat exchanger

A. Based on the nature of heat exchange process, heat exchangers are classified into three categories:

   a. Open or direct contact type heat exchangers: There is continuous heat and mass transfer by complete mixing of hot and cold fluid. Its use is restricted to situations where mixing between hot and cold fluid is harmless and desirable. Examples are water cooling towers.

   b. Regenerators type heat exchangers: Its operation is intermittent. Heat is accumulated in a certain medium known as matrix by passing hot fluid. Subsequently, this heat is transferred to the cold fluid by allowing the cold fluid to pass through the heated matrix. In case of rotating matrix, the process is continuous. Again, its use is restricted to condition that hot and cold fluid mixing is harmless and desirable.

   c. Recuperator type heat exchangers: The hot and cold fluid flow is separated by a wall. And the heat transfer takes place in the order. There is a convection phenomenon to transfer heat between hot fluid and wall, then conduction phenomena to transfer heat through the wall followed by again convection phenomena to transfer heat between wall and cold fluid. There is no mixing of fluids.

B. Based on the relative direction of motion of fluids heat exchangers are classified as follows:
    a. Parallel or co-current type heat exchangers: Both the hot and cold fluids enter, flow and leave in the same direction.
    b. Counter-flow or counter current type heat exchangers: In this hot and cold fluid enter, flow and leave in the opposite direction.
    c. Cross flow type heat exchangers: Hot and cold fluid enter, flow and leave it at right angle.

C. Based on the design and other constructional features heat exchangers are classified as follows:
    a. Mechanical design of heat exchange surface
        i. Concentric tubes: Two concentric tubes are used for carrying fluids one for each. The flow direction may be same or opposite.
        ii. Shell and tube: One fluid is carried through a bundle of tubes enclosed by a shell. The other fluid is forced to pass through shell over the outside surface of tubes. The flow direction for either or both the fluids may change during its passage through it. A shell and tube heat exchanger is shown in the Figure 1.8.
    b. Physical state of heat exchanging surface
        i. Condenser: The hot fluid changes its phase from vapour to liquid during its passage.
        ii. Evaporator: Cold fluid changes its phase from liquid to vapour during its passage.

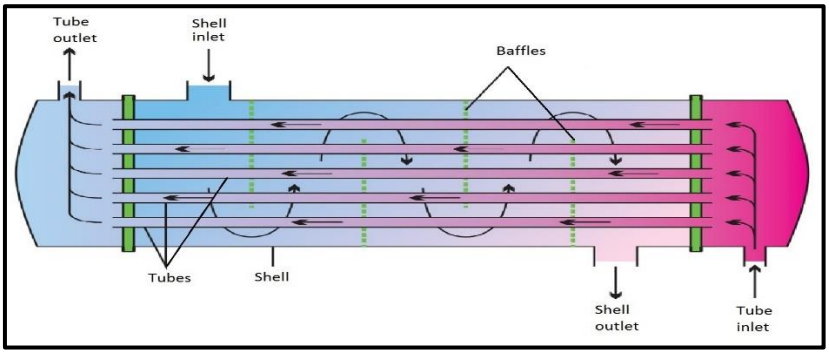

Figure 1.8: Shell and tube heat exchanger

1.4 Need of the study

The energy shortage has now become a worldwide critical problem. Looking to the energy crisis, it is important to find alternative resources to replace conventional fuel energy and also to reduce the conventional fuel energy usage. Consequently, intensive efforts should be made to reduce the energy consumption for different processes. As the conventional jaggery making process is thermally inefficient. Therefore, there are different ways to make it thermally efficient like use of exhaust gases or solar energy, either to preheat the sugarcane juice or to preheat the air entering the furnace and use of solar energy to dry the bagasse.

1.5 Objectives

In order to replace the use of dry bagasse as raw material for heating of sugarcane juice a renewable source of energy i.e. solar energy based conversion system is proposed in the present study. Following are the main objectives of the present study:

1) Design, fabrication and installation of a shell and tube heat exchanger used to transfer energy from primary fluid (water) to sugarcane juice.

2) Installation of an evacuated tube solar collector to absorb solar energy.

3) Testing and Performance analysis of heat recovery unit (combination of solar collector and heat exchanger) to transfer heat energy in Jaggery making process.

1.6 Organisation of thesis

The work presented in the report has been organised as follows:

Chapter 1: Introduction

The conventional jaggery making process was introduced in this chapter. The general losses associated with this process and the possible methods to improve its thermal efficiency were discussed. Objectives of the present study have been stated.

Chapter 2: Literature review

Various studies done on improvement of thermal efficiencies of Jaggery making units, Flat Plate Collectors, Evacuated Tube Solar Collectors and Heat Exchangers have been discussed in this chapter.

Chapter 3: Design and fabrication of heat exchanger

An algorithm was developed to design a Shell and Tube Heat Exchanger in two different tube configurations: Aligned grid and Staggered grid. Two configurations of STHE were theoretically studied based on the results obtained from this algorithm. STHE with Staggered tube grid was being selected for the experimental work based on the results of obtained from algorithm. The design values of the STHE are also presented in this chapter. The geometries of the staggered STHE made in SOLIDWORKS were presented. At the end images of the fabricated staggered STHE are shown in this chapter.

Chapter 4: Development of experimental setup and experimentation

The experimental setup was developed after selecting the ETSC for heating of the primary fluid (water), designing and fabricating of the STHE. The methodology of the experimentation is also presented in this chapter.

Chapter 5: Results and discussion

This chapter contains performance study of both heat exchanger and ETSC. Heat exchanger was being optimised based on the results obtained from the experimentation.

Chapter 6: Conclusion

In this chapter, conclusions were made based on the experimental results and the future scope of the work is recommended.

Chapter 2 LITERATURE REVIEW

With the rapid increase in population and economic growth of countries worldwide and especially in the tropical regions, it is important that efficient techniques are deployed to reduce energy consumption. Efficient processes with the help of technology, reduce the energy consumption significantly. Modified processes utilising waste heat recovery and solar energy can be very promising from the economic point of view in the long run. Bagasse which is used as fuel for conventional jaggery making process, can be used in different industries for producing useful products. A review of the comprehensive study carried out on the different methods to improve the thermal efficiency of jaggery making process is presented in this chapter.

2.1 Difficulties with the conventional jaggery making process:

The thermal efficiency of the furnace depends mainly on the flow patterns inside the furnace, which are highly non-ideal in nature because of the irregular geometries of the units. Chimney height, chimney top and bottom diameters, furnace depth, area of air inlet and outlet, and orientation of furnace air inlet and duct are several design and operating parameters that influence the flow patterns inside the furnace. The construction of the jaggery making units are being done by the local artisans based on their past experience and not based on the proper designing skills of the units. Therefore, the thermal efficiency of the jaggery making units, is very less. Many research scholars have stated that there is a lot of scope for saving more bagasse in many of the existing jaggery making units. Many parameters which reduce the efficiency of the jaggery making units, are as follows:

1) It contains significant amount of water around 20% even after drying in the open solar radiation **(Agalave, 2015)**. Energy is lost to evaporate this water from the bagasse which makes the combustion process less efficient **(Munsamy, 2008)**.
2) The pan used to heat the sugarcane juice is not properly designed so it takes a lot of energy to transfer heat from furnace to sugarcane juice **(Agalave, 2015)**.

3) Improper sizing of chimney results in decreasing combustion efficiency of open earthen furnace used for conventional jaggery making process **(Shiralkar et al., 2014)**. As radiation is the main cause of the heat transfer to the pan and is a strong function of temperature. Therefore, in case of oversized chimney following problems can be encountered:
    a) It requires extra energy to heat this extra air present in the furnace and it requires extra feeding of the bagasse to maintain the flame temperature.
    b) If bagasse feeding is not matched with the increased air flow rate then it increases the batch period because of the low flame temperature resulting in the less production.
4) Energy lost through combustion gases from the open earthen furnace is around 30 to 35% of the total energy supplied which is not being utilised **(Manjare et al., 2016)**.

Hence, the overall thermal efficiency of the conventional jaggery making process is very poor.

2.2 Possible solutions

There are many ways to improve the thermal efficiency of the conventional jaggery making process as follows:

1) For removing moisture or dewatering the bagasse, either cane diffuser can be used **(Munsamy, 2008)** or solar drier (solar air heater) can be used **(Jakkamputi and Mandapati, 2016)** or both can be used.
2) Fins can be provided at the bottom of the main pan and gutter pan for efficient heat transfer from furnace **(Anwar, 2010; Agalave, 2015)**.
3) By blocking excess air from entering the furnace by the use of dampers at the air inlet of the furnace or at the exit of the chimney **(Shiralkar et al., 2014)**.
4) By preheating the sugarcane juice with the help of the exhaust gases of the chimney **(Manjare et al., 2016)**.
5) By preheating of the air entering the furnace with the help of the exhaust gases of the chimney **(Jakkamputi and Mandapati, 2016)**.

Non-conventional sources of energy like solar energy can also be used as a substitute of bagasse in the conventional jaggery making process **(Jakkamputi and Mandapati, 2016)**. Solar energy can be used:

1) To preheat the air entering the furnace,
2) To remove the water content from the bagasse,
3) To supply partly or completely the heat energy required for the jaggery making process.

Recently, **(Jakkamputi and Mandapati, 2016)** suggested a method to utilise the solar energy for the jaggery making process. The modified jaggery making process is shown in Figure 2.1. A solar collector in combination with a heat exchanger is used to preheat the sugarcane juice. The solar energy collected by using collectors is transferred to the sugarcane juice in a heat exchanger. The liquid flowing across the solar collector and heat exchanger can be treated as a primary fluid and the sugarcane juice is considered as a secondary fluid.

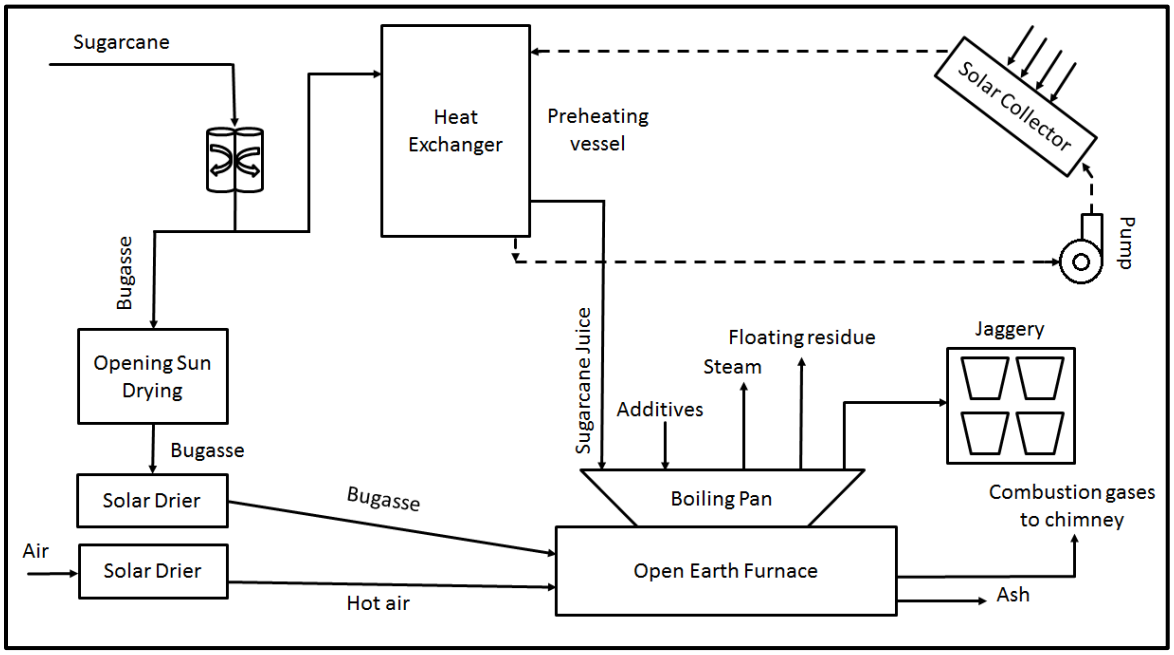

Figure 2.1: Modified jaggery making process (Jakkamputi et al., 2016)

The temperature of sugarcane juice can be raised very close to its boiling point using FPC or ETSC so that energy required in the first stage of boiling process can be supplied from solar energy. Similarly, the latent heat of energy required to remove the water from

the sugarcane juice can also be supplied using solar energy. This requires highly efficient solar collectors like parabolic through collectors or parabolic dish collectors. Solar energy can also be used to preheat the air used for combustion process using solar air heaters. It can also be used to remove the water content in the bagasse. Water content can be reduced to 5 to 7% by using solar driers against 20% in conventional open drying process **(Jakkamputi et al., 2016)**.

2.3 Past research work on jaggery making process

(Anwar, 2010) proposed an improved design of pan to improve the efficiency of the jaggery making process. By providing parallel fins at the bottom of the main pan and gutter pan, it was found that heat utilisation efficiency of jaggery making unit having 2-pan furnace was improved by 9.44% resulting into 31.34% saving of fuel and energy.

(Sardeshpande et al., 2010) put forward a procedure for thermal evaluation of a jaggery making furnace based on the heat and mass transfer analysis. In the thermal evaluation, it was indicated that theoretically only 29% of the energy supplied by bagasse combustion, is required for jaggery making. The oxygen content present in the flue gases is a measure of degree of combustion. The thermal efficiency of the furnace along with inside furnace temperature, increases with the decrease in excess air intake. A method of supplying controlled fuel to the furnace was proposed based on the oxygen percentage in the flue gases. This method reduced the bagasse requirement for 1 kg of jaggery preparation from 2.39 kg to 1.73 kg, making around 27% of fuel savings.

(Solomon, 2011) The economic evaluation of different products which can be made from the byproducts of sugarcane is presented. 10-12 million tonnes of molasses are produced every year in India. Sugarcane byproducts can be utilised to produce pulp and paper, panel or insulating board, particle board, biogas, bioelectricity, ethanol, alcohol, etc. which have good economic value. These industries will result in producing some good products, giving employment opportunities to the villagers, reducing pollution hazards.

(Arya et al., 2013) improved the design of three pan jaggery making plant by some modifications which includes

i. Instead of ordinary masonry bricks, fire bricks (40-50% alumina) were used in the construction of the furnace.
ii. A cast iron fire grate was provided in the furnace for proper mixing of the fuel and air.
iii. Air was sucked in to the furnace both from the front wall opening and the bottom opening of the fire grates.
iv. Ash was being automatically dropped through these grates from where it can be easily taken out time to time.
v. They also improved design of the chimney by keeping the optimum height of the circular chimney. The chimney height is optimised by creating sufficient draft and also by providing two additional dampers of mild steel plate to control the draft.

The conventional three pan jaggery making plant used 2.26 kg of bagasse for making 1 kg of sugarcane juice whereas the modified three pan jaggery making plant used 1.99 kg bagasse with an improvement in plant efficiency. Productivity was also increased as 1800 kg of sugarcane juice was used to make jaggery instead of 1500 kg in the modified jaggery making plant. CO_2 percentage was also increased in the modified plant which indicates better combustion.

(Shiralkar et al., 2014) made analytical calculations for single, double and four pan furnaces of jaggery making units. It was pointed out that thermal efficiency of single pan units is 45-60%, double pan units 45-55% and four pan units is 40-50%. Productivity increases with the increase in number of pans but the increase in unit efficiency is comparatively smaller. Efficiency of the furnace depends on the mass flow rate of intake air. In case of excess air, heat is lost in preheating the excess air resulting in lower furnace temperature and thermal efficiency. It was suggested that existing furnace efficiency can be increased by controlling the mass flow rate of air with the use of dampers. Two jaggery making furnaces consisting two pans and four pans were tested and it was observed that their efficiencies were increased from 53% to 76% and 50% to 57% respectively.

(Agalave, 2015) provided fins at the bottom of the pan in the single pan furnace and also provided baffles from the top side at the center of the furnace near the exit of the flue gases. These two factors resulted in improvement in the thermal efficiency by 9.44%. This

improvement resulted into utilising 1.1 kg of bagasse instead of 2.3 kg of bagasse per kg of jaggery for the furnace.

(Jakkamputi and Mandapati, 2016) described various factors which reduces the thermal efficiency of a conventional jaggery making unit. Many factors including inefficient combustion in the furnace, energy lost through exhaust gases, energy lost through furnace wall convection and radiation, accounts around 55% of the total energy produced by the combustion of bagasse. Various methods to improve the thermal efficiency of a conventional jaggery making unit are: (a) preheating the air entering the furnace (b) increasing the sugarcane juice temperature up to 100°C by using waste heat available in exhaust flue gases from the furnace or by industrial waste heat available or by the use of solar energy. Analytical calculations were also presented to find the heat balances in the jaggery making unit.

(Manjare et al., 2016) performed experimental analysis on a single pan furnace to prepare jaggery. It was pointed out that the incomplete combustion in the furnace results due to improper design of pan and furnace prepared by local artisans without any optimisation measures. It was observed that the efficiency of the jaggery making unit was increased from 16.16% to 24.36% and bagasse consumption was reduced by 1.2 kg per kg of jaggery production, by preheating the sugarcane juice in the preheating vessel or pre-heater by the exhaust gases.

The literature survey proposes that the thermal efficiency of jaggery making units is very poor and needs significant improvement. Preheating of the sugarcane juice and inlet air either by exhaust gases or by solar energy, modifying pan design and controlling the bagasse and air entering the furnace are some modifications to improve the thermal performance of the jaggery making units. It will result in saving of bagasse which can be utilised for different purposes like pulp and paper production, insulation board production and so on.

2.4 Flat plate collector

Around the world, a lot of experimental work has been carried out for evaluating and enhancing the performance of Flat Plate Collector (FPC). To validate the results of simulation and mathematical modeling by varying different parameters has been put forward by many research scholars. Below is a review of work done by many research scholars on FPC:

(Winter, 1975) Double loop or indirect solar water heating system reduces the problem of corrosion, freezing, etc. Same time the performance of solar water heating system decreases because the collector has to work at a higher temperature. In this paper, a heat exchanger factor was being developed in order to calculate the penalty or decrement in the performance of the solar water heating system due to the use of an integrated heat exchanger.

(Fanney et al., 1988) In this paper, the effect of flow rate on the performance of direct as well as indirect domestic solar water heating system was being studied experimentally and numerically by simulations.

Two methods to improve the performance of solar water heating system were presented. It can be done either by reducing the flow rate or by enhancing the thermal stratification in the storage tank. The running and initial cost were reduced by reducing the flow rate, but flow imbalances were observed in the solar collector below a certain minimum flow rate. In case of indirect domestic solar hot water system, the performance of heat exchanger decreases with the decrease in flow rate. It was also pointed out that the performance of the solar water heating system is independent of the tank side flow rate.

There was no occurrence of flow imbalance by using improved stratification within storage tank. Thermal stratification increases the performance along with the initial cost of the project.

(Hobbi et al., 2009) conducted an experimental study on a flat plate collector to investigate the effect of passive heat enhancement devices (simple tube, twisted strip, coil spring wire and conical ridges) on its thermal performance. Experimental results showed

negligible difference in the heat flux to the fluid. High values of Grashoff number, Richardson and Rayleigh number were observed. This showed that heat transfer mode was mixed convection type in which free convection was dominant.

(Mossad et al., 2012) presented numerical simulations using ANSYS FLUENT of a flat plate collector with two different configurations. The first configuration consisted of a single row heat exchanger with length 10.8 m and inside pipe diameter as ¾ or ½ inch. The second one consisted of a double row heat exchanger with length 16.2 m and diameter ½ or ¾ inch. It was found that single row heat exchanger of first configuration was more economical than double row heat exchanger.

(AL-Khaffajy et al., 2013) In this paper, the effect of different parameters on the thermal performance of the system along with reducing the cost (both initial and running) were being investigated. From the results, it was found that the single row heat exchanger of 10.8m length for both elliptical and type B tube gave high service outlet temperature while reducing both initial and running or pumping cost. The size of tubes used were ¾ or ½ inch. Hence, size of the flat plate collector can be selected from the results presented in this paper.

(Abubakar et al., 2014) conducted experiments on a solar flat plate collector (model TE39) in hot weather conditions of Bauchi. The experiments were being carried out daily for 2 hours (11:00 to 13:00 hours) for a period of 28 days. It was found that collector's optimum efficiency was around 70.5% and the maximum outlet water temperature was 55°C. It was concluded from the experimental results that that model TE39 is best suitable for the domestic use in the Bauchi weather conditions.

(Arslan et al., 2015) performed numerical analysis to optimise the performance of storage tank in a solar water heating system. It was concluded that thermal stratification was better with the increase in the temperature of the fluid through covered heat exchanger. Storage tank capability to deliver the amount of hot water decreases with the increase in discharge time.

(Singh et al., 2016) The parabolic trough collector is used in the industries for a very high temperature (~200`C or above). So, by reducing its size, it can also be used for household applications even in case of free convection.

(Kumavat et al., 2016) In this paper, four different configurations of a flat plate collector were being simulated in ANSYS FLUENT. Flat plate collector with better output results was selected from the numerical analysis and then fabricated for experimental analysis. Experimental results showed that, collector outlet temperature is directly proportional to the solar intensity and the best output temperatures were found on clear sunny days.

The literature survey suggests that a number of researchers have conducted parametric studies on the performance of FPC systems considering geometric and climatic variations and found that collector tilt angle, climatic conditions like solar intensity, wind velocity. Therefore, by keeping the optimum tilt angle, highest output temperatures are found on clear sunny days with minimum wind velocity.

2.5 Evacuated tube solar collector

A lot of experimental work has been carried out for evaluating the performance of Evacuated Tube Solar Collector (ETSC) all over world. To study the impact of different parameters affecting the performance of ETSC system and to validate the results of simulations and mathematical modelling, various researchers had developed experimental set ups consisting different types and sizes of ETSC with different concentrations of different nano-fluids.

(Budihardjo et al., 2002) conducted an experiment on ETSC consisting 21 evacuated tubes and a tank with 150 litre capacity. ISO9459-2 method was used as test procedure for experimentation. Performance evaluation of ETSC with numerical simulations was also presented based on the experimental results. It was found that the natural mass flow rate through the evacuated tubes was around 20-25 kg/hr which was around 3 to 4 times flow rate through the tank volume per hour. Investigation show that natural convection flow rate in the evacuated tube is high. A correlation for ETSC was also

developed for the flow rate as a function of heat transfer and fluid flow inside water in glass tube.

(Gao et al., 2009) conducted experiments and compared two types of ETSCs, Water in glass Evacuated Tube Solar Collector (WGETsc) and U-pipe Evacuated Tube Solar Collector (UpETsc). It was found that thermal storage (around 25 to 30%) as well as thermal efficiency of WGETsc was lower than UpETsc. As in case of UpETsc evacuated tubes are not completely insulated and are always filled with water therefore at night water in the tubes loses its energy. It was observed that the optimum mass flow rate at maximum thermal efficiency for WGETsc and UpETsc were 20-60 kg/hr m^2 and 20-40 kg/hr m^2 respectively.

(Mahendran et al., 2012) experimented on the ETSC with different concentrations of Al_2O_3 and TiO_2 in water and compared the performance of the ETSC with water as the working fluid. The mass flow rate of the water or water with nano particles was fixed at 2.7 litre/min. The efficiencies of the collector were found to be 58% and 73% with water and water based TiO_2 (0.3% concentration) as the working fluid respectively. The efficiency increased by 16.67% with 0.3% TiO_2 nanofluid as compared to water. Similarly, it was found that water based Al_2O_3 nanofluid gives 8% higher efficiency as compared to water as a working fluid in ETSC.

(Mahendran et al., 2013) experimentally studied the efficiency of the ETSC as per ASHRAE standard 93-2000. They used 0, 1, 2 and 3% by volume of water based TiO2 nanofluid and keeping mass flow rate constant at 2.0 litre/min. They found that the efficiency of ETSC with 2% by volume TiO2 in water was higher and it was 42.5% higher compared with water as working fluid.

(Mishra, 2015) Thermal efficiency of an evacuated U-tube collector was found to be more than water in glass evacuated tube solar water heater from the experimental results. It was suggested that water in the tubes should be carefully handled otherwise as the temperature of water reaches very high, causes thermal shock in the tubes resulting in formation of cracks. This may result in loss of vacuum and even failure of tubes.

(Sabiha et al., 2015) The effect of nanofluids and Single Walled Carbon Nanotube (SWCNT) on the performance of the ETSC was studied. It was found that the suspension

of SWCNT and Sodium Dodecyl Sulfate (SDS) were stable for a period of one month. It was point out that for a mass flow rate of 1.5 kg/sec and for the case of 0.05 and 0.25% by volume SWCNT, maximum temperature difference between inlet and outlet was 9.85°C and 11.43°C respectively. The efficiency increased from 36.57% to 62.51% for 0.05 and 0.25 % by volume SWCNT respectively i.e. the efficiency for 0.25 volume% of SWCNT was 15.66% higher than 0.05 volume % SWCNT.

(Naik et al., 2016) developed a mathematical model to find the performance of a U-tube Evacuated Tube Solar Collector (ETSC). Analytical results with the help of mathematical model developed were also presented and results had been validated with experimental results. It was found that the results of the analytical solution were quite similar with the experimental results. Lithium Chloride aqueous solution (LiCl-H_2O), air and water had been used as the working fluid. Experimental results show that the effect of mass flow rate of the working fluid, length of the collector and solar intensity are significant whereas the effect of the inlet temperature of the working fluid has very little or no effect on the performance of the U-tube Evacuated Tube Solar Collector.

(Ghaderian et al., 2017) performed experiments on a passive Evacuated Tube Collector using Triton X-100 as the surfactant and nanoparticles having particle size of 40nm. The collector is having a spherical coil inside the storage tank. The experiments were carried out with different volume fraction of the nanoparticles ranging from 0.03 to 0.06% and volume flow rate inside the spherical coil ranging from 20 litre/hr to 60 litre/hr. It was found from the experimental results that the maximum efficiency of 57.3% was obtained when the nanoparticles volume fraction was 0.06% and flow rate was 60 litre/hr. It was observed that the stability of the nanoparticles decreases with increase in the ionic strength. The stability of the nanoparticles inside the pure water against deposition was checked using sedimentation technique. In sedimentation technique, the mixture is kept still for some days of around 30-40 days to check the deposition. It was also pointed out that by the use of nanoparticles, the heat capacity of the mixture was reduced but there was an increment in the output temperature and as the concentration of Al_2O_3 and CuO increased, heat transfer coefficient also increased.

These literatures review suggest that a lot of research work has been done on ETSC systems for evaluating thermal performance considering different types and sizes of ETSC with different concentrations of nano fluids at different mass flow rates of the working fluid.

2.6 Shell and tube heat exchanger

Around the globe, different algorithms have been developed by research scholars for designing Shell and Tube Heat Exchanger (STHE) with different configurations of tube arrangements in order to reduce the time for designing of STHE. Researchers have also done experimental work for evaluating the performance of STHE, to study the impact of different parameters on the performance of STHE and to validate the results of simulations and mathematical modelling.

(Caputo et al., 2008) Three case studies were presented in this paper to check the capabilities of the proposed heat exchanger design. An algorithm was developed to optimise the design of heat exchanger. Hence, the initial and running costs of the heat exchanger were minimised. Using the algorithm, total cost of the heat exchanger was reduced to half. It was suggested that this algorithm should be used to design the heat exchanger as it consumes less time, provides the designer with more degree of freedom to design and select more number of design alternatives.

(Patel et al., 2010) Heat exchanger design is a complex process which involves optimisation of many of the operating and geometric parameters. Rating a large number of heat exchanger geometries to find those who satisfy required heat transfer rate, operational and geometric constraints, was the traditional design approach. It was found that traditional design approach was quite time consuming and did not give surety of finding the optimum design. In this paper, particle swamp optimisation (PSO) technique was discussed which optimises the heat exchanger design from economic point of view i.e. based on the annual running cost of the heat exchanger. The results of the PSO technique were also compared with the genetic algorithms (GA) to design a heat exchanger. The geometric parameters of the heat exchanger including: baffle spacing, outer and internal diameters were considered for optimisation. Optimisation also included two tube layouts: triangular and square tube layouts.

(Jayachandriah et al., 2015) designed a double pass helical coil heat exchanger and compared its results with heat exchanger with segmental baffle using Kern Method. The designed model has 7 tubes of diameter 20 mm and length 500 mm, shell diameter 90 mm and shell length 600 mm respectively. Steel AISI 1010, Copper and Aluminium are the material of the shell, tube and baffles respectively. It concludes that shell and tube heat exchanger with continuous helical baffle has maximum overall heat transfer coefficient. The pressure drop is found to be decreasing with an increase in the helix angle.

(Ambekar et al., 2016) studied the effect of different configurations of the baffles (helical baffles, single, double and triple segmental baffles and Flower A and B type baffles) inside Shell and Tube Heat Exchanger. The CFD simulations were carried out in SOLIDWORKS flow simulation software version 2015. The simulation results showed that the single segmental baffles were giving more heat transfer rate while keeping all the other parameters constant such as mass flow rate, pressure drop and heat transfer coefficient. Helical baffles showed almost zero stagnation zones resulting reduced fouling and long operational life of the heat exchanger because vibrations due to flow were low.

The literature survey proposes that a large number of research scholars put forward different algorithms for designing STHE with different types of tube banks with the help of different optimisation techniques like GA, PSO, etc. to reduce the time taken for designing the STHE. Effect of different parameters like different tube arrangements, different types of baffles, etc. on the performance of STHE are significant.

2.7 Summary of literature review

Based on the literature review presented in this chapter, the research findings are as follows:

Research work had been carried out to improve the performance of jaggery making unit by adapting different methods. Sugarcane juice can be preheated close to its saturation temperature by using the waste heat available in the exhaust gases from the open earthen furnace using multiple number of pans instead a single pan. In a modified jaggery making unit we can utilise the solar energy to preheat the sugarcane juice, inlet air for combustion and to remove the moisture content in the bagasse. Solar collector in combination with a heat

exchanger is a basic unit in the modified jaggery making unit by which we can absorb solar energy to preheat the sugarcane juice. The literature collected on solar collectors found that experimental as well as theoretical work had been carried out to improve the performance of FPC and ETSC. Use of reflector sheet, glazing on glass cover and selective coating on the absorber surface of the FPC are some ways to improve the efficiency of FPC. Different studies had been carried out to compare the efficiency of different types of ETSC. Literature with different ways of improving the external as well as internal heat transfer coefficients in a shell and tube heat exchanger were also presented in this chapter. Experimental as well theoretical analysis had been carried out to optimise the design of STHE and to improve its performance.

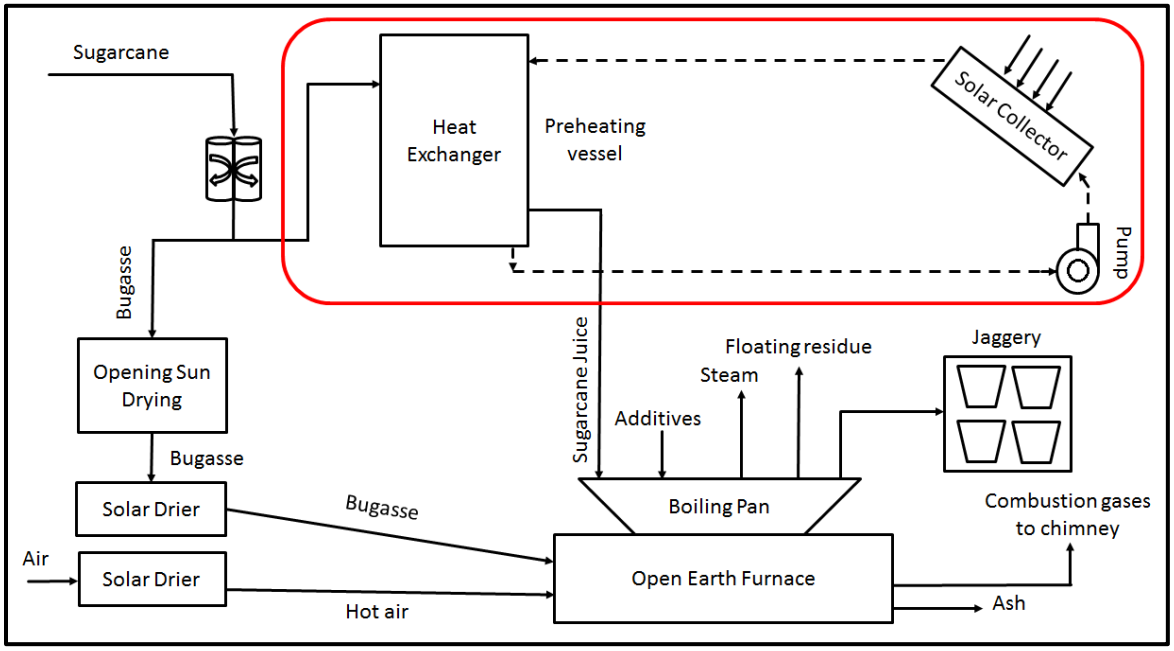

Figure 2.2: Modified jaggery making process indicating the work done in the report by red rectangle (Jakkamputi and Mandapati, 2016)

Work done in this report (indicated by a rectangle in red color in Figure 2.2), was selected based on the literature survey.

Chapter 3 DESIGN AND FABRICATION OF HEAT EXCHANGER

Because of the relatively simple manufacturing and adaptability to different operating conditions, shell and tube heat exchangers (STHE) are most widely used heat exchangers in the industry. The design process of STHE is an iterative process involving a large number of geometric and operating variables as a part of the search for a heat exchanger geometry that meets the heat transfer requirement and given design constraints. First, an algorithm is discussed for designing STHE. A Microsoft excel program was made based on the algorithm for designing STHE in order to reduce the time taken for designing process. First the algorithm for designing the STHE is discussed. Later, STHE design is shown after presenting input and output of the Microsoft excel program. Then, the steps followed to fabricate the heat exchanger are discussed. The challenges faced during the fabrication are presented at the end of this chapter.

3.1 Data reduction

In the present work, two different arrangements of tubes or tube banks of STHE as shown in Figure 3.1, were being studied and designed:

1) Aligned or In Line or Square tube arrangement (tube bank) as indicated in Figure 3.1 (a).
2) Staggered or Triangle tube arrangement (tube bank) as indicated in Figure 3.1 (b).

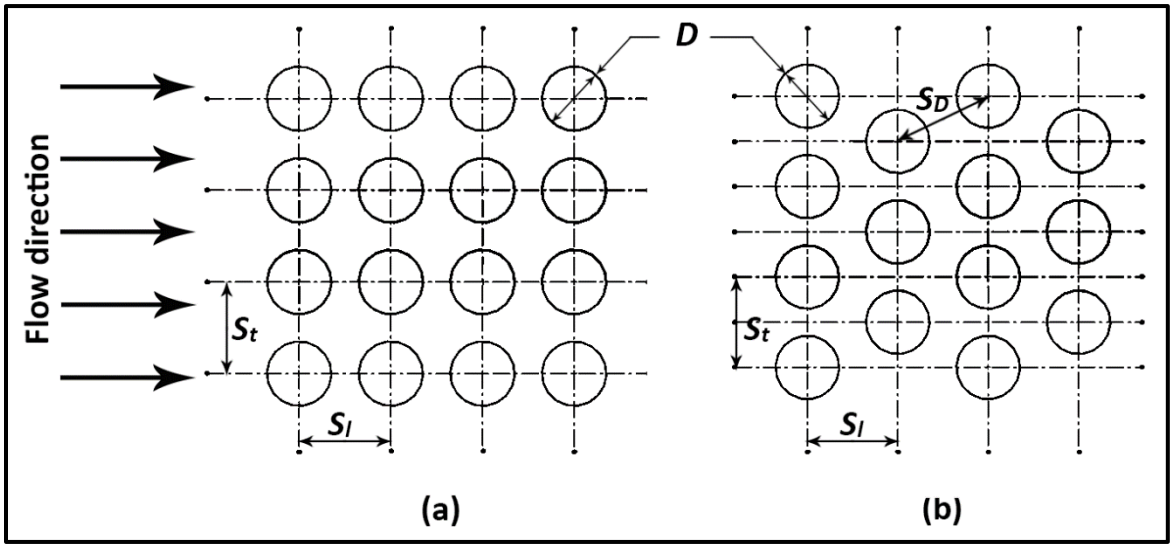

Figure 3.1: Different types of tube arrangements (a) aligned and (b) staggered

At the initial stage of design, water was being considered as working fluid in both shell and tube side for both the arrangements. Property values of water in saturated condition are given in table 3.1.

The design calculations of heat exchanger were made considering the total volume of water to be heated (V_c) as 15 liters. The volume of the heat exchanger (V_{hx}) is considered to be half of total volume of water to be heated.

$$V_{hx} = \frac{2 \times V_t}{3} \tag{3.1}$$

Shell inside diameter to length ratio (L/D_s) is considered to be between 5 to10 **(Kakac et al., 2002)**. Considering the shape of the shell as cylindrical, the volume of the heat exchanger is given in Eq. (3.2).

$$V_{hx} = \frac{\pi}{4} \times D_s^2 \times L \tag{3.2}$$

Where D_s represents shell inside diameter (m) and

L represents tube length (m),

Table 3.2 indicates the values of C and n_1 taken from **(Hewitt, 1998)** for both staggered (triangle) tube arrangement or staggered tube bank and aligned (square) tube arrangement or aligned tube bank.

Transverse tube pitch (S_t) as shown in Figure 3.1, is calculated from Eq. (3.3)

$$S_t = 1.25 * d_o \tag{3.3}$$

Shell hydraulic diameter (d_e) **(Patel et al., 2010)** is being given by

1) For aligned tube bank

$$d_e = \frac{4\left(S_t^{\,2} - (\pi d_o^{\,2}/4)\right)}{\pi d_o} \tag{3.4}$$

2) For staggered tube bank

$$d_e = \frac{4\left(0.43 * S_t^{\,2} - (0.5\pi d_o^{\,2}/4)\right)}{0.5\pi d_o} \tag{3.5}$$

Baffle spacing (pitch): represented by B , is taken as 30 to 70% of the total shell length **(Edwards, 2008)**.

Baffle cuts: It is expressed as the ratio of segment opening height to shell inside diameter and should be kept between 40 to 60%. The upper limit of baffle cut ensures that every 2 consecutive pairs of baffles will support each tube.

Tube Diameters: Commonly used sizes are tubes having diameters ¾" or 1". Mostly ¾" tubes are used for better heat transfer area and provision for cleaning and preventing vibrations. ½ inch tubes can be used for shorter tube lengths i.e. less than 4 feet **(Primo, 2012).**

Table 3.1: The Property Values of water in saturated state (Rohsenow et al., 1973)

Temperature, T (°C)	Density, (kg/m^3)	Kinetic viscosity, (mm^2/sec)	Thermal Diffusivity, (mm^2/sec)	Prandtl number (Pr)	Specific Heat, c (J/kg K)	Thermal Conductivity, k (W/m K)	Dynamic Viscosity, (kg/m sec)
20	1000	1.006	0.1431	7.02	4178	0.5978	0.1006
40	995	0.657	0.1511	4.34	4178	0.628	0.0653715
60	985	0.478	0.1553	3.02	4183	0.6513	0.047083
80	974	0.364	0.1636	2.22	4195	0.6687	0.0354536

Table 3.2: Values of constants C and n_1 (Rohsenow et al., 1973)

No. of passes	Triangle tube pitch		Square tube pitch	
	C	n_1	C	n_1
1	0.319	2.142	0.215	2.207
2	0.249	2.207	0.156	2.291
4	0.175	2.285	0.158	2.263
6	0.0743	2.499	0.0402	2.617
8	0.0365	2.675	0.0331	2.643

Shell cross-sectional area - A_s (m^2) is given in Eq. (3.6)

$$A_s = \frac{\pi D_s^{\,2}}{4} \tag{3.6}$$

Cross-sectional area of baffle - A_b (m^2) is expressed in Eq. (3.7)

$$A_b = 0.75 * A_s \tag{3.7}$$

Shell side cross-sectional area - A_s (m^2), normal to the flow direction is shown in Eq. (3.8)

$$A_s = D_s B\left(1 - \frac{d_o}{S_t}\right) \tag{3.8}$$

Shell side flow velocity v_s (m/sec) **(Selbas et al., 2006)** can be obtained from Eq. (3.9)

$$v_s = \frac{\dot{m}_s}{\rho_s A_s} \tag{3.9}$$

Where $\dot{m}_s$ shows shell side mass flow rate (kg/sec) and

ρ_s indicates density of shell side fluid (kg/m^3),

Shell side Reynolds number - Re_s (unit less) can be obtained as follows,

$$Re_s = \frac{m_s d_e}{A_s \mu_s} \tag{3.10}$$

Shell side fluid Prandtl number - Pr_s (unit less) (can also be obtained from data handbook) which follows

$$Pr_s = \frac{\mu_s C_{ps}}{k_s} \tag{3.11}$$

Where μ_s is the dynamic viscosity of the shell side fluid (Pa sec),

C_{ps} is the specific heat of shell side fluid (J/kg K),

k_s is the thermal conductivity of the shell side fluid (W/m K),

Overall heat transfer coefficient - U (W/m^{2}K) is expressed as

$$U = \frac{1}{(1/h_s) + R_{fs} + (d_o/d_i)\left(R_{ft} + (1/h_t)\right)} \tag{3.12}$$

Where h_s is the shell side convective heat transfer coefficient (W/m^{2}K),

R_{fs} is shell side fouling resistance (m^{2}K/W),

d_o is the outside tube diameter (m),

d_i is the inside tube diameter (m),

R_{ft} is the tube side fouling resistance (m^{2}K/W),

h_t is the tube side convective heat transfer coefficient (W/m^{2}K),

Logarithmic mean temperature difference - $LMTD$ (K), is obtained as

$$LMTD = \frac{(T_{hi} - T_{co}) - (T_{ho} - T_{ci})}{\ln\left((T_{hi} - T_{co})/(T_{ho} - T_{ci})\right)} \tag{3.13}$$

Temperature difference correction factor - F (unit less), can be obtained as follows

$$F = \sqrt{\frac{R^2+1}{R-1}} * \frac{\ln\left((1-P)/(1-PR)\right)}{\ln\left(\left(2-PR+1-\sqrt{R^2+1}\right)/\left(2-PR+1+\sqrt{R^2+1}\right)\right)} \tag{3.14}$$

Where R is the correction coefficient (unit less) and is given by following relation

$$R = \frac{(T_{hi} - T_{ho})}{(T_{co} - T_{ci})} \tag{3.15}$$

P is the efficiency (unit less) and is expressed as follows

$$P = \frac{(T_{co} - T_{ci})}{(T_{hi} - T_{ci})} \tag{3.16}$$

Heat exchanger surface area - A (m^2) is given by

$$A = \frac{\dot{Q}}{U * F * LMTD} \tag{3.17}$$

Heat transfer rate - $\dot{Q}$ (W) is given by

$$\dot{Q} = \dot{m}_h C_h (T_{hi} - T_{ho}) = \dot{m}_c C_c (T_{co} - T_{ci}) \tag{3.18}$$

Number of tubes - N_t (unit less) is given by,

$$N_t = C \times \left(\frac{D_s}{d_o} \right)^{n_1} \tag{3.19}$$

The number of tubes is finally rounded off to the lower even number.

Tube side fluid velocity - v_t (m/sec) is calculated from Eq. (3.20).

$$v_t = \frac{\dot{m}_t}{(\pi / 4) d_t^2 \rho_t} \left(\frac{n}{N_t} \right) \tag{3.20}$$

Where $\dot{m}_t$ is the tube side mass flow rate(kg/sec),

d_i is the tube inside diameter(m),

ρ_t is the density of the tube side fluid (kg/m^3),

n is the number of tube passes (unit less),

N_t is the nuber of tubes (unit less)

The tube side Prandtl number - Pr_t (unit less) and is given by

$$Pr_t = \frac{\mu_t C_{pt}}{k_t} \tag{3.21}$$

Where μ_t is the dynamic viscosity of the tube side fluid (Pa sec),

C_{pt} is the specific heat of tube side fluid (J/kg K),

k_t is the thermal conductivity of tube side fluid (W/m K),

Tube side heat transfer coefficient -h_t (W/m^{2}K), can be calculated from the following correlation depending upon Reynold's number (Re_t) of the tube side **(Caputo et al., 2008)**:

a. If $Re_t < 2300$:

$$h_t = \frac{k_t}{d_i}\left[3.657 + \frac{0.0677(Re_t\, Pr_t(d_i/L))^{1.33^{1/3}}}{1+0.1Pr_t(Re_t(d_i/L))^{0.3}}\right] \tag{3.22}$$

b. If $2300 < Re_t < 10000$

$$h_t = \frac{k_t}{d_i}\left[\frac{(f_t/8)(Re_t - 1000)Pr_t}{1+12.7(f_t/8)^{1/2}(Pr_t^{2/3}-1)}\left(1+\frac{di}{L}\right)^{0.67}\right] \tag{3.23}$$

c. If $Re_t > 10000$

$$h_t = 0.027\frac{k_t}{d_o} Re_t^{0.8}\, Pr_t^{1/3}\left(\frac{\mu_t}{\mu_{wt}}\right)^{0.14} \tag{3.24}$$

Where f_t is Darcy's friction factor **(Hewitt, 1998)** and is given by

$$f_t = \left[1.82 * log_{10}(Re_t) - 1.64\right]^{-2} \tag{3.25}$$

Tube side Reynold's number - Re_t (unit less) and can be obtained from

$$Re_t = \frac{\rho_t v_t d_t}{\mu_t} \tag{3.26}$$

Shell side cross-sectional area - A_s (m^2) is given by

$$A_s = \frac{\pi D_s^{\,2}}{4} \tag{3.27}$$

Tube length - L (m) can be calculated from Eq. (3.28) as,

$$L = \frac{A}{\pi d_o N_t} \tag{3.28}$$

A simple program was developed in Microsoft Excel using Equation (3.1) to Equation (3.28) to design a shell and tube heat exchanger. The input and the final output of the program after number of trials, are given in Table 3.3 and Table 3.4.

Table 3.3: Input to the program: Heat Exchanger design input data

Parameters	**Tube Pitch**		**Unit**
	Staggered Grid	**Aligned Grid**	
Total volume of sugarcane juice to be heated	15	15	Litre
The volume of the heat exchanger (V_{hx})	5	5	Litre
Shell Length to diameter ratio (L / D_s)	7.5	7.5	Unit less
Tube side inlet fluid temperature (T_{hi})	85	85	℃
Shell side inlet fluid temperature (T_{ci})	20	20	℃
Tube side mass flow rate (m_t)	150	150	kg / hr
Mass flow rate of the shell side fluid (m_s)	200	200	kg / hr
No. of tube passes (n)	1	1	Unit less
Correction Factor from data hand book (F)	0.93	0.93	Unit less

Table 3.4: Output from the program: Calculated parameters

Parameters	Tube Pitch		Unit
	Staggered Grid	Aligned Grid	
Shell inside diameter (D_s)	10.47	10.47	cm
Shell length (L)	71.01	71.01	cm
Tube inside diameter (d_i)	11.00	11.00	mm
Tube outside diameter (d_o)	12.50	12.50	mm
Baffle spacing (B)	0.25	0.25	m
Tube side Reynolds number (Re_t)	307.40	388.30	Unit less
Reynold's number for shell (Re_s)	145.13	201.99	Unit less
Overall heat transfer coefficient (U)	167.16	165.57	$\mathrm{W/m^2K}$
Heat Transfer rate (Q)	4.51	3.88	kW
Heat transfer area, sq. meter	0.67	0.53	$\mathrm{m^2}$
Temp difference at inlet $((\Delta T)_{inlet})$	65.00	65.00	℃
Temp difference at outlet $((\Delta T)_{outlet})$	19.62	26.04	℃
Temp lost by hot fluid $((\Delta T)_h)$	25.93	22.26	℃
Temp gain by cold fluid $((\Delta T)_c)$	19.45	16.70	℃
Calculated correction factor (F)	0.29	0.24	Unit less
Effectiveness (ε)	0.40	0.34	Unit less
Tube side outlet fluid temperature (T_{ho})	59.07	62.74	℃
Shell side outlet fluid temperature (T_{co})	39.45	36.70	℃
Logarithmic Mean Temperature Difference $(LMTD)$	42.23	45.46	Unit less
Heat exchanger surface area (A)	0.69	0.55	$\mathrm{m^2}$
No. of tubes (N_t)	24	19	Unit less

3.2 Heat exchanger design

Shell and tube heat exchanger (STHE) 3D geometry was created in Solidworks using the optimised design parameters obtained from the MS Excel program presented in

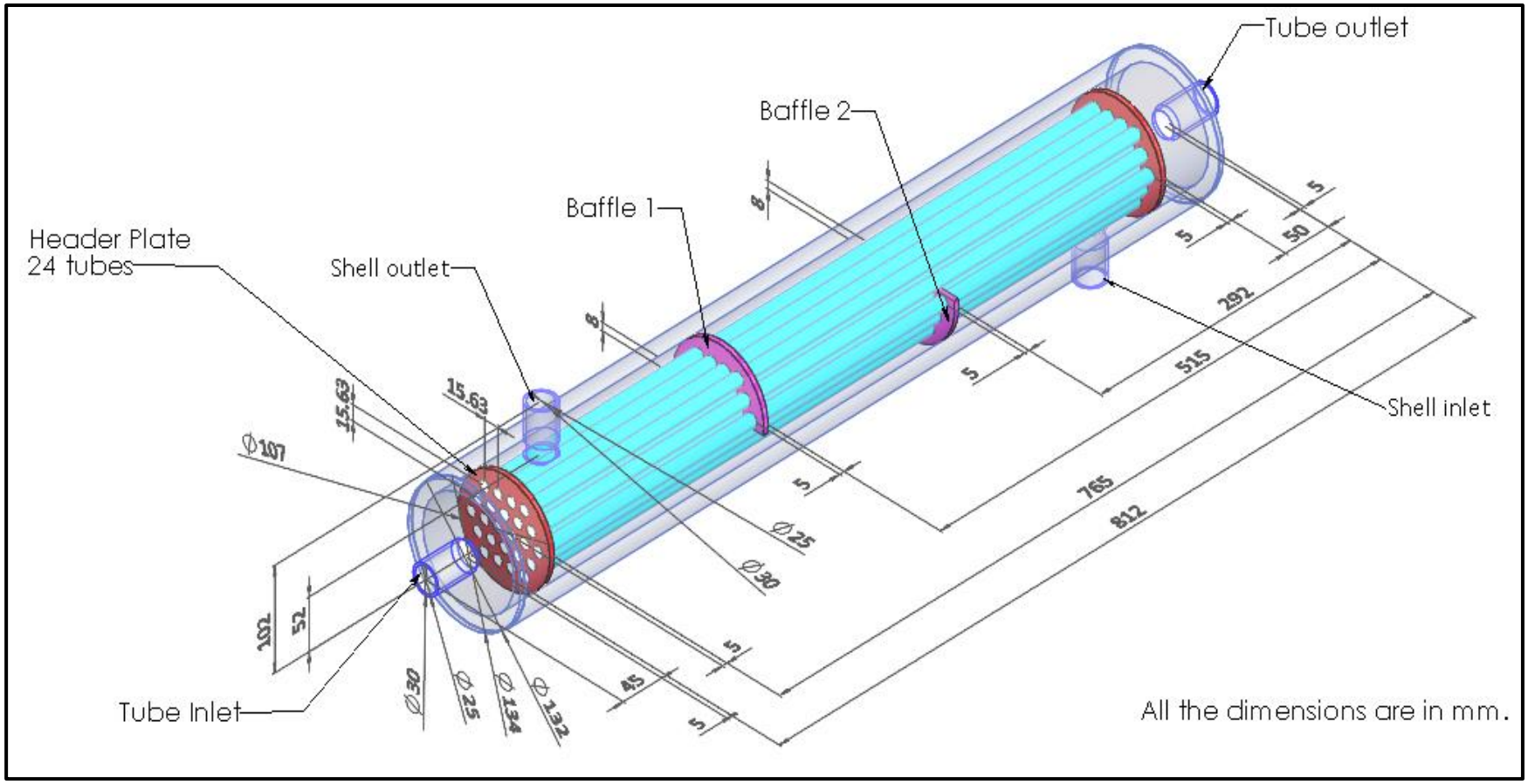

Figure 3.2: Heat exchanger isometric view by keeping the shell part partially transparent

Table 3.3 and Table 3.4 of section 3.1. The complete assembly of STHE in 3D view is shown in Figure 3.2.

3.3 Fabrication of heat exchanger

The fabrication of heat exchanger was carried outside of MNIT, Jaipur. The steps followed during fabrication are as follows:

i. Baffles plates and header plates are attached all together using light welding. This process ensures
    a. Alignment of the drilled holes with each other,
    b. No mismatching of the holes in any of the plates during drilling process.
ii. One holder is attached with the plates for the purpose of holding it better during the drilling process.
iii. Points where the drilling of holes to be done for placing tubes, were marked with the help of a marker as shown in Figure 3.3.
iv. Using a center punch (shown in Figure 3.4 with a tip angle of 60° to 90°), the centers for the holes were marked. These centers stop the wandering tendency of the drill.

Figure 3.3: Marking of the plates

Figure 3.4: Centre Punch (Allant, 2008)

Figure 3.5: Drilling of the plates

Figure 3.6: Plates after drilling

Figure 3.7: after grinding or finishing of the plates

Figure 3.8: Grinder (GmbH, 2017)

v. The plates are then drilled using the drilling machine as shown in Figure 3.5. The plates after drilling are shown in Figure 3.6.

vi. Grinding operation was being carried out using a small angled grinder (Figure 3.8) in order to remove any metal chips left on the plates after the drilling operation as in Figure 3.7.

vii. Before separating the plates, the finishing of the plates is carried out in such a way that it fits inside the shell pipe without mismatching of the holes using lathe machine.

viii. Baffle plates are cut according to the required size as shown in figure 3.10.

ix. The baffle plates are inserted inside the shell one by one as shown in Figure 3.11. Tubes were inserted inside the baffle plates to ensure the proper alignment of the holes. Point welding at 2/3rd joining points of baffle plates and shell pipe, is done so that when tubes are removed to weld the baffle plates with shell, there will not be misplacing and misalignment of the baffle plates.

Figure 3.9: After separating all the plates

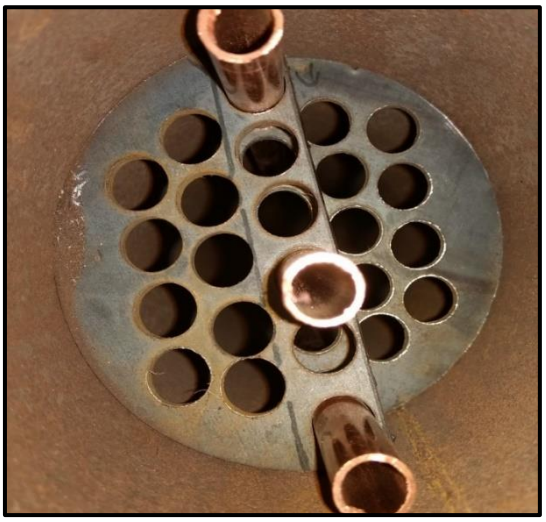

Figure 3.11: Inserting the baffle plates in the shell

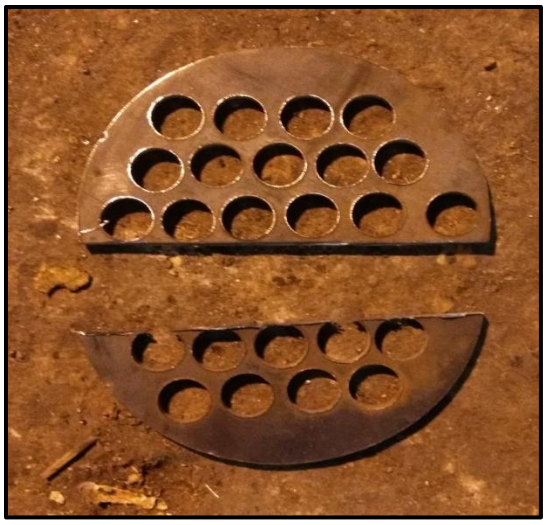

Figure 3.10: Baffle plate after cutting

Figure 3.12: After welding one baffle plate

Figure 3.13: After welding of both the baffle plates

Figure 3.14: Inserting the main plate

x. Similarly, the header plates are being placed inside the shell and their alignment is being checked by placing the tubes inside the header and baffle plates as shown in Figure 3.14. Similar to the baffle plates point welding, 3/4 point welds are done to ensure the alignment and place of the header plates. After removing the tubes, gas welding is done properly at the joining circle of header plate and shell. As this plate separates the shell fluid and tube fluid therefore proper welding needs to be carried out.

Figure 3.15: After welding of the main plate

Figure 3.16: After insertion of the Copper (*Cu*) Tubes

Figure 3.17: After gas tungsten arc welding of the Copper (*Cu*) tubes

Figure 3.18: Outside view of the header

xi. The copper tubes are then cut a little longer (0.5 cm) than the actual size. The copper tubes are then inserted into the shell through the header plates and baffles. While gas welding of *Cu* tubes with the cast iron header plate, the tubes should not move therefore their mouth is being punched.

xii. After making the hole using the drill machine for the connector pipe, the main plate is welded to the connector pipe. The main plate is then welded to the shell.

xiii. The hole for the shell inlet and outlet are being made using the drill machine. And connector for shell inlet and outlet are connected to these holes as shown in Figure 3.19 and 3.20.

Figure 3.19: Inside view of the header

Figure 3.20: Inlet or outlet to the shell

Figure 3.21: Putting insulation and cover

Figure 3.22: Top view of the heat exchanger

Figure 3.23: Front view of the heat exchanger

xiv. A sheet (aluminium) is required to hold the insulation material (glasswool). Therefore first the sheet is led on the floor and heat exchanger is kept on it. Then the insulation is put on it as required thickness as shown in Figure 3.21. Then it is covered with the sheet and hold with the help of 3/4 screws. And on the sides cover sheet is folded.

xv. The final heat exchanger is shown in Figure 3.22 and 3.23.

3.4 Challenges faced during fabrication process

In many of the practical applications, brazing is commonly used to weld components made with the Copper (*Cu*) material. The brazing operation should be continuous to make leak-proof joint between the dissimilar materials. Heat exchanger manufacturing in the present work involves many joints which are to be done at different locations. This joining operation by brazing is discontinuous which may lead to direct mixing of both shell and tube side fluids. Therefore, after thorough literature and market survey on Copper joints, it was decided to weld the Copper to the Cast Iron by using Tungsten arc welding (GTAW) process **(Daniel et al., 2016)**.

Chapter 4 DEVELOPMENT OF EXPERIMENTAL SETUP

The experimental process of shell and tube heat exchanger being tested for any leakages is initially described in this chapter. Then the experimental setup of heat recovery unit i.e. the combination of Evacuated Tube Solar Collector (ETSC) and Shell and Tube Heat Exchanger (STHE) and their specifications expressed under development of experimental setup is being described. The experimental procedure adopted and instrumentation used is discussed in the subsequent sections of this chapter.

An experimental setup of heat recovery unit i.e. ETSC and STHE systems have been developed at the rooftop of the Mechanical Engineering Department, M.N.I.T., Jaipur (Rajasthan, India) for the analysis. Jaipur is situated in the eastern side of Rajasthan state, which is the western part of India and its geographic and weather details are mentioned in Table 4.1.

Table 4.1: Geographical and weather data of Jaipur (ISHRAE, 2014)

S. No.	Parameters	Details
1	Latitude	N 26°49`
2	Longitude	E 75°48`
3	Altitude	390.00 m
4	Annual maximum temperature	43.6 ℃
5	Annual minimum temperature	5.5 ℃
6	Average direct normal irradiance	5.56 $kWhr/m^2/day$

4.1 Description of the experimental setup

The heat recovery unit consists of 1) ETSC used for heating of primary fluid (water) as shown in Figure 4.1(a), and 2) STHE for exchanging heat in primary fluid to secondary fluid as shown in Figure 4.1(b). Therefore both the components ETSC and STHE and their experimental setups are discussed separately:

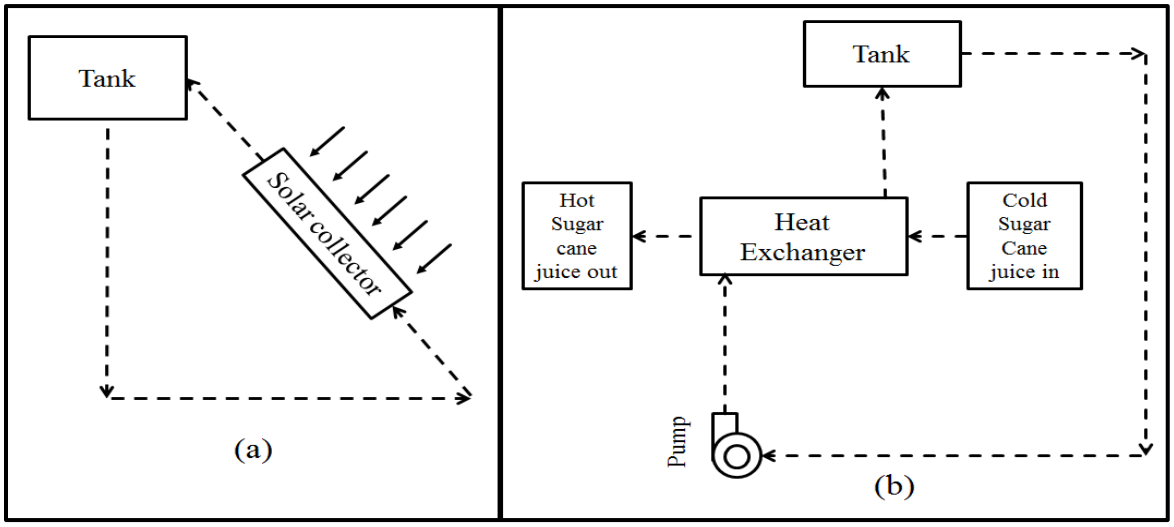

Figure 4.1: Block diagram of experimental procedure (a) Heating of primary fluid with the help Evacuated Tube Solar Collector and (b) Exchange of this heat to the secondary fluid with the help of Shell and Tube Heat Exchanger

4.1.1 Evacuated tube solar collector

The ETSC specifications are given in Table 4.2. The locations of all the temperature sensors used during experimentation are represented in Figure 4.2.

Table 4.2: Specification of Evacuated Tube Solar Collector

Specifications	**Unit**	**Details (explanation)**
Collector gross area	m^2	1.45 (1.70*0.855)
Collector absorber area	m^2	0.986 (1.70*0.058*10)
Collector aperture area	m^2	0.731 (1.70*0.043*10)
Evacuated tube length (total)	m	1.80
Evacuated tube length (exposed to solar radiation after installation)	m	1.70
Max. operating pressure	kg/cm^2	0
Temperature working	K	283-372
Collector angle	Degree(°)	30
Absorber		Aluminium
Absorption (α)/emission (ε)		0.96/0.06
Collector housing		Aluminium
Collector glazing		Evacuated tubes (borosilicate glass)
Number of tubes		10 evacuated tubes
Outer glass tube diameter	cm	5.8
Inner glass tube diameter	cm	4.3
Sealing material		Silicone
Frame material		Stainless steel

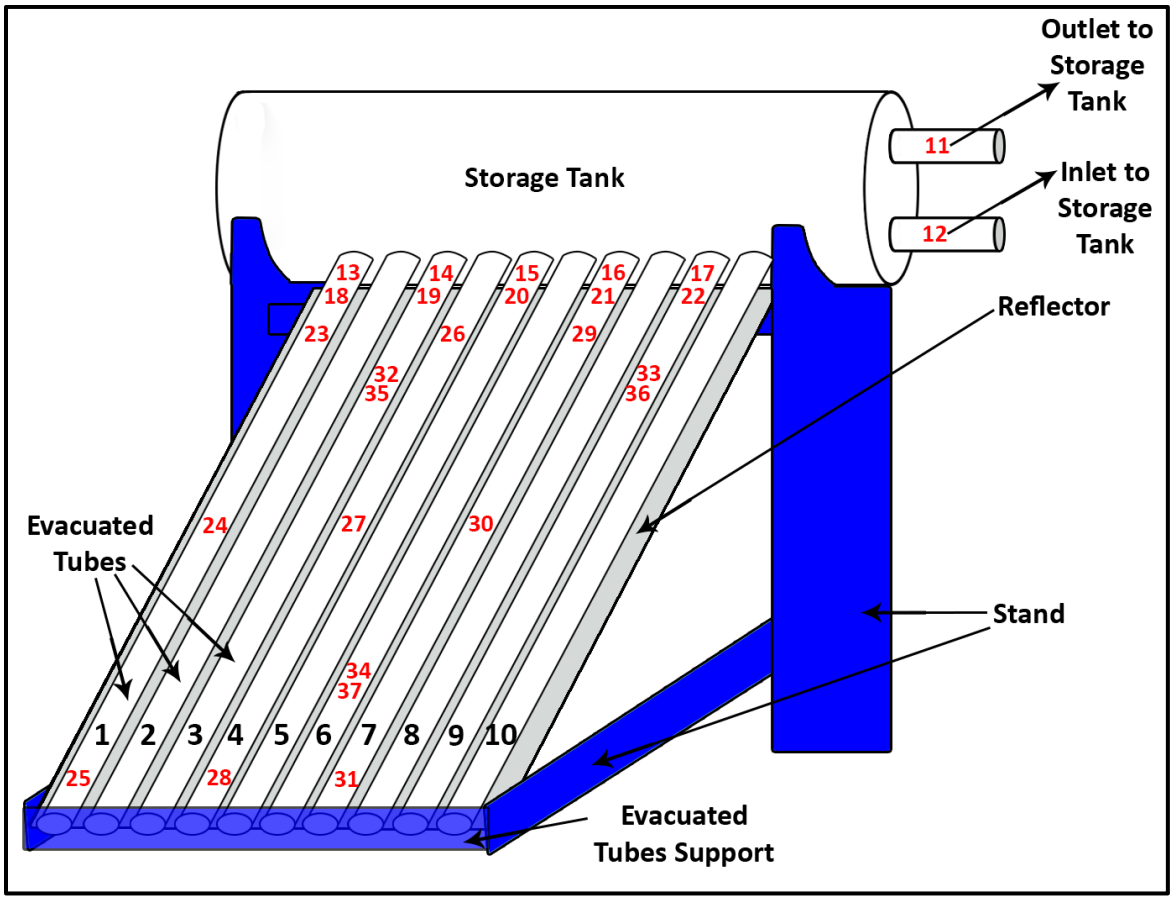

Figure 4.2: Schematic view of evacuated tube solar collector showing location of temperature sensors

The details of the temperature sensors are indicated in Table 4.3. An evacuated tube with inlet and outlet temperature sensors is presented in Figure 4.3.

Table 4.3 Notation of temperature sensors used in Evacuated Tube Solar Collector

Numbering	Representing
1-10	Numbering of evacuated tubes
11, 12	Inlet and outlet of storage tank temperature
13-17	Outlet temperatures of evacuated tube no - 1,3,5,7,9
18-22	Inlet temperatures of evacuated tube no - 1,3,5,7,9
23-25	Outer surface temperatures of evacuated tube 1
26-28	Outer surface temperatures of evacuated tube 6
29-31	Upper surface temperatures of reflector sheet
32-35	Lower surface temperatures of reflector sheet

Figure 4.3: An evacuated tube with inlet and outlet temperature sensors

4.1.2 Shell and tube heat exchanger

Shell and tube heat exchanger specifications are shown in Table 4.4. The schematic diagram of the experimental setup and location of the temperature sensors are shown in Figure 4.4.

Table 4.4: Heat exchanger specification

Part	Specification	Detail	Material
Tube side	Tube Pitch	Staggered grid	Copper (*Cu*)
	No. of tube passes (n)	1	
	No. of tubes (N_t)	24	
	Tube inside diameter (d_i) [mm]	11.00	
	Tube outside diameter (d_o) [mm]	12.50	
Shell side	Shell length (L) [cm]	71.0	Mild steel (M.S.)
	Shell inside diameter (D_s) [cm]	10.7	
	Shell outside diameter [cm]	11.2	
Baffle	Baffle spacing (B) [cm]	22.3	Mild steel (M.S.)
Insulation	Thickness [cm]	1	Glass wool
Cover	Thickness [mm]	1	Aluminium sheet

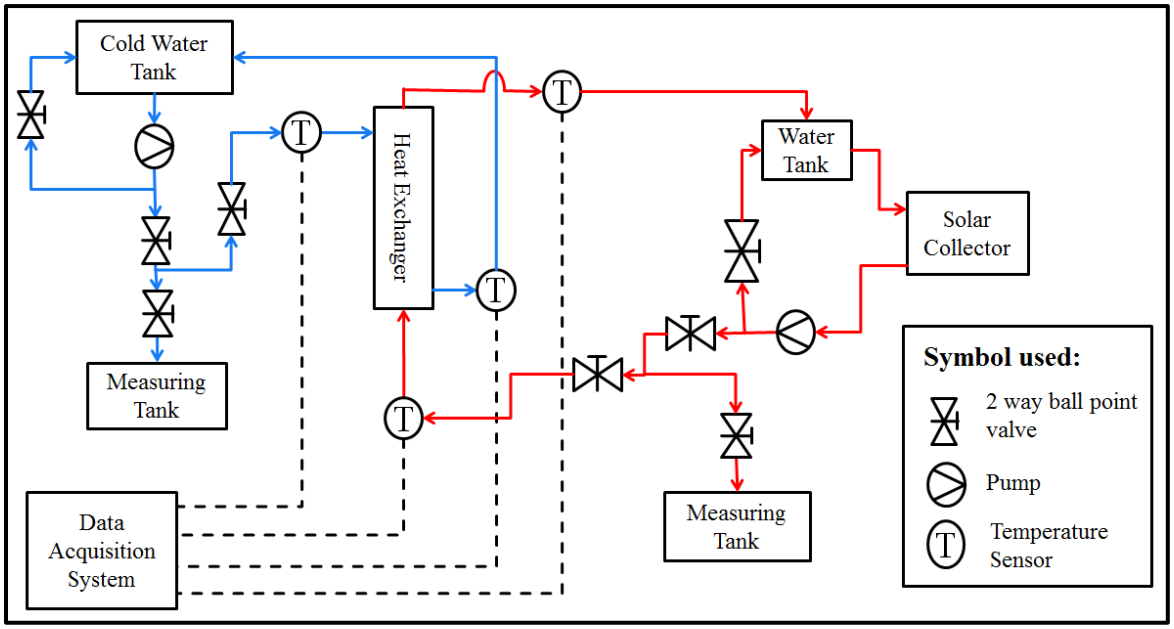

Figure 4.4: Schematic diagram of the experimental setup of the heat exchanger.

4.1.3 Pump, tank and connecting pipe specification

The specifications of pump, tank and connecting pipes used, are presented in Table 4.5.

Table 4.5: Specification of pump, tank and connecting pipes

Specification	Detail	Remark
Pump	Make : Alpha	50 W / Head 25 Feet, quantity 2
Tank	Capacity 25 liters	Overhead tank
	Capacity 25 liters	Measuring tank
	Capacity 30 liters	Cold fluid tank
Piping	CPVC and flexible pipe	¾ inch CPVC pipe and ½ inch flexible pipe
Flow control valve	Ball type	¾ inch diameter CPVC
Frame or Stand	Mild steel (M. S.)	Height (1 meter), quantity 2
Insulation of pipes	Nitrile sleeves	¾ inch diameter

The complete experimental setup is shown in Figure 4.4.

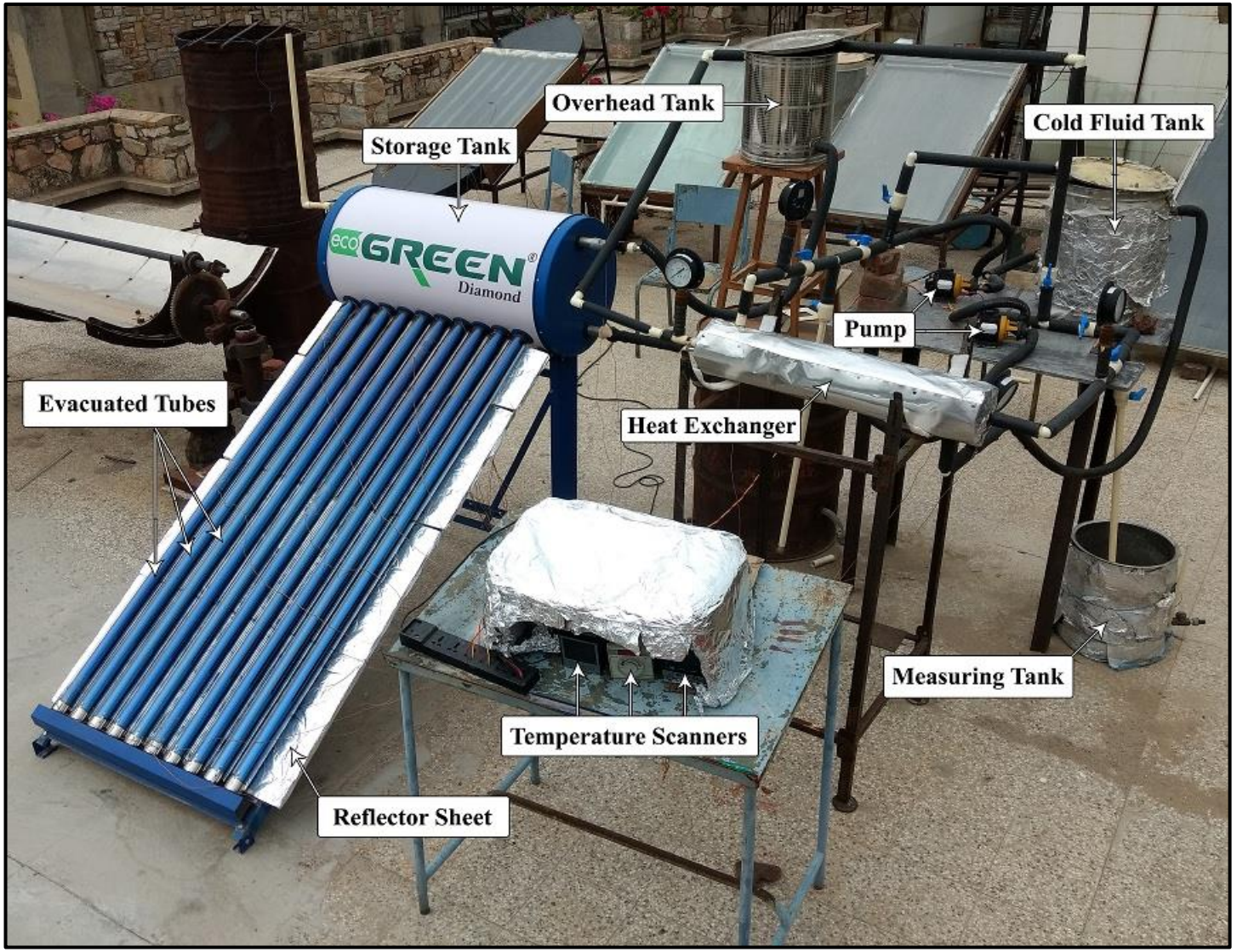

Figure 4.5: Experimental Setup

4.2 Experimental procedure

The experiment was divided into two parts depending upon the two separate processes as indicated in Figure 4.1 and is discussed as follows:

i. Experimental study on Evacuated Tube Solar Collector (ETSC)
   a) Turn on the pump in the morning at around 8:30 AM to circulate water in the overhead and storage tank until the temperature of water collected in the storage tank becomes uniform.
   b) Once the water is filled the pump is turned off.
   c) Uncover the evacuated tubes.
   d) Observe the readings of solar intensity, temperatures of ambient air, evacuated tubes inlet and outlet, storage tank inlet and outlet, reflector sheet upside and downside, and temperature of the evacuated tube surface.
   e) Repeat the step 4 for every 30 minutes till the evening 5:00 PM.
   f) Cover the evacuated tubes.
   g) Plot the records in a graph.

ii. Experimental study on Shell and Tube Heat Exchanger (STHE)
   a) Switch on the hot fluid pump.
   b) Measure and adjust the mass flow rate of the hot fluid to the required mass flow rate.
   c) Switch off the hot fluid pump.
   d) Similarly, repeat the steps 1, 2 and 3 to adjust the cold fluid mass flow rate.
   e) Start both hot fluid and cold fluid pumps.
   f) Observe the temperature reading for every 3 minutes and finally note down all the temperature readings once the cold fluid temperature reaches the steady state.
   g) Switch off both the pumps.
   h) Plot the records in a graph.

4.3 Instrumentation

Instruments used during the experiment for the measurement of various quantities such as temperature, air velocity, solar irradiance, etc., are described as follows:

4.3.1 Thermocouple

Thermocouples are widely used type of temperature sensors. They work on the principle of two effects **(Beckwith, et al., 2006)**:

i. Seebeck (Thomson) effect: States that when two dissimilar metals are joined at two different junctions, an electromotive force (emf) is generated between the two junctions. Different combination of the metals generates different amounts of emf.
ii. Peltier effect: Due to the difference in temperatures of the two junctions, an emf is generated within the circuit.

In most of the cases, the emf generated by the Seebeck (Thomson) effect is very small and it can be neglected. Therefore, thermocouples using Peltier effect are common in commercial applications. The emf or voltage generated in thermocouples is very small and generally is in micrometers (μm). The current flowing due to the emf or voltage generated across the junctions can be measured by using temperature scanners. The temperature at one junction is measured by considering another end temperature as the reference value.

Different types of thermocouples like J, K, T, E, R, S, B, etc., are commercially available in the market. Type T (copper-constantan) thermocouples are nickel alloy based thermocouples. Since both the conductors are non-magnetic in nature, therefore, there is no Curie point and there is no abrupt change in its characteristics in its working range. In the current study, T type thermocouples are used for measuring temperatures. T-type thermocouples can measure temperature in the range of -270℃ to 370℃ (-380°F to 392 °F) with a sensitivity of about $43 \mu V / °C$.

The thermocouples were calibrated in the operating range 15-90$℃$ with the help of Fluke 1586A Super-DAQ Precision Temperature Scanner (as shown in Figure 4.5). The calibration results are presented in Appendix B.

Figure 4.6: Calibration of the temperature sensors using Fluke 1586A Super-DAQ Precision Temperature Scanner

4.3.2 Weather station

A weather station is a set of instruments for measuring climatic conditions to provide weather data. As shown in Figure 4.6, a weather station is located at the top of MNIT Director's office which records the surrounding air temperature, relative humidity, wind velocity and solar radiation at an interval of 15 minutes and sends this recorded data at http://www.moinee.com/mnit/.

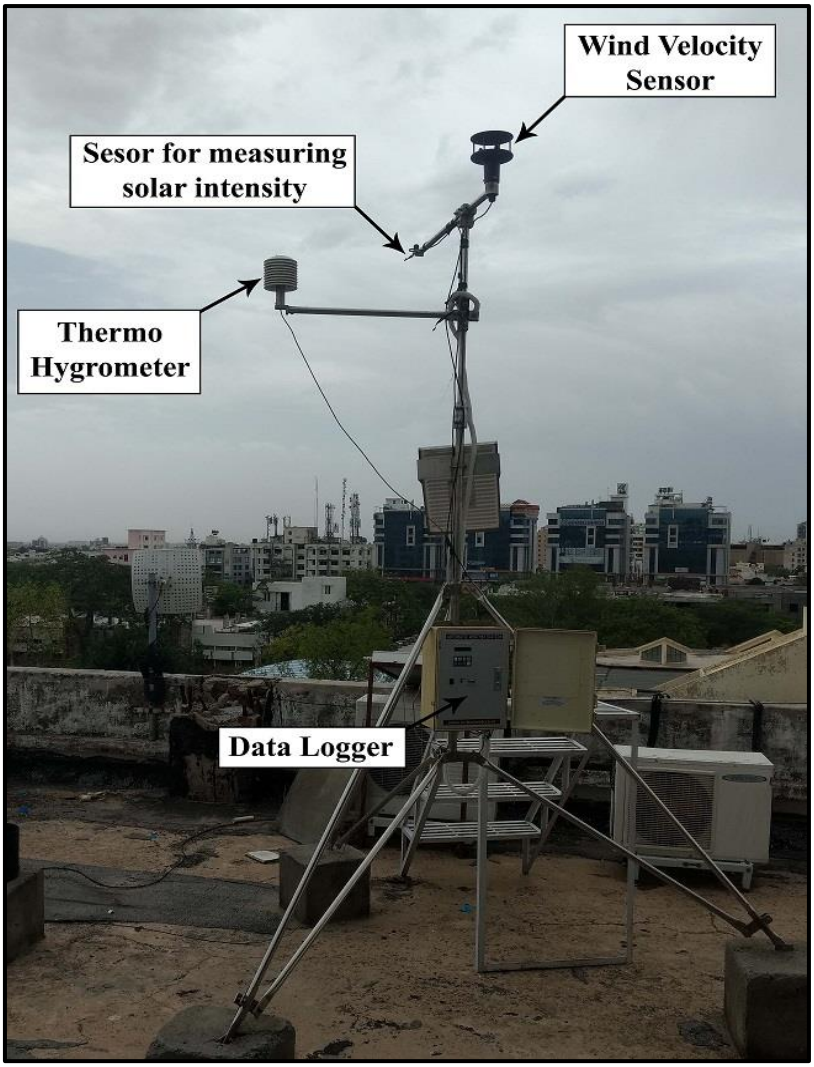

Figure 4.7: MNIT weather station

4.3.3 Temperature scanners

Different temperature scanners were used to show or indicate the temperature detected by the thermocouples. In the present study following digital scanners were used:

Table 4.6: Specifications of the temperature scanners

Make	Multispan	Multispan	Masibus
Model no	MS-1208	MDI-1106	8208
Channel	8	6	8
Resolution	1℃	1℃	0.1/1℃
Quantity used	2	1	1

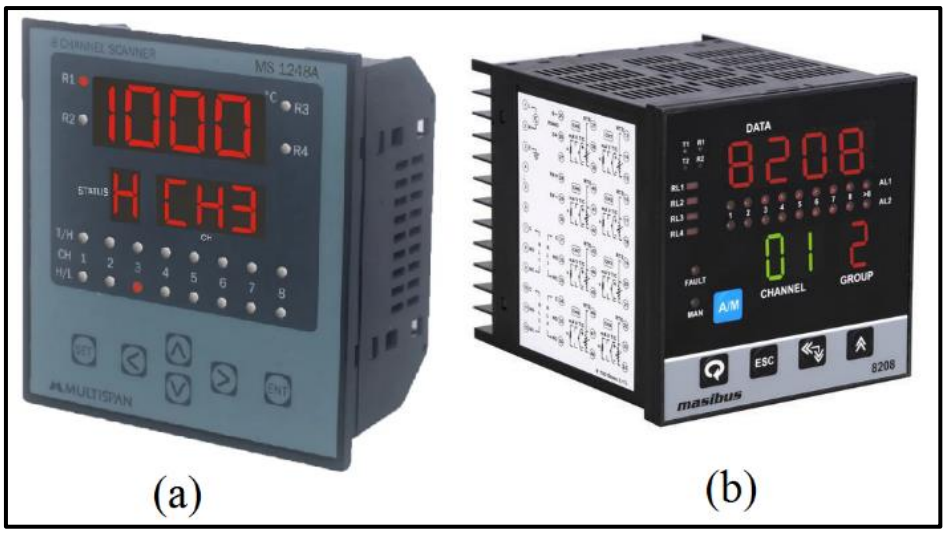

Figure 4.8: Scanners (a) Multispan MS 1208 (b) Masibus 8208

4.4 Problems faced during experimentation

In case of ETSC, the thermocouple wires used to measure the inlet and outlet temperature of evacuated tubes, were taken out through the storage tank. The temperature readings were affected by the hot water present in the storage tank. Therefore, the thermocouple wire was drawn out with the evacuated tubes as shown in Figure 4.9(b). It arose the leakage problem but the temperature readings were more accurate.

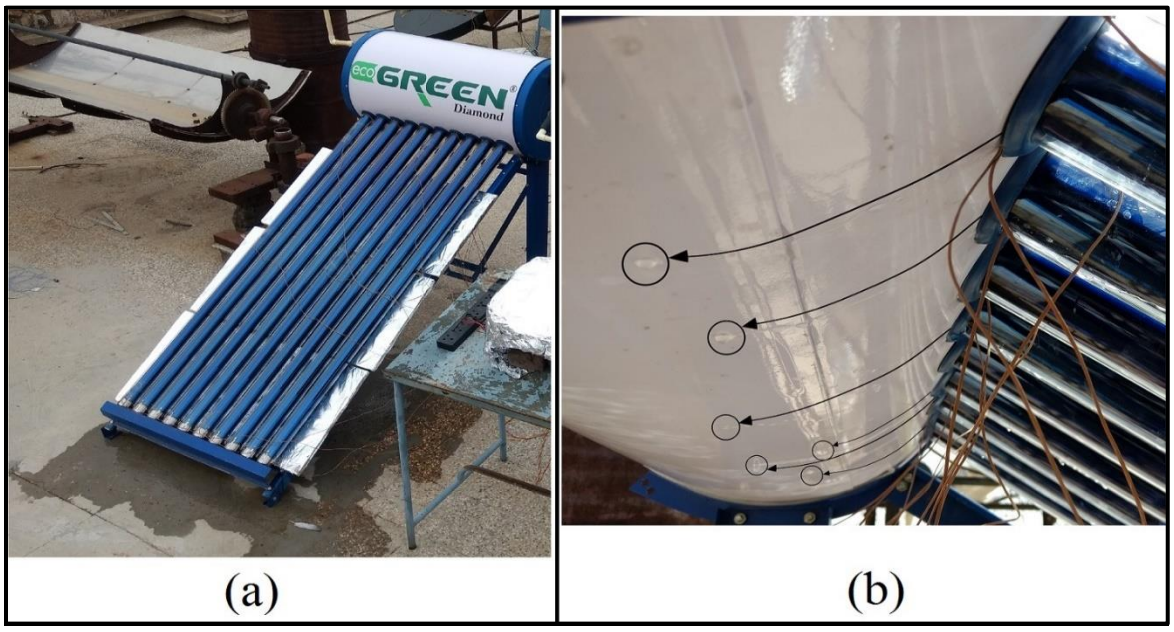

Figure 4.9: Leakage from tubes

Chapter 5 DATA COLLECTION AND ANALYSIS

The experimental setup was built at the rooftop of Mechanical Engineering Department building of M.N.I.T., Jaipur (Rajasthan, India), as shown in Figure 5.1. Experiments were carried to find out the thermal performance of solar based heat recovery unit. Initially the Evacuated Tube Solar Collector (ETSC) was operated to produce hot water (primary fluid). Heat stored in hot water is transferred to the secondary fluid (water or sugarcane juice) using a Shell and Tube Heat Exchanger (STHE). The thermal performance of heat recovery unit was calculated as the ratio of heat absorbed by the secondary fluid in STHE to the heat collected by the primary fluid in ETSC. Experimental results obtained are presented in this Chapter.

5.1 Experimental results of evacuated tube solar collector

In order to carry out the experiment ETSC was run for 25 days same as the STHE. The readings were also taken for 25 days but as there was no variation in the any parameter other than solar radiation, air velocity. Therefore, all the graphs are also similar throughout the experimental work. Therefore, here one day experimental results are shown in Appendix A.3.The useful data are indicated in Table 5.1.

The thermal efficiency of a solar collector is its quality to convert incident solar radiation into thermal energy. Efficiency can shift depending upon the solar radiation, outside temperature, and encompassing temperature. The thermal efficiency is calculated from the following mathematical statement:

$$\text{Thermal efficiency} = \frac{\text{Useful solar energy}}{\text{Total incident solar energy}} \tag{5.1}$$

Or it can be expressed as

$$\eta = \frac{Q_u}{A_c I} \tag{5.2}$$

Table 5.1: Variation of different parameters of Evacuated tube solar collector on 4th June 2017

Time	Evacuated tube temperature	Storage tank temperature	Evacuated tube surface temperature	Reflector sheet upper temperature	Reflector sheet lower surface temperature	Ambient temperature	Solar Intensity
9:00	57	57.5	42.8	30.4	28.4	31.87	368
9:30	61	58.5	44.1	31.6	29.6	32.32	425
10:00	65	60.5	45.3	32.2	30.2	33.21	475
10:30	69	62	45.6	32.7	30.7	32.68	538
11:00	71	63.5	46.2	33.9	31.9	33.01	608
11:30	72.6	65	46.8	35.1	33.1	33.96	654
12:00	74.9	67.5	47.2	36.3	34.3	34.99	686
12:30	77.2	69	48.2	36.8	34.8	35.73	690
13:00	79	71.5	48.3	38	36	36.39	724
13:30	80.1	72.5	49.5	39.2	37.2	36.61	756
14:00	82.8	73.5	43.5	39.8	37.8	37.64	752
14:30	82.3	75	42.3	40.3	38.3	37.51	728
15:00	83.9	76.5	42	40.8	38.8	37.69	673
15:30	81	77.3	42.5	40	38	38.02	509
16:00	76.4	77	44.8	42	40	38.13	552
16:30	76.1	76.5	44.7	41.3	39.3	37.98	480
17:00	77.6	76.3	43.5	40.5	38.5	37.65	414

5.2 Performance analysis of evacuated tube solar collector

Variations of temperatures including temperatures of evacuated tube, storage tank, evacuated tube surface, ambient, reflector sheet top and bottom surfaces, with respect to time is represented in Figure 5.1. It was observed that the temperature of the liquid in the storage tank is constantly increasing with time and reaching to its maximum by the evening 17:00 hrs even though the solar intensity is observed to be decreasing after 14:00 hrs.

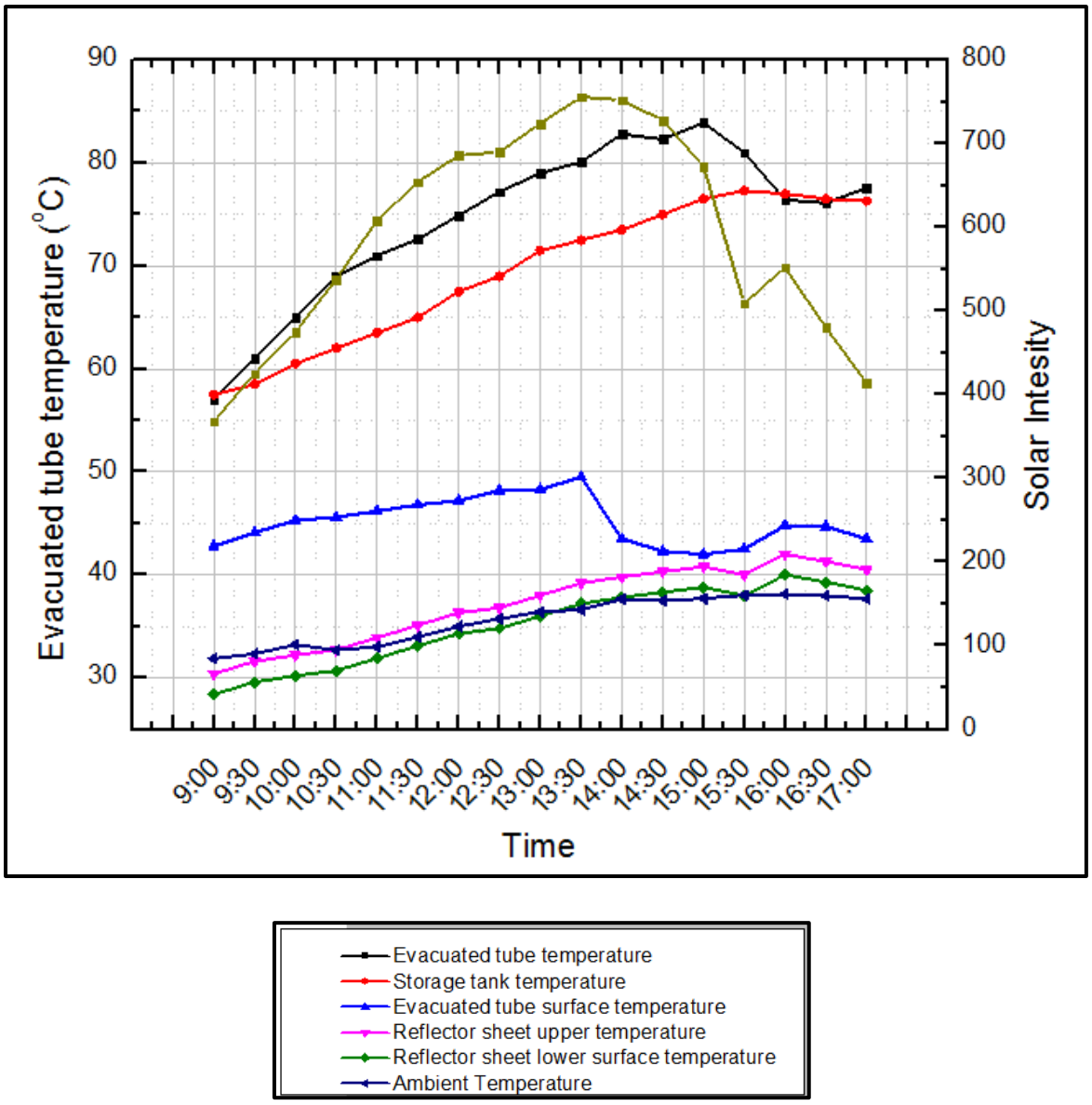

Figure 5.1: Evacuated tube solar collector (a) Variation of different parameters w.r.t. time (b) notations used

The useful solar energy (Q_u) is given by equation 5.3

$$Q_u = MCp\left(T_{out} - T_{in}\right) \tag{5.3}$$

Therefore efficiency can be rewritten as follows:

$$\eta = \frac{MCp\left(T_{out} - T_{in}\right)}{A_c G} \tag{5.4}$$

$\eta = 63.28\%$

For the given experimental results the efficiency was found to be 63.28%.

The efficiency of the Evacuated Tube Solar Collector (ETSC) was found to be changing from 55 to 68%, depending on the availability of solar radiation, clouds and other factors.

5.3 Experimental results of shell and tube heat exchanger

The primary fluid (water) at higher temperature from ETSC exit is allowed to flow through the STHE and heat is transferred to the secondary fluid (water or sugarcane juice) in the STHE. The primary fluid flows through the tubes and secondary fluid flow through the shell of the STHE. The secondary fluid is circulated again and again through the STHE until and unless the temperature difference between inlet temperature of tube fluid and exit temperature of shell fluid becomes more or less equal. Experiments were carried out by changing the tube fluid and shell fluid mass flow rates to different values.

The effectiveness of STHE is defined as the ratio of actual heat transferred between the tube and shell fluids to the maximum heat that can be transferred between the two. It is given by,

$$\varepsilon = \frac{\dot{Q}_{avg}}{\dot{Q}_{\max}} = \frac{\dot{Q}_{avg}}{\left(\dot{m}c\right)_{\min}\left(T_{hi} - T_{ci}\right)} \tag{5.5}$$

In Equation 5.1, $\dot{Q}_{avg}$ is the average heat transferred between the tube and shell side fluids and is equal to the average of heat lost by the tube side fluid and the heat gained by the shell side fluid.

5.3.1 Experiment on 28th April 2017:

Initially, the mass flow rate of hot fluid ($\dot{m}_h$) and cold fluid ($\dot{m}_c$) were kept at 60 kg/hr. Variations of inlet and outlet temperatures of hot and cold fluids with respect to the time are given in Figure 5.2 (a). Logarithmic Mean Temperature Difference (*LMTD*), Effectiveness (ε), heat lost by hot fluid, $\dot{Q}_h$, heat gained by the cold fluid, $\dot{Q}_c$ and average heat transfer rate between the fluids ($\dot{Q}_{avg}$) of the STHE are calculated using the temperature values. Variations of $\dot{Q}_h$, $\dot{Q}_c$, $\dot{Q}_{avg}$ with respect to time and variations of *LMTD*, ε with respect to time are shown in Figure 5.2 (b) and (c) respectively. The hot fluid Reynold's number (Re_h) was found to be 122.96 and for cold fluid (Re_c) was found to be 43.75 with the set mass flow rates of the fluids. It was observed that the temperature difference between hot fluid inlet and cold fluid exit of the STHE is continuously decreasing with time from a maximum value of 18.2 ℃ at 17:57 hours to a minimum value of 1.5 ℃ at 18:30 hours. The exit temperature of cold fluid was found to be very close to the inlet temperature of hot fluid after 35 min of the working of STHE. The average heat transfer rate between the two fluids and *LMTD* was found to be decreasing with time as the exit temperature of cold fluid is increasing with time. The effectiveness of the STHE is found to be constant through the experiment and found to be an average value of 0.514.

Table 5.2: Fluid temperatures and performance parameters of heat exchanger on 28th April 2017

Conditions	$\dot{m}_h$ **= 60 kg/hr**		$\dot{m}_c$ **= 60 kg/hr**			(Re_t)**=122.96**		(Re_s)**=43.75**	
Time	T_{hi}	T_{ci}	T_{ho}	T_{co}	$\dot{Q}_c$	$\dot{Q}_h$	$\dot{Q}_{avg}$	*LMTD*	ε
	℃	**℃**	**℃**	**℃**	**kW**	**kW**	**kW**		
17:57	78.9	46.2	59.5	60.7	1.01	1.35	1.18	18.2	0.518
18:00	77.7	51.6	62.2	63.1	0.8	1.08	0.94	14.5	0.517
18:03	76.6	55.9	64.4	65.1	0.65	0.85	0.75	11.5	0.520
18:06	75.9	59.4	66.1	66.6	0.5	0.69	0.59	9.3	0.513

18:09	75.3	62.1	67.5	67.9	0.4	0.54	0.47	7.4	0.511
18:12	74.8	64.3	68.6	68.9	0.32	0.43	0.37	5.9	0.506
18:15	74.4	66.1	69.4	69.7	0.25	0.34	0.3	4.7	0.519
18:18	74	67.5	70.2	70.3	0.2	0.27	0.23	3.6	0.508
18:21	73.8	68.6	70.7	70.9	0.15	0.22	0.19	2.9	0.524
18:24	73.6	69.4	71.2	71.3	0.13	0.17	0.15	2.3	0.512
18:27	73.4	70.1	71.5	71.6	0.1	0.13	0.12	1.8	0.522
18:30	73.3	70.7	71.8	71.8	0.08	0.1	0.09	1.5	0.497
								Average	0.514

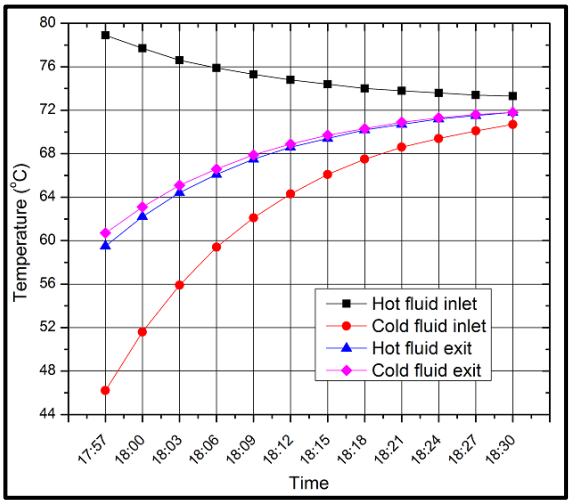

(a) *T* vs *t*

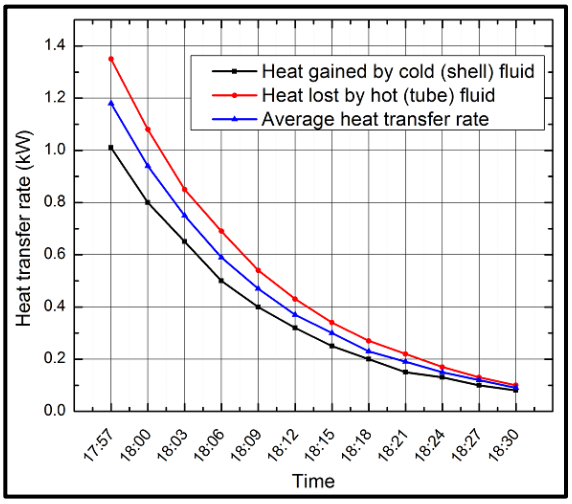

(b) *Q* vs *t*

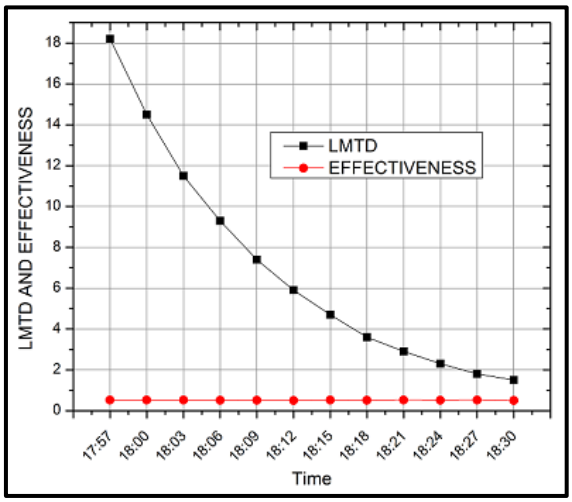

(c) *LMTD* vs *t* and ε vs *t*

Figure 5.2: Variation of different heat exchanger parameters with time based on the experimental results of 28th April 2017

5.3.2 Experiment on 29th April 2017:

The mass flow rate of hot fluid ($\dot{m}_h$) and cold fluid ($\dot{m}_c$) kept at 60 kg/hr and 120 kg/hr respectively. Variations of inlet and outlet temperatures of hot and cold fluids with respect to the time are given in Figure 5.3 (a). Variations of $\dot{Q}_h$, $\dot{Q}_c$, $\dot{Q}_{avg}$ with respect to time and variations of *LMTD*, ε with respect to time are shown in Figure 5.3 (b) and (c) respectively. The Reynold's number of hot fluid (Re_h) was found to be 122.96 and for cold fluid (Re_c) was found to be 87.5 with the set mass flow rates of the fluids. It was observed that the temperature difference between hot fluid inlet and cold fluid exit of the STHE is continuously decreasing with time from a maximum value of 24.7 ℃ at 17:39 hrs to a minimum value of 2.2 ℃ at 18:24 hrs. The exit temperature of cold fluid was found to be very close to the inlet temperature of hot fluid at the end of the experiment. The average heat transfer rate between the two fluids and *LMTD* was found to be decreasing with time as the exit temperature of cold fluid is increasing with time. The effectiveness of the STHE is found to be constant through the experiment and found to be an average value of 0.629.

Table 5.3: Fluid temperatures and performance parameters of heat exchanger on 29th April 2017

Conditions	$\dot{m}_h$ **= 60 kg/hr**		$\dot{m}_c$ **= 120 kg/hr**			(Re_t)**=122.96**		(Re_s)**=87.5**	
Time	T_{hi}	T_{ci}	T_{ho}	T_{co}	$\dot{Q}_c$	$\dot{Q}_h$	$\dot{Q}_{avg}$	*LMTD*	ε
	℃	**℃**	**℃**	**℃**	**kW**	**kW**	**kW**		
17:39	75.2	41.2	50.2	50.5	1.3	1.74	1.52	15.6	0.641
17:42	73.6	44.7	52.4	52.5	1.08	1.48	1.28	13.2	0.635
17:45	72.1	47.7	54.3	54.3	0.93	1.24	1.08	11.3	0.635
17:48	71	50.3	55.8	55.9	0.78	1.06	0.92	9.5	0.638
17:51	70.1	52.3	57.1	57.1	0.67	0.91	0.79	8.2	0.637
17:54	69.3	54.2	58.2	58.2	0.55	0.77	0.66	6.9	0.627
17:57	68.6	55.7	59.2	59.2	0.5	0.65	0.57	6	0.634
18:00	68	57	60	60	0.43	0.56	0.49	5	0.639
18:03	67.3	58.2	60.7	60.7	0.34	0.47	0.4	4.2	0.631
18:06	66.9	59.1	61.3	61.2	0.28	0.39	0.34	3.7	0.625
18:09	66.5	59.9	61.8	61.7	0.25	0.33	0.29	3.2	0.630
18:12	66.2	60.6	62.2	62.1	0.21	0.28	0.25	2.7	0.641
18:15	65.9	61.2	62.5	62.5	0.18	0.24	0.21	2.2	0.641

18:18	65.8	61.7	62.8	62.8	0.15	0.21	0.18	1.9	0.630
18:21	65.6	62.2	63.1	63	0.11	0.17	0.14	1.6	0.591
18:24	65.4	62.5	63.3	63.2	0.1	0.15	0.12	1.4	0.594
								Average	0.629

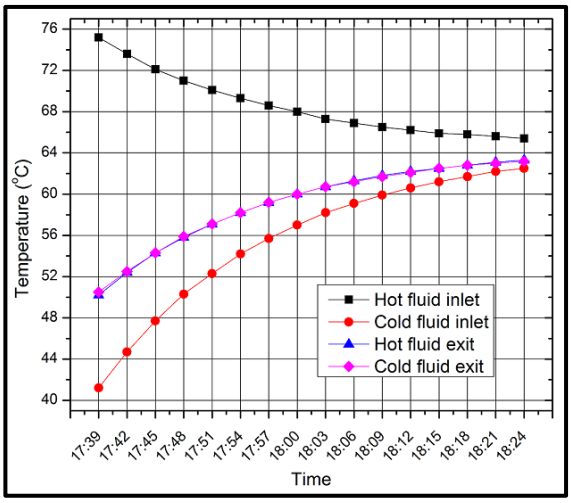

(a) *T* vs *t*

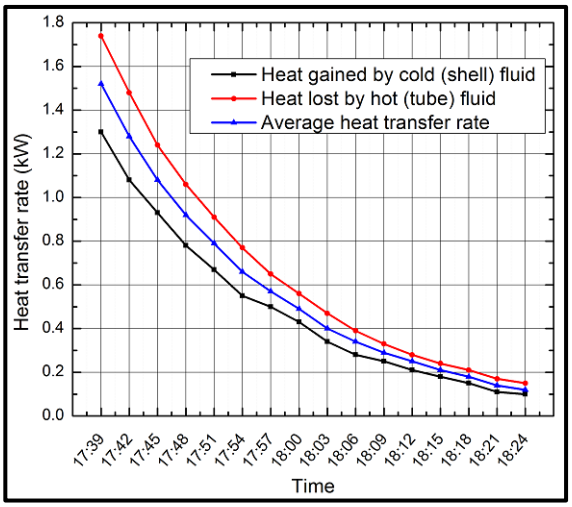

(b) *Q* vs *t*

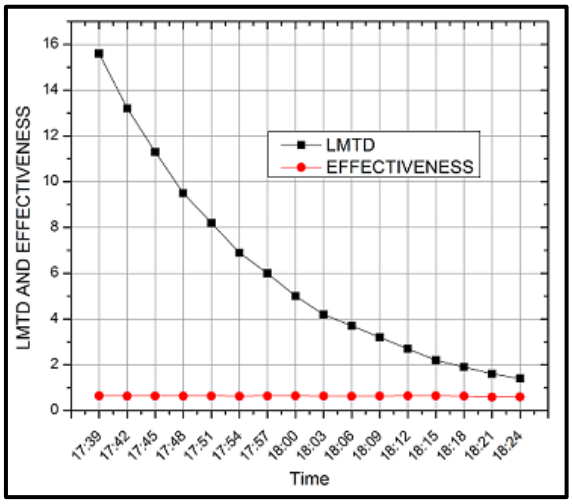

(c) *LMTD* vs *t* and ε vs *t*

Figure 5.3: Variation of different heat exchanger parameters with time based on the experimental results of 29th April 2017

5.3.3 Experiment on 30th April 2017:

The mass flow rate of hot fluid ($\dot{m}_h$) and cold fluid ($\dot{m}_c$) kept at 60 kg/hr and 180 kg/hr respectively. Variations of inlet and outlet temperatures of cold and hot fluids with

respect to the time are given in Figure 5.4 (a). Variations of $\dot{Q}_h$, $\dot{Q}_c$, $\dot{Q}_{avg}$ with respect to time and variations of *LMTD*, ε with respect to time are shown in Figure 5.4 (b) and (c) respectively. The Reynold's number of hot fluid (Re_h) was found to be 122.96 and for cold fluid (Re_c) was found to be 131.24 with the set mass flow rates of the fluids. It was observed that the temperature difference between hot fluid inlet and cold fluid exit of the STHE is continuously decreasing with time from a maximum value of 45.5 ℃ at 18:12 hrs to a minimum value of 4 ℃ at 19:06 hrs. The exit temperature of cold fluid was found to be very close to the inlet temperature of hot fluid at the end of the experiment. The average heat transfer rate between the two fluids and *LMTD* was found to be decreasing with time as the exit temperature of cold fluid is increasing with time. The effectiveness of the STHE is found to be constant through the experiment and found to be an average value of 0.691.

Table 5.4: Fluid temperatures and performance parameters of heat exchanger on 30th April 2017

Conditions	$\dot{m}_h$ **= 60 kg/hr**		$\dot{m}_c$ **= 180 kg/hr**			(Re_t)**=122.96**		(Re_s)**=131.24**	
Time	T_{hi}	T_{ci}	T_{ho}	T_{co}	$\dot{Q}_c$	$\dot{Q}_h$	$\dot{Q}_{avg}$	*LMTD*	ε
	℃	**℃**	**℃**	**℃**	**kW**	**kW**	**kW**		
18:12	81.5	24.8	36.4	36	2.34	3.15	2.74	24.77	0.693
18:15	78.7	29	39.1	38.8	2.06	2.76	2.41	21.67	0.696
18:18	76.1	32.7	41.6	41.3	1.8	2.41	2.1	18.99	0.694
18:21	73.9	36	43.7	43.4	1.56	2.1	1.83	16.59	0.693
18:24	71.9	38.8	45.5	45.3	1.35	1.84	1.59	14.49	0.689
18:27	70.3	41.3	47.2	46.9	1.18	1.61	1.39	12.72	0.688
18:30	68.8	43.4	48.6	48.4	1.05	1.41	1.23	11.11	0.695
18:33	67.6	45.2	49.8	49.6	0.92	1.23	1.08	9.78	0.692
18:36	66.3	47	51	50.8	0.79	1.07	0.93	8.49	0.691
18:39	65.4	48.4	51.9	51.7	0.68	0.94	0.81	7.45	0.684
18:42	64.5	49.6	52.7	52.5	0.6	0.82	0.71	6.54	0.684
18:45	63.8	50.8	53.4	53.3	0.53	0.72	0.63	5.69	0.695
18:48	63.1	51.8	54	53.9	0.45	0.63	0.54	4.9	0.686
18:51	62.4	52.6	54.6	54.5	0.41	0.54	0.48	4.33	0.703
18:54	61.9	53.3	55.2	55	0.34	0.47	0.41	3.85	0.684
18:57	61.5	54	55.6	55.5	0.3	0.42	0.36	3.29	0.689
19:00	61.1	54.5	56	55.8	0.26	0.36	0.31	2.97	0.674

19:03	60.8	55.1	56.3	56.2	0.23	0.32	0.28	2.56	0.705
19:06	60.5	55.5	56.6	56.5	0.21	0.27	0.24	2.27	0.689
								Average	0.691

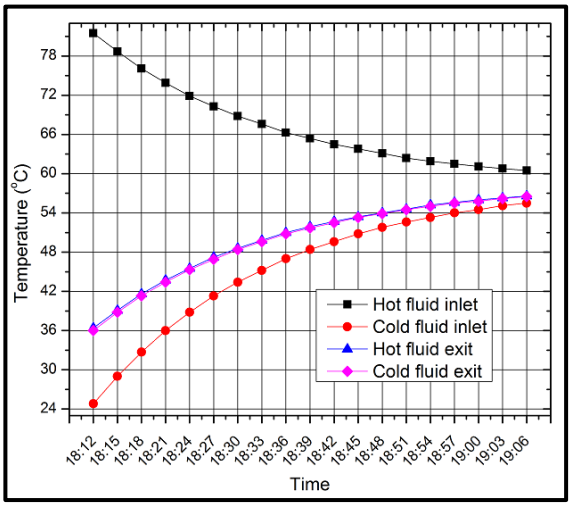

(a) *T* vs *t*

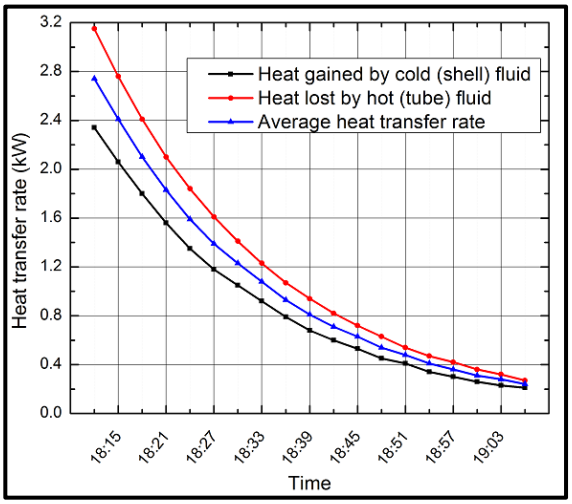

(b) *Q* vs *t*

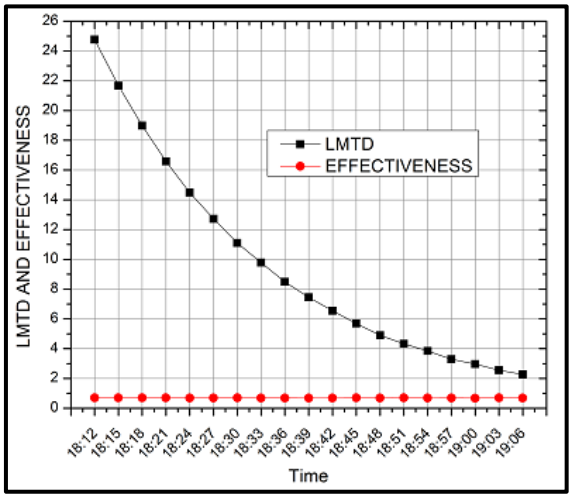

(c) *LMTD* vs *t* and *ε* vs *t*

Figure 5.4: Variation of different heat exchanger parameters with time based on the experimental results of 30th April 2017

5.3.4 Experiment on 1st May 2017:

The mass flow rate of hot fluid ($\dot{m}_h$) and cold fluid ($\dot{m}_c$) kept at 60 kg/hr and 240 kg/hr respectively. Variations of inlet and outlet temperatures of shell and tube side fluids with respect to the time are given in Figure 5.5 (a). Variations of $\dot{Q}_h$, $\dot{Q}_c$, $\dot{Q}_{avg}$ with

respect to time and variations of *LMTD,* ε with respect to time are shown in Figure 5.5 (b) and (c) respectively. The hot fluid Reynold's number (Re_h) was found to be 122.96 and for shell side (Re_c) was found to be 174.99 with the set mass flow rates of the fluids. It was observed that the temperature difference between hot fluid inlet and cold fluid exit of the STHE is continuously decreasing with time from a maximum value of 38.5℃ at 18:03 hrs to a minimum value of 5.8℃ at 18:51 hrs. The exit temperature of cold fluid was found to be very close to the inlet temperature of hot fluid at the end of the experiment. The average heat transfer rate between the two fluids and *LMTD* was found to be decreasing with time as the exit temperature of cold fluid is increasing with time. The effectiveness of the STHE is found to be constant through the experiment and found to be an average value of 0.719.

Table 5.5: Fluid temperatures and performance parameters of heat exchanger on 01st May 2017

Conditions	$\dot{m}_h$ **= 60 kg/hr**			$\dot{m}_c$ **= 240 kg/hr**		(Re_t)**=122.96**		(Re_s)**=174.99**	
Time	T_{hi}	T_{ci}	T_{ho}	T_{co}	$\dot{Q}_c$	$\dot{Q}_h$	$\dot{Q}_{avg}$	*LMTD*	ε
	℃	**℃**	**℃**	**℃**	**kW**	**kW**	**kW**		
18:03	75.6	30.1	37.7	37.1	1.95	2.64	2.29	19	0.722
18:06	73.2	32.8	39.5	39	1.75	2.34	2.04	16.9	0.724
18:09	71	35.1	41.2	40.7	1.55	2.08	1.81	15	0.723
18:12	69.1	37.2	42.6	42.1	1.37	1.85	1.61	13.4	0.724
18:15	67.4	39.1	43.8	43.4	1.2	1.65	1.42	11.8	0.720
18:18	65.9	40.8	44.9	44.6	1.06	1.46	1.26	10.5	0.720
18:21	64.6	42.2	46	45.7	0.97	1.3	1.14	9.4	0.730
18:24	63.4	43.5	46.9	46.6	0.86	1.15	1	8.3	0.721
18:27	62.2	44.6	47.6	47.4	0.77	1.02	0.9	7.4	0.734
18:30	61.3	45.8	48.3	48.1	0.66	0.91	0.78	6.5	0.722
18:33	60.5	46.7	48.9	48.7	0.57	0.81	0.69	5.7	0.717
18:36	59.8	47.4	49.5	49.3	0.54	0.72	0.63	5.2	0.729
18:39	59.1	48.2	50	49.9	0.46	0.63	0.54	4.6	0.711
18:42	58.5	48.8	50.5	50.3	0.4	0.56	0.48	4.1	0.710
18:45	58	49.3	50.9	50.7	0.37	0.49	0.43	3.7	0.709
18:48	57.6	49.8	51.2	51	0.32	0.44	0.38	3.3	0.699
18:51	57.1	50.4	51.5	51.3	0.26	0.4	0.33	2.9	0.707
								Average	0.719

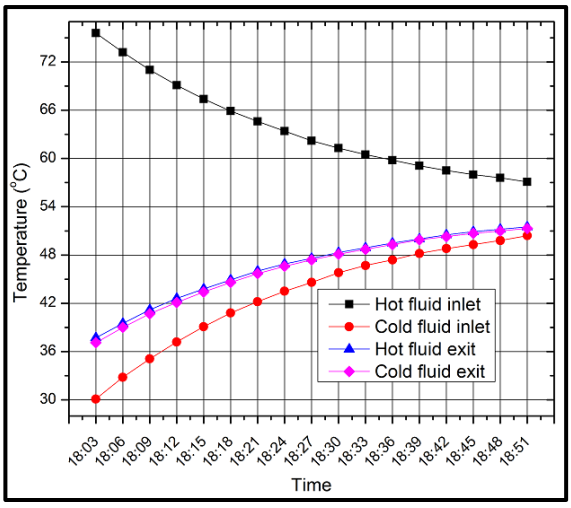

(a) T vs t

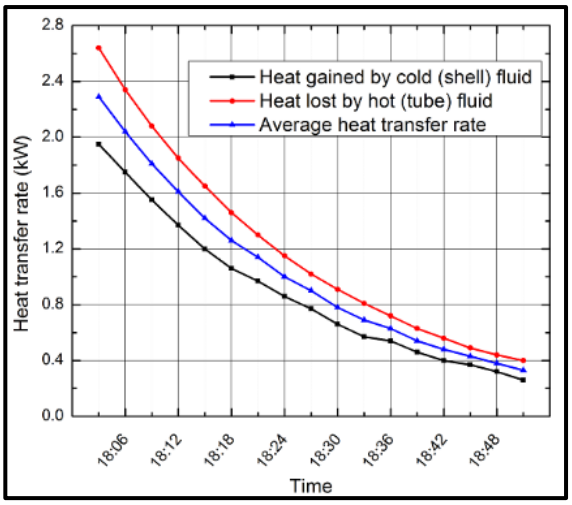

(b) Q vs t

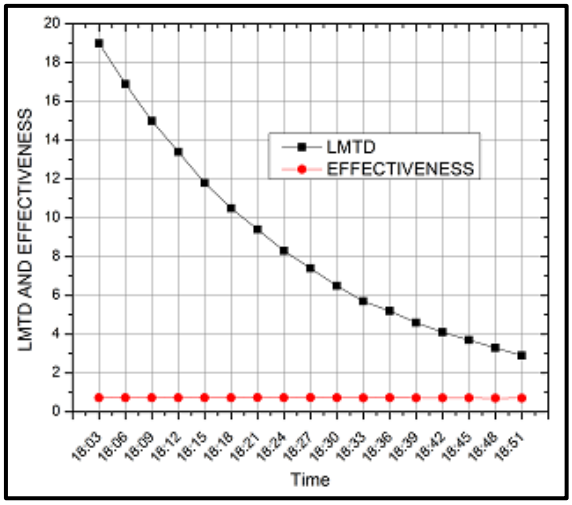

(c) *LMTD* vs t and ε vs t

Figure 5.5: Variation of different heat exchanger parameters with time based on the experimental results of 01st May 2017

5.3.5 Experiment on 3rd May 2017:

The mass flow rate of hot fluid ($\dot{m}_h$) and cold fluid ($\dot{m}_c$) kept at 120 kg/hr and 60 kg/hr respectively. Variations of inlet and outlet temperatures of shell and tube side fluids with respect to the time are given in Figure 5.6 (a). Variations of $\dot{Q}_h$, $\dot{Q}_c$, $\dot{Q}_{avg}$ with respect to time and variations of *LMTD*, ε with respect to time are shown in Figure 5.6 (b) and (c) respectively. The hot fluid Reynold's number (Re_h) was found to be 245.92 and for cold fluid (Re_c) was found to be 43.75 with the set mass flow rates of the fluids. It was observed

that the temperature difference between hot fluid inlet and cold fluid exit of the STHE is continuously decreasing with time from a maximum value of 30.5 ℃ at 18:30 hrs to a minimum value of 1.2 ℃ at 19:09 hrs. The exit temperature of cold fluid was found to be very close to the inlet temperature of hot fluid at the end of the experiment. The average heat transfer rate between the two fluids and *LMTD* was found to be decreasing with time as the exit temperature of cold fluid is increasing with time. The effectiveness of the STHE is found to be constant through the experiment and found to be an average value of 0.604.

Table 5.6: Fluid temperatures and performance parameters of heat exchanger on 03rd May 2017

Conditions	$\dot{m}_h$ **= 120 kg/hr**		$\dot{m}_c$ **= 60 kg/hr**			(Re_t) **=245.92**		(Re_s) **=43.75**	
Time	T_{hi}	T_{ci}	T_{ho}	T_{co}	$\dot{Q}_c$	$\dot{Q}_h$	$\dot{Q}_{avg}$	*LMTD*	ε
	℃	**℃**	**℃**	**℃**	**kW**	**kW**	**kW**		
18:30	84.9	20	61.9	54.4	2.4	3.21	2.8	35.9	0.619
18:33	83.4	32.9	65.6	59.6	1.86	2.48	2.17	28	0.617
18:36	82.2	42.9	68.3	63.7	1.45	1.94	1.7	21.8	0.621
18:39	81.3	50.8	70.6	67	1.13	1.5	1.31	16.9	0.616
18:42	80.6	56.8	72.3	69.4	0.88	1.16	1.02	13.2	0.615
18:45	80.1	61.6	73.6	71.4	0.68	0.9	0.79	10.3	0.613
18:48	79.7	65.3	74.7	72.9	0.53	0.7	0.62	8	0.618
18:51	79.4	68.1	75.5	74.1	0.42	0.55	0.48	6.3	0.609
18:54	79.1	70.4	76.1	75	0.32	0.42	0.37	4.8	0.610
18:57	78.9	72.1	76.6	75.7	0.25	0.32	0.29	3.8	0.612
19:00	78.8	73.5	77	76.3	0.19	0.25	0.22	3	0.596
19:03	78.7	74.6	77.3	76.7	0.15	0.19	0.17	2.4	0.595
19:06	78.6	75.4	77.5	77.1	0.12	0.15	0.13	1.8	0.583
19:09	78.5	76.1	77.7	77.3	0.08	0.1	0.09	1.4	0.538
								Average	0.604

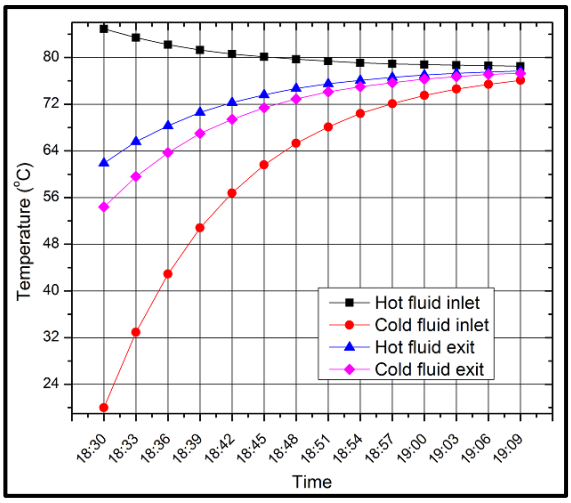

(a) *T* vs *t*

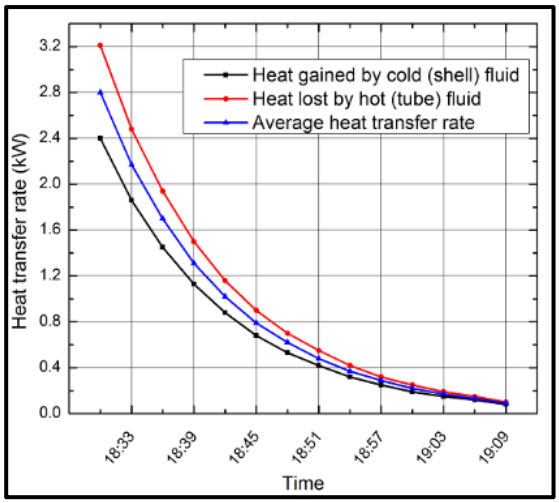

(b) *Q* vs *t*

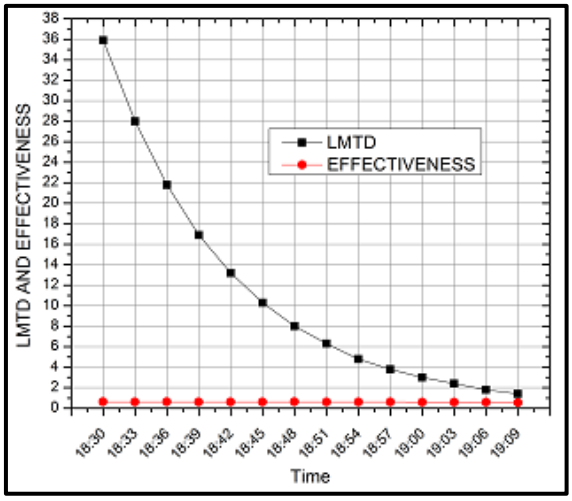

(c) *LMTD* vs *t* and ε vs *t*

Figure 5.6: Variation of different heat exchanger parameters with time based on the experimental results of 03rd May 2017

5.3.6 Experiment on 4th May 2017:

The mass flow rate of hot fluid ($\dot{m}_h$) and cold fluid ($\dot{m}_c$) kept at 120 kg/hr and 120 kg/hr respectively. Variations of inlet and outlet temperatures of shell and hot fluids with respect to the time are given in Figure 5.7 (a). Variations of $\dot{Q}_h$, $\dot{Q}_c$, $\dot{Q}_{avg}$ with respect to time and variations of *LMTD*, ε with respect to time are shown in Figure 5.7 (b) and (c) respectively. The hot fluid Reynold's number (Re_h) was found to be 245.92 and for cold fluid (Re_c) was found to be 87.5 with the set mass flow rates of the fluids. It was observed

that the temperature difference between hot fluid inlet and cold fluid exit of the STHE is continuously decreasing with time from a maximum value of 29.4℃ at 18:03 hrs to a minimum value of 2.8℃ at 18:42 hrs. The exit temperature of cold fluid was found to be very close to the inlet temperature of hot fluid at the end of the experiment. The average heat transfer rate between the two fluids and *LMTD* was found to be decreasing with time as the exit temperature of cold fluid is increasing with time. The effectiveness of the STHE is found to be constant through the experiment and found to be an average value of 0.408.

Table 5.7: Fluid temperatures and performance parameters of heat exchanger on 04th May 2017

Conditions	$\dot{m}_h$ **= 120 kg/hr**		$\dot{m}_c$ **= 120 kg/hr**			(Re_t)**=245.92**		(Re_s)**=87.5**	
Time	T_{hi}	T_{ci}	T_{ho}	T_{co}	$\dot{Q}_c$	$\dot{Q}_h$	$\dot{Q}_{avg}$	*LMTD*	ε
	℃	**℃**	**℃**	**℃**	**kW**	**kW**	**kW**		
18:03	81.2	35.7	59.7	51.8	2.24	2.99	2.62	29.4	0.413
18:06	79.9	41.8	61.9	55.3	1.88	2.51	2.19	24.6	0.412
18:09	78.7	46.9	63.7	58.1	1.57	2.08	1.82	20.6	0.411
18:12	77.8	51.1	65.2	60.5	1.31	1.76	1.53	17.3	0.411
18:15	76.9	54.6	66.5	62.5	1.09	1.46	1.28	14.4	0.412
18:18	76.2	57.6	67.5	64.1	0.91	1.22	1.06	12.1	0.409
18:21	75.7	60.1	68.3	65.6	0.77	1.03	0.9	10.2	0.414
18:24	75.2	62.2	69.1	66.8	0.64	0.84	0.74	8.4	0.408
18:27	74.8	63.9	69.8	67.7	0.52	0.7	0.61	7.1	0.401
18:30	74.5	65.4	70.3	68.5	0.44	0.59	0.51	6	0.402
18:33	74.2	66.6	70.7	69.2	0.37	0.49	0.43	5	0.406
18:36	74	67.6	71	69.8	0.31	0.42	0.36	4.1	0.404
18:39	73.8	68.4	71.3	70.3	0.27	0.35	0.31	3.4	0.412
18:42	73.6	69.1	71.6	70.8	0.22	0.28	0.25	2.8	0.399
								Average	0.408

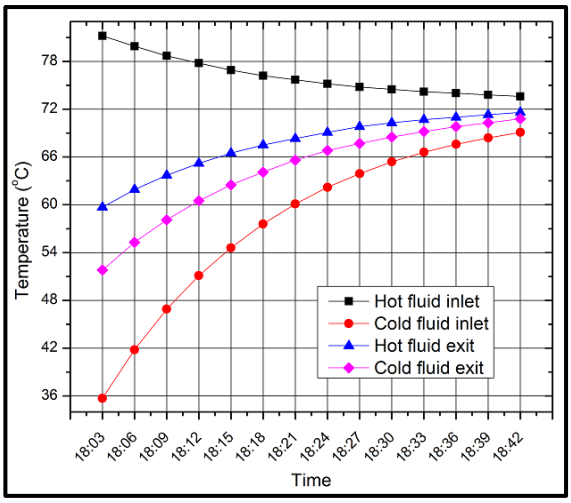

(a) *T* vs *t*

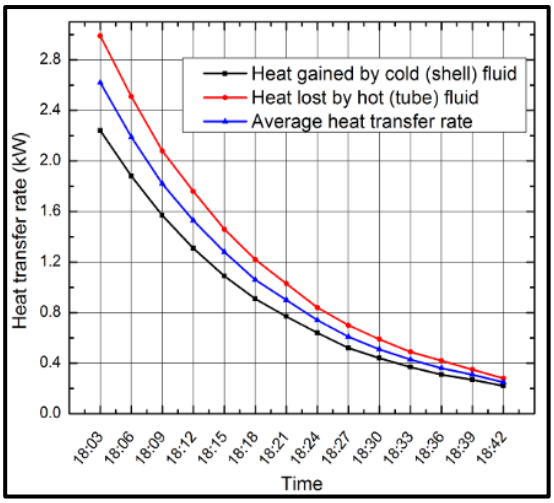

(b) *Q* vs *t*

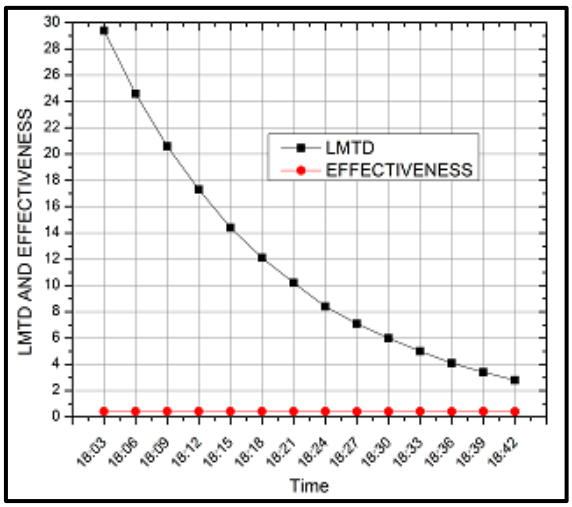

(c) *LMTD* vs *t* and ε vs *t*

Figure 5.7: Variation of different heat exchanger parameters with time based on the experimental results of 04th May 2017

5.3.7 Experiment on 5th May 2017:

The mass flow rate of hot fluid ($\dot{m}_h$) and cold fluid ($\dot{m}_c$) kept at 120 kg/hr and 180 kg/hr respectively. Variations of inlet and outlet temperatures of shell and hot fluid fluids with respect to the time are given in Figure 5.8 (a). Variations of $\dot{Q}_h$, $\dot{Q}_c$, $\dot{Q}_{avg}$ with respect to time and variations of *LMTD*, ε with respect to time are shown in Figure 5.8 (b) and (c) respectively. The hot fluid Reynold's number (Re_h) was found to be 245.92 and for cold fluid (Re_c) was found to be 131.24 with the set mass flow rates of the fluids. It was observed

that the temperature difference between hot fluid inlet and cold fluid exit of the STHE is continuously decreasing with time from a maximum value of 31.1 ℃ at 18:12 hrs to a minimum value of 3.1 ℃ at 19:00 hrs. The exit temperature of cold fluid was found to be very close to the inlet temperature of hot fluid at the end of the experiment. The average heat transfer rate between the two fluids and *LMTD* was found to be decreasing with time as the exit temperature of cold fluid is increasing with time. The effectiveness of the STHE is found to be constant through the experiment and found to be an average value of 0.459.

Table 5.8: Fluid temperatures and performance parameters of heat exchanger on 05th May 2017

Conditions	$\dot{m}_h$ **= 120 kg/hr**		$\dot{m}_c$ **= 180 kg/hr**			(Re_t)**=245.92**		(Re_s)**=131.24**	
Time	T_{hi}	T_{ci}	T_{ho}	T_{co}	$\dot{Q}_c$	$\dot{Q}_h$	$\dot{Q}_{avg}$	***LMTD***	ε
	℃	**℃**	**℃**	**℃**	**kW**	**kW**	**kW**		
18:12	79.1	36.9	56.7	48	2.33	3.12	2.73	25	0.464
18:15	77.7	41.1	58.2	50.7	2.01	2.71	2.36	21.7	0.463
18:18	76.4	44.6	59.5	53	1.75	2.35	2.05	18.8	0.462
18:21	75.3	47.8	60.8	55.1	1.52	2.03	1.77	16.3	0.462
18:24	74.4	50.6	61.8	56.8	1.3	1.76	1.53	14.2	0.461
18:27	73.6	52.9	62.6	58.3	1.13	1.53	1.33	12.3	0.461
18:30	72.9	55	63.4	59.6	0.98	1.32	1.15	10.7	0.461
18:33	72.2	56.8	64	60.8	0.83	1.14	0.99	9.2	0.461
18:36	71.7	58.3	64.6	61.8	0.72	0.99	0.86	8	0.460
18:39	71.2	59.6	65.2	62.7	0.64	0.85	0.74	6.9	0.458
18:42	70.8	60.8	65.6	63.4	0.55	0.73	0.64	6	0.459
18:45	70.5	61.8	66	64	0.47	0.63	0.55	5.2	0.454
18:48	70.2	62.7	66.3	64.6	0.4	0.55	0.47	4.5	0.450
18:51	70	63.4	66.6	65.1	0.36	0.48	0.42	3.9	0.457
18:54	69.7	64.1	66.8	65.6	0.29	0.4	0.35	3.3	0.448
18:57	69.5	64.7	67	66	0.27	0.35	0.31	2.9	0.463
19:00	69.4	65.2	67.2	66.3	0.23	0.3	0.27	2.5	0.461
								Average	0.459

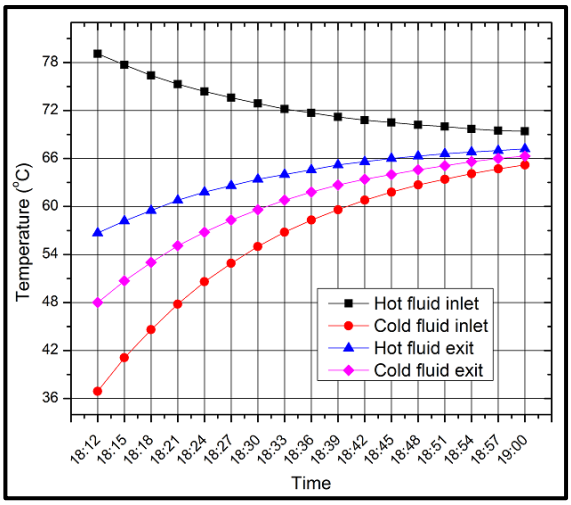

(a) *T* vs *t*

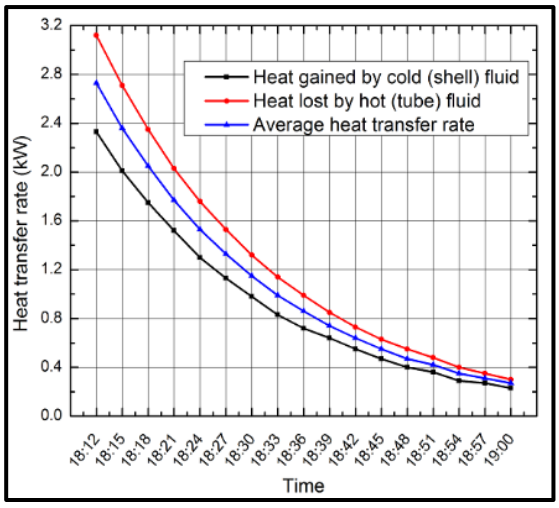

(b) *Q* vs *t*

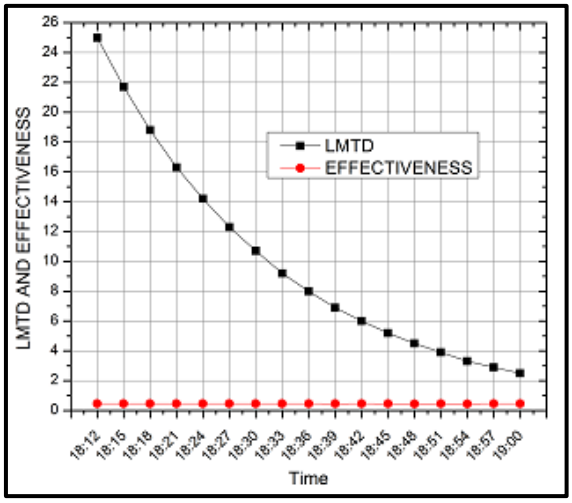

(c) *LMTD* vs *t* and ε vs *t*

Figure 5.8: Variation of different heat exchanger parameters with time based on the experimental results of 05th May 2017

5.3.8 Experiment on 6th May 2017:

The mass flow rate of hot fluid ($\dot{m}_h$) and cold fluid ($\dot{m}_c$) kept at 120 kg/hr and 240 kg/hr respectively. Variations of inlet and outlet temperatures of shell and tube side fluids with respect to the time are given in Figure 5.9 (a). Variations of $\dot{Q}_h$, $\dot{Q}_c$, $\dot{Q}_{avg}$ with respect to time and variations of *LMTD*, ε with respect to time are shown in Figure 5.9 (b) and (c) respectively. The hot fluid Reynold's number (Re_h) was found to be 245.92 and for cold fluid (Re_c) was found to be 174.99 with the set mass flow rates of the fluids. It was

observed that the temperature difference between hot fluid inlet and cold fluid exit of the STHE is continuously decreasing with time from a maximum value of 35.5℃ at 17:54 hrs to a minimum value of 4.9℃ at 18:42 hrs. The exit temperature of cold fluid was found to be very close to the inlet temperature of hot fluid at the end of the experiment. The average heat transfer rate between the two fluids and *LMTD* was found to be decreasing with time as the exit temperature of cold fluid is increasing with time. The effectiveness of the STHE is found to be constant through the experiment and found to be an average value of 0.489.

Table 5.9: Fluid temperatures and performance parameters of heat exchanger on 06th May 2017

Conditions	$\dot{m}_h$ **= 120 kg/hr**		$\dot{m}_c$ **= 240 kg/hr**			(Re_t) **=245.92**		(Re_s) **=174.99**	
Time	T_{hi}	T_{ci}	T_{ho}	T_{co}	$\dot{Q}_c$	$\dot{Q}_h$	$\dot{Q}_{avg}$	*LMTD*	ε
	℃	**℃**	**℃**	**℃**	**kW**	**kW**	**kW**		
17:54	78.6	33.7	53.2	43.1	2.63	3.54	3.08	26.7	0.492
17:57	76.9	37.3	54.5	45.7	2.34	3.12	2.73	23.6	0.495
18:00	75.5	40.4	55.7	47.8	2.05	2.77	2.41	20.8	0.493
18:03	74.3	43.2	56.7	49.8	1.83	2.45	2.14	18.5	0.494
18:06	73.2	45.7	57.6	51.5	1.62	2.17	1.9	16.3	0.496
18:09	72.1	47.9	58.4	52.9	1.4	1.91	1.65	14.4	0.489
18:12	71.2	49.8	59.1	54.2	1.22	1.69	1.46	12.8	0.489
18:15	70.4	51.5	59.7	55.5	1.11	1.49	1.3	11.3	0.493
18:18	69.8	53	60.4	56.5	0.97	1.32	1.14	10	0.487
18:21	69.2	54.3	60.8	57.4	0.85	1.17	1.01	8.8	0.486
18:24	68.6	55.6	61.3	58.2	0.74	1.02	0.88	7.8	0.486
18:27	68.2	56.6	61.6	58.9	0.65	0.92	0.78	6.9	0.482
18:30	67.8	57.5	62	59.6	0.6	0.8	0.7	6.1	0.488
18:33	67.3	58.3	62.3	60.2	0.51	0.7	0.61	5.4	0.486
18:36	67	59	62.5	60.7	0.45	0.63	0.54	4.8	0.484
18:39	66.7	59.6	62.8	61.2	0.42	0.55	0.49	4.2	0.495
18:42	66.4	60.3	63	61.5	0.34	0.48	0.41	3.7	0.482
								Average	0.489

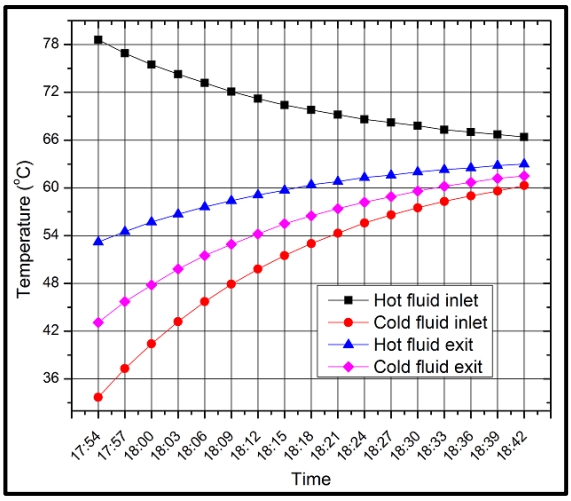

(a) *T* vs *t*

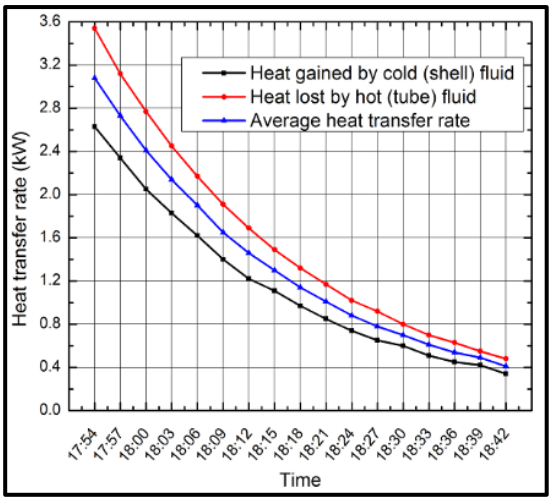

(b) *Q* vs *t*

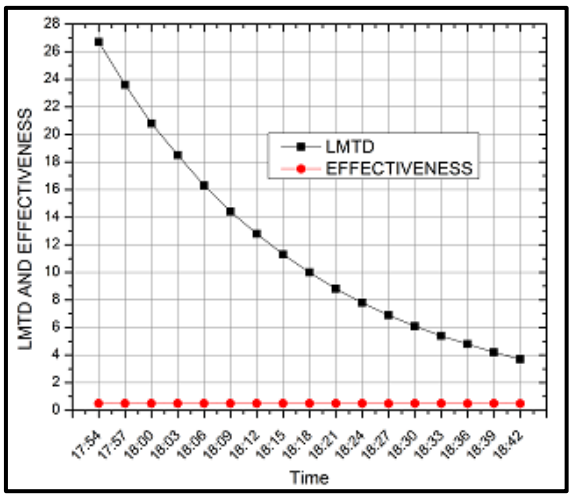

(c) *LMTD* vs *t* and ε vs *t*

Figure 5.9: Variation of different heat exchanger parameters with time based on the experimental results of 06th May 2017

5.3.9 Experiment on 7th May 2017:

The mass flow rate of hot fluid ($\dot{m}_h$) and cold fluid ($\dot{m}_c$) kept at 180 kg/hr and 60 kg/hr respectively. Variations of inlet and outlet temperatures of shell and tube side fluids with respect to the time are given in Figure 5.10 (a). Variations of $\dot{Q}_h$, $\dot{Q}_c$, $\dot{Q}_{avg}$ with respect to time and variations of *LMTD*, ε with respect to time are shown in Figure 5.10 (b) and (c) respectively. The hot fluid Reynold's number (Re_h) was found to be 368.88 and for cold fluid (Re_c) was found to be 43.75 with the set mass flow rates of the fluids. It was

observed that the temperature difference between hot fluid inlet and cold fluid exit of the STHE is continuously decreasing with time from a maximum value of 12.6℃ at 18:00 hrs to a minimum value of 2℃ at 18:21 hrs. The exit temperature of cold fluid was found to be very close to the inlet temperature of hot fluid at the end of the experiment. The average heat transfer rate between the two fluids and *LMTD* was found to be decreasing with time as the exit temperature of cold fluid is increasing with time. The effectiveness of the STHE is found to be constant through the experiment and found to be an average value of 0.651.

Table 5.10: Fluid temperatures and performance parameters of heat exchanger on 07th May 2017

Conditions	$\dot{m}_h$ **= 180 kg/hr**		$\dot{m}_c$ **= 60 kg/hr**			(Re_t)**=368.88**		(Re_s)**=43.75**	
Time	T_{hi}	T_{ci}	T_{ho}	T_{co}	$\dot{Q}_c$	$\dot{Q}_h$	$\dot{Q}_{avg}$	*LMTD*	ε
	℃	**℃**	**℃**	**℃**	**kW**	**kW**	**kW**		
18:00	82.3	52.8	75	69.7	1.18	1.54	1.36	16.9	0.661
18:03	81.8	59.1	76.2	72.2	0.91	1.18	1.04	13	0.657
18:06	81.5	64	77.1	74	0.7	0.92	0.81	10	0.664
18:09	81.2	67.8	77.9	75.4	0.53	0.69	0.61	7.7	0.653
18:12	81	70.7	78.4	76.6	0.41	0.54	0.48	6	0.669
18:15	80.8	72.9	78.9	77.5	0.32	0.39	0.35	4.5	0.636
18:18	80.7	74.7	79.3	78.1	0.24	0.31	0.27	3.5	0.646
18:21	80.6	76	79.6	78.6	0.18	0.22	0.2	2.7	0.624
								Average	0.651

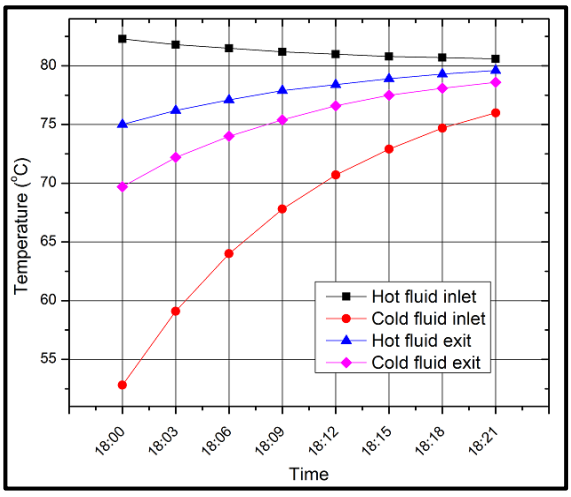

(a) *T* vs *t*

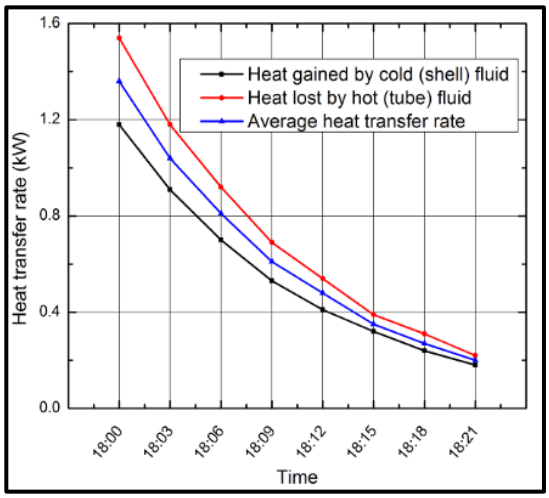

(b) *Q* vs *t*

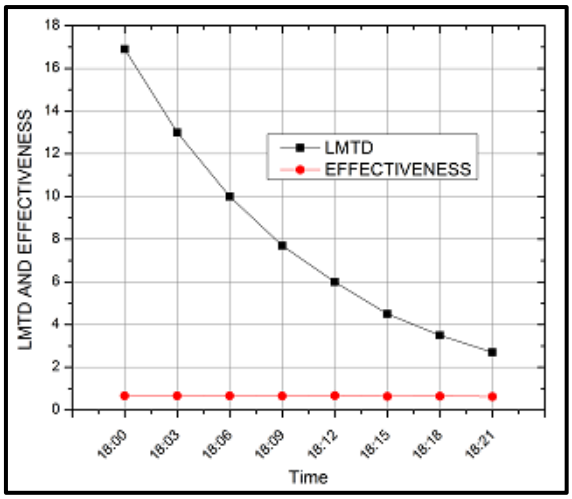

(c) *LMTD* vs *t* and ε vs *t*

Figure 5.10: Variation of different heat exchanger parameters with time based on the experimental results of 07th May 2017

5.3.10 Experiment on 8th May 2017:

The mass flow rate of hot fluid ($\dot{m}_h$) and cold fluid ($\dot{m}_c$) kept at 180 kg/hr and 120 kg/hr respectively. Variations of inlet and outlet temperatures of shell and tube side fluids with respect to the time are given in Figure 5.11 (a). Variations of $\dot{Q}_h$, $\dot{Q}_c$, $\dot{Q}_{avg}$ with respect to time and variations of *LMTD*, ε with respect to time are shown in Figure 5.11 (b) and (c) respectively. The hot fluid Reynold's number (Re_h) was found to be 368.88 and for cold fluid (Re_c) was found to be 87.5 with the set mass flow rates of the fluids. It was observed that the temperature difference between hot fluid inlet and cold fluid exit of the STHE is continuously decreasing with time from a maximum value of 22.6℃ at 17:42 hrs to a minimum value of 1.6℃ at 18:24 hrs. The exit temperature of cold fluid was found to be very close to the inlet temperature of hot fluid at the end of the experiment. The average heat transfer rate between the two fluids and *LMTD* was found to be decreasing with time as the exit temperature of cold fluid is increasing with time. The effectiveness of the STHE is found to be constant through the experiment and found to be an average value of 0.449.

Table 5.11: Fluid temperatures and performance parameters of heat exchanger on 08th May 2017

Conditions	$\dot{m}_h$ **= 180 kg/hr**		$\dot{m}_c$ **= 120 kg/hr**			(Re_t)**=368.88**		(Re_s)**=87.5**	
Time	T_{hi}	T_{ci}	T_{ho}	T_{co}	$\dot{Q}_c$	$\dot{Q}_h$	$\dot{Q}_{avg}$	*LMTD*	ε
	°C	**°C**	**°C**	**°C**	**kW**	**kW**	**kW**		
17:42	81.2	44.1	68.2	58.6	2.02	2.72	2.37	23.3	0.458
17:45	80.4	49.5	69.7	61.7	1.69	2.25	1.97	19.4	0.457
17:48	79.7	54.1	70.8	64.1	1.39	1.86	1.63	16.1	0.457
17:51	79.1	57.9	71.7	66.2	1.15	1.54	1.35	13.3	0.457
17:54	78.6	61	72.5	67.9	0.96	1.27	1.12	11.1	0.457
17:57	78.2	63.6	73.1	69.3	0.79	1.05	0.92	9.2	0.452
18:00	77.9	65.8	73.7	70.5	0.67	0.86	0.76	7.6	0.451
18:03	77.7	67.6	74.1	71.5	0.54	0.73	0.63	6.4	0.447
18:06	77.3	69	74.6	72.3	0.45	0.58	0.52	5.3	0.449
18:09	77.1	70.4	74.9	73	0.37	0.48	0.42	4.3	0.450
18:12	77	71.4	75.2	73.6	0.31	0.39	0.35	3.6	0.448
18:15	76.9	72.2	75.4	74	0.25	0.33	0.29	3	0.443
18:18	76.8	72.9	75.5	74.4	0.21	0.28	0.25	2.5	0.460
18:21	76.7	73.5	75.7	74.7	0.17	0.22	0.19	2.1	0.426
18:24	76.6	73.9	75.8	75	0.15	0.18	0.16	1.7	0.425
								Average	0.449

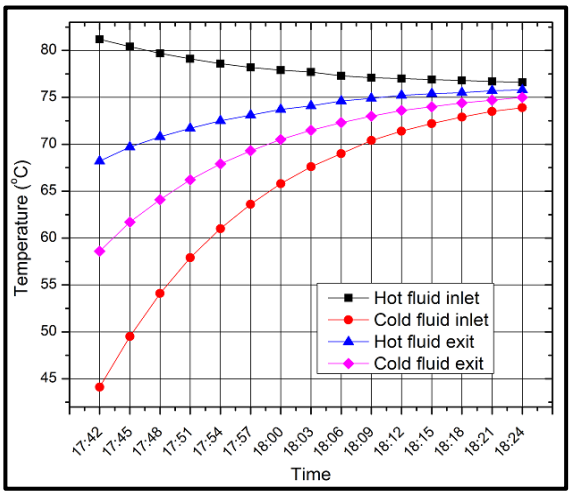

(a) *T* vs *t*

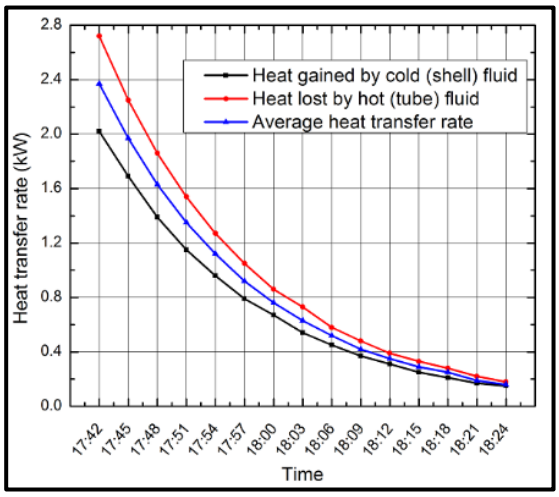

(b) *Q* vs *t*

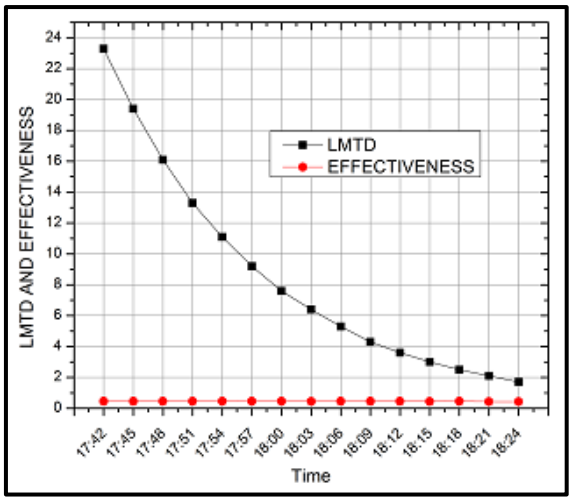

(c) *LMTD* vs *t* and ε vs *t*

Figure 5.11: Variation of different heat exchanger parameters with time based on the experimental results of 08th May 2017

5.3.11 Experiment on 9th May 2017:

The mass flow rate of hot fluid ($\dot{m}_h$) and cold fluid ($\dot{m}_c$) kept at 180 kg/hr and 180 kg/hr respectively. Variations of inlet and outlet temperatures of shell and tube side fluids with respect to the time are given in Figure 5.12 (a). Variations of $\dot{Q}_h$, $\dot{Q}_c$, $\dot{Q}_{avg}$ with respect to time and variations of *LMTD*, ε with respect to time are shown in Figure 5.12 (b) and (c) respectively. The hot fluid Reynold's number (Re_h) was found to be 368.88 and for cold fluid (Re_c) was found to be 131.24 with the set mass flow rates of the fluids. It was observed that the temperature difference between hot fluid inlet and cold fluid exit of the STHE is continuously decreasing with time from a maximum value of 25.2℃ at 18:06 hrs to a minimum value of 2.6℃ at 18:51 hrs. The exit temperature of cold fluid was found to be very close to the inlet temperature of hot fluid at the end of the experiment. The average heat transfer rate between the two fluids and *LMTD* was found to be decreasing with time as the exit temperature of cold fluid is increasing with time. The effectiveness of the STHE is found to be constant through the experiment and found to be an average value of 0.493.

Table 5.12: Fluid temperatures and performance parameters of heat exchanger on 09th May 2017

Conditions	$\dot{m}_h$ = 180 kg/hr			$\dot{m}_c$ = 180 kg/hr		(Re_t)=368.88		(Re_s)=131.24	
Time	T_{hi}	T_{ci}	T_{ho}	T_{co}	$\dot{Q}_c$	$\dot{Q}_h$	$\dot{Q}_{avg}$	*LMTD*	ε
	°C	°C	°C	°C	kW	kW	kW		
18:06	79.5	43.7	65.2	54.3	3	4.44	3.72	25.1	0.497
18:09	78.6	47.7	66.2	56.9	2.59	3.84	3.22	21.7	0.498
18:12	77.8	51.2	67.1	59.1	2.23	3.33	2.78	18.6	0.500
18:15	77	54.1	67.9	61	1.91	2.86	2.38	16.1	0.497
18:18	76.4	56.8	68.6	62.6	1.63	2.43	2.03	13.8	0.495
18:21	75.9	58.9	69.2	64	1.4	2.13	1.76	11.9	0.495
18:24	75.5	60.9	69.8	65.2	1.2	1.83	1.52	10.3	0.498
18:27	75.1	62.5	70.2	66.3	1.03	1.57	1.3	8.8	0.493
18:30	74.8	63.9	70.6	67.2	0.88	1.36	1.12	7.6	0.491
18:33	74.5	65.2	70.9	68	0.76	1.19	0.97	6.5	0.499
18:36	74.3	66.3	71.2	68.6	0.65	0.97	0.81	5.7	0.484
18:39	74.1	67.2	71.4	69.2	0.56	0.84	0.7	4.9	0.485
18:42	73.9	67.9	71.6	69.7	0.48	0.76	0.62	4.1	0.494
18:45	73.8	68.6	71.8	70.1	0.41	0.63	0.52	3.6	0.478
18:48	73.6	69.3	71.9	70.5	0.35	0.54	0.45	3	0.500
18:51	73.5	69.8	72.1	70.9	0.29	0.46	0.37	2.6	0.478
								Average	0.493

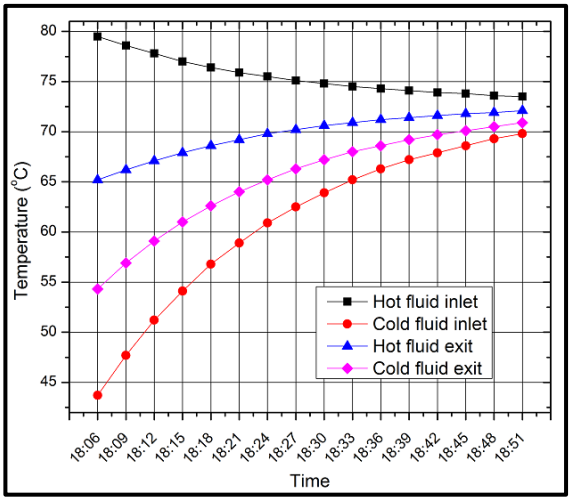

(a) *T* vs *t*

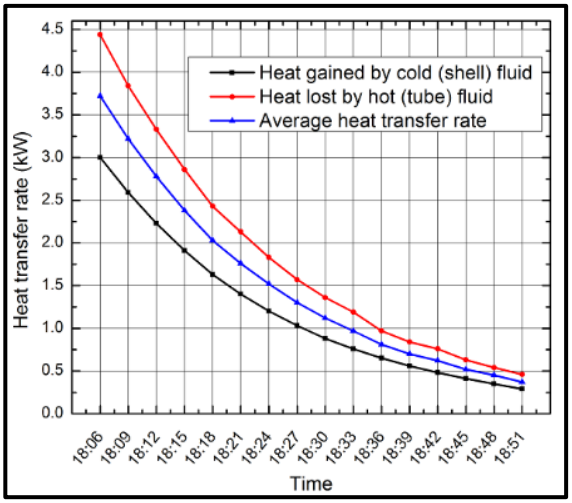

(b) *Q* vs *t*

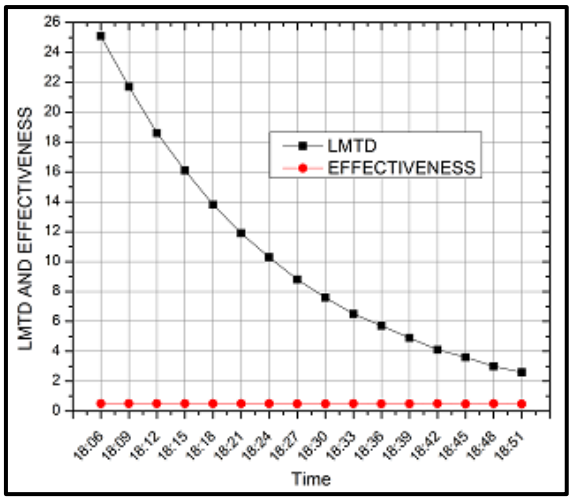

(c) *LMTD* vs *t* and ε vs *t*

Figure 5.12: Variation of different heat exchanger parameters with time based on the experimental results of 09th May 2017

5.3.12 Experiment on 10th May 2017:

The mass flow rate of hot fluid ($\dot{m}_h$) and cold fluid ($\dot{m}_c$) kept at 180 kg/hr and 240 kg/hr respectively. Variations of inlet and outlet temperatures of shell and tube side fluids with respect to the time are given in Figure 5.13 (a). Variations of $\dot{Q}_h$, $\dot{Q}_c$, $\dot{Q}_{avg}$ with respect to time and variations of *LMTD*, ε with respect to time are shown in Figure 5.13 (b) and (c) respectively. The hot fluid Reynold's number (Re_h) was found to be 368.88 and for cold fluid (Re_c) was found to be 174.99 with the set mass flow rates of the fluids. It was observed that the temperature difference between hot fluid inlet and cold fluid exit of the STHE is continuously decreasing with time from a maximum value of 33.7℃ at 17:45 hrs to a minimum value of 4.4℃ at 18:33 hrs. The exit temperature of cold fluid was found to be very close to the inlet temperature of hot fluid at the end of the experiment. The average heat transfer rate between the two fluids and *LMTD* was found to be decreasing with time as the exit temperature of cold fluid is increasing with time. The effectiveness of the STHE is found to be constant through the experiment and found to be an average value of 0.372.

Table 5.13: Fluid temperatures and performance parameters of heat exchanger on 10th May 2017

Conditions	$\dot{m}_h$ = 180 kg/hr			$\dot{m}_c$ = 240 kg/hr		(Re_t)=368.88		(Re_s)=174.99	
Time	T_{hi}	T_{ci}	T_{ho}	T_{co}	$\dot{Q}_c$	$\dot{Q}_h$	$\dot{Q}_{avg}$	*LMTD*	ε
	°C	°C	°C	°C	kW	kW	kW		
17:45	80.1	35.6	60.9	46.4	2.99	4.02	3.51	29.3	0.377
17:48	78.9	39.7	62	49.1	2.62	3.53	3.08	25.8	0.376
17:51	77.8	43.3	62.9	51.6	2.31	3.1	2.71	22.7	0.376
17:54	76.8	46.4	63.7	53.7	2.05	2.74	2.4	20.1	0.378
17:57	75.9	49.2	64.4	55.7	1.79	2.4	2.1	17.6	0.376
18:00	75.2	51.6	65.1	57.3	1.59	2.12	1.86	15.6	0.377
18:03	74.6	53.8	65.7	58.8	1.39	1.87	1.63	13.7	0.375
18:06	74	55.7	66.1	60	1.22	1.65	1.44	12.1	0.376
18:09	73.5	57.3	66.6	61.2	1.08	1.44	1.26	10.7	0.372
18:12	73.1	58.8	66.9	62.2	0.94	1.29	1.11	9.4	0.371
18:15	72.7	60.2	67.3	63.1	0.82	1.12	0.97	8.3	0.371
18:18	72.2	61.3	67.6	63.9	0.74	0.97	0.85	7.3	0.373
18:21	71.9	62.3	67.8	64.5	0.62	0.86	0.74	6.4	0.369
18:24	71.7	63.1	68.1	65.1	0.56	0.76	0.66	5.8	0.367
18:27	71.4	63.9	68.3	65.8	0.51	0.65	0.58	5	0.370
18:30	71.2	64.7	68.4	66.2	0.42	0.58	0.5	4.4	0.368
18:33	71	65.3	68.6	66.6	0.36	0.5	0.43	3.9	0.361
								Average	0.372

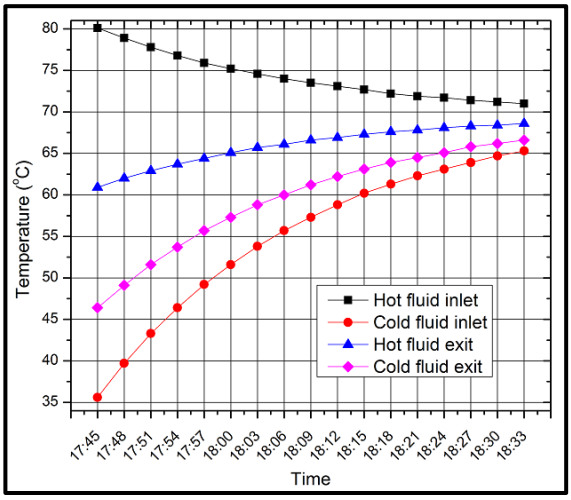

(a) *T* vs *t*

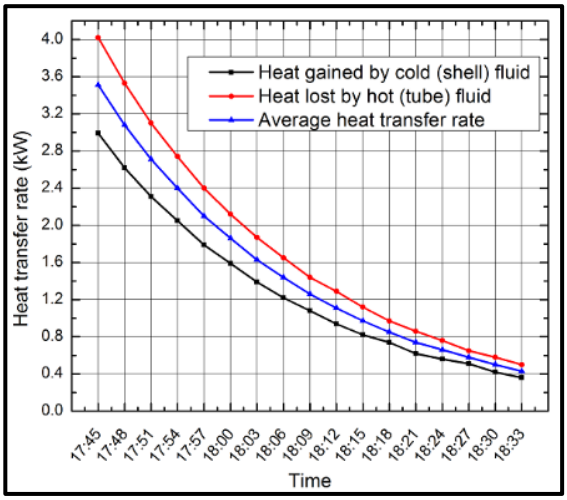

(b) *Q* vs *t*

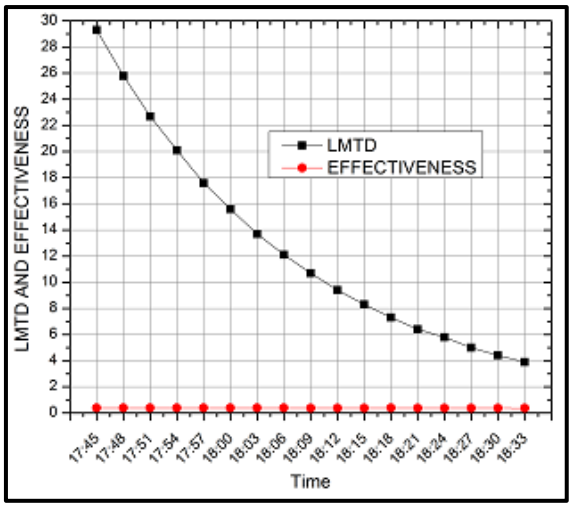

(c) *LMTD* vs *t* and ε vs *t*

Figure 5.13: Variation of different heat exchanger parameters with time based on the experimental results of 10th May 2017

5.3.13 Experiment on 11th May 2017:

The mass flow rate of hot fluid ($\dot{m}_h$) and cold fluid ($\dot{m}_c$) kept at 240 kg/hr and 60 kg/hr respectively. Variations of inlet and outlet temperatures of shell and tube side fluids with respect to the time are given in Figure 5.14 (a). Variations of $\dot{Q}_h$, $\dot{Q}_c$, $\dot{Q}_{avg}$ with respect to time and variations of *LMTD*, ε with respect to time are shown in Figure 5.14 (b) and (c) respectively. The hot fluid Reynold's number (Re_h) was found to be 491.84 and for cold fluid (Re_c) was found to be 43.75 with the set mass flow rates of the fluids. It was observed that the temperature difference between hot fluid inlet and cold fluid exit of the STHE is continuously decreasing with time from a maximum value of 20.0℃ at 18:03 hrs to a minimum value of 0.7℃ at 18:39 hrs. The exit temperature of cold fluid was found to be very close to the inlet temperature of hot fluid at the end of the experiment. The average heat transfer rate between the two fluids and *LMTD* was found to be decreasing with time as the exit temperature of cold fluid is increasing with time. The effectiveness of the STHE is found to be constant through the experiment and found to be an average value of 0.665.

Table 5.14: Fluid temperatures and performance parameters of heat exchanger on 11th May 2017

Conditions	$\dot{m}_h$ = 240 kg/hr			$\dot{m}_c$ = 60 kg/hr		(Re_t)=491.84		(Re_s)=43.75	
Time	T_{hi}	T_{ci}	T_{ho}	T_{co}	$\dot{Q}_c$	$\dot{Q}_h$	$\dot{Q}_{avg}$	*LMTD*	ε
	°C	°C	°C	°C	kW	kW	kW		
18:03	84.1	34.5	74.2	64.1	2.06	2.74	2.4	28.7	0.694
18:06	83.4	45.7	76	68.2	1.57	2.06	1.81	21.9	0.689
18:09	83	54.1	77.2	71.4	1.2	1.6	1.4	16.7	0.695
18:12	82.6	60.6	78.2	73.7	0.92	1.2	1.06	12.7	0.691
18:15	82.2	65.5	79	75.5	0.7	0.89	0.8	9.7	0.687
18:18	82	69.3	79.6	76.9	0.53	0.69	0.61	7.4	0.689
18:21	81.8	72.2	80.1	78	0.4	0.49	0.45	5.6	0.673
18:24	81.7	74.4	80.4	78.8	0.31	0.38	0.34	4.3	0.668
18:27	81.6	76.1	80.7	79.4	0.23	0.26	0.25	3.3	0.652
18:30	81.6	77.3	80.9	79.8	0.17	0.21	0.19	2.6	0.634
18:33	81.5	78.3	81	80.2	0.13	0.15	0.14	1.9	0.628
18:36	81.5	79.1	81.1	80.5	0.1	0.12	0.11	1.4	0.658
18:39	81.4	79.7	81.2	80.7	0.07	0.07	0.07	1	0.591
								Average	0.665

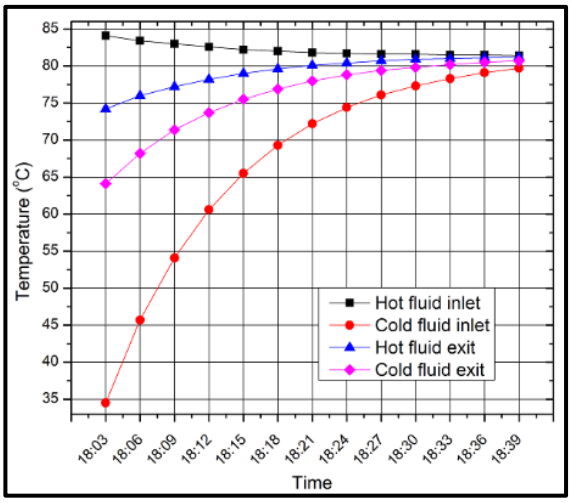

(a) *T* vs *t*

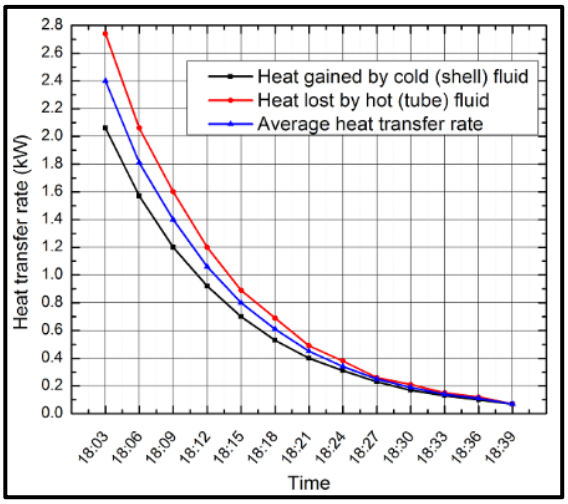

(b) *Q* vs *t*

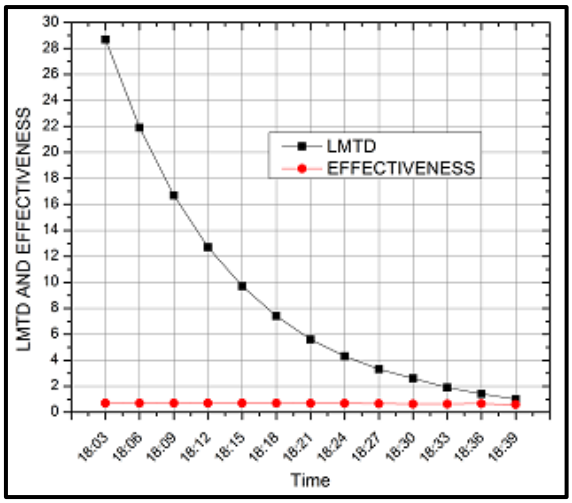

(c) *LMTD* vs *t* and ε vs *t*

Figure 5.14: Variation of different heat exchanger parameters with time based on the experimental results of 11th May 2017

5.3.14 Experiment on 12th May 2017:

The mass flow rate of hot fluid ($\dot{m}_h$) and cold fluid ($\dot{m}_c$) kept at 240 kg/hr and 120 kg/hr respectively. Variations of inlet and outlet temperatures of shell and tube side fluids with respect to the time are given in Figure 5.15 (a). Variations of $\dot{Q}_h$, $\dot{Q}_c$, $\dot{Q}_{avg}$ with respect to time and variations of *LMTD*, ε with respect to time are shown in Figure 5.15 (b) and (c) respectively. The hot fluid Reynold's number (Re_h) was found to be 491.84 and for cold fluid (Re_c) was found to be 87.5 with the set mass flow rates of the fluids. It was observed that the temperature difference between hot fluid inlet and cold fluid exit of the STHE is continuously decreasing with time from a maximum value of 17.4℃ at 17:57 hrs to a minimum value of 2.0℃ at 18:30 hrs. The exit temperature of cold fluid was found to be very close to the inlet temperature of hot fluid at the end of the experiment. The average heat transfer rate between the two fluids and *LMTD* was found to be decreasing with time as the exit temperature of cold fluid is increasing with time. The effectiveness of the STHE is found to be constant through the experiment and found to be an average value of 0.477.

Table 5.15: Fluid temperatures and performance parameters of heat exchanger on 12th May 2017

Conditions	$\dot{m}_h$ **= 240 kg/hr**		$\dot{m}_c$ **= 120 kg/hr**			(Re_t) **=491.84**		(Re_s) **=87.5**	
Time	T_{hi}	T_{ci}	T_{ho}	T_{co}	$\dot{Q}_c$	$\dot{Q}_h$	$\dot{Q}_{avg}$	*LMTD*	ε
	°C	**°C**	**°C**	**°C**	**kW**	**kW**	**kW**		
17:57	81.3	51.3	72.9	63.9	1.76	2.34	2.05	19.4	0.490
18:00	80.7	56.1	73.8	66.4	1.44	1.92	1.68	16	0.490
18:03	80.3	60	74.7	68.5	1.19	1.57	1.38	13.2	0.488
18:06	79.9	63.1	75.3	70.2	0.99	1.29	1.14	10.9	0.487
18:09	79.6	65.8	75.9	71.6	0.81	1.03	0.92	9	0.478
18:12	79.4	68	76.3	72.8	0.66	0.86	0.76	7.4	0.478
18:15	79.2	69.9	76.6	73.7	0.54	0.72	0.63	6.1	0.486
18:18	79	71.3	76.9	74.5	0.45	0.58	0.51	5	0.475
18:21	78.9	72.5	77.2	75.1	0.36	0.46	0.41	4.2	0.460
18:24	78.8	73.5	77.4	75.7	0.31	0.38	0.34	3.4	0.460
18:27	78.7	74.4	77.5	76.2	0.25	0.32	0.29	2.8	0.484
18:30	78.6	75.1	77.7	76.6	0.21	0.24	0.22	2.3	0.451
								Average	0.477

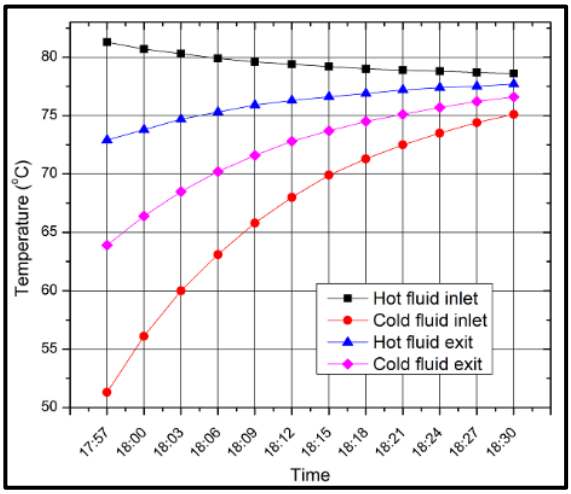

(a) *T* vs *t*

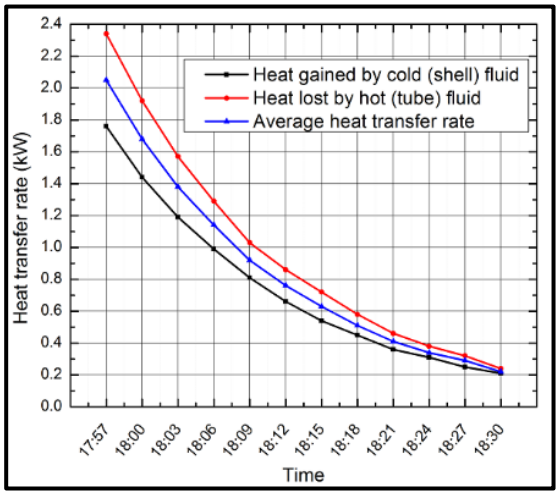

(b) *Q* vs *t*

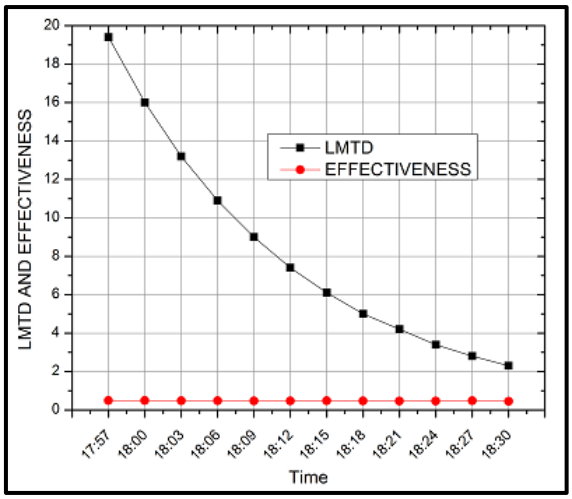

(c) *LMTD* vs *t* and ε vs *t*

Figure 5.15: Variation of different heat exchanger parameters with time based on the experimental results of 12th May 2017

5.3.15 Experiment on 13th May 2017:

The mass flow rate of hot fluid ($\dot{m}_h$) and cold fluid ($\dot{m}_c$) kept at 240 kg/hr and 180 kg/hr respectively. Variations of inlet and outlet temperatures of shell and tube side fluids with respect to the time are given in Figure 5.16 (a). Variations of $\dot{Q}_h$, $\dot{Q}_c$, $\dot{Q}_{avg}$ with respect to time and variations of *LMTD*, ε with respect to time are shown in Figure 5.16 (b) and (c) respectively. The hot fluid Reynold's number (Re_h) was found to be 491.84 and for cold fluid (Re_c) was found to be 131.24 with the set mass flow rates of the fluids. It was observed that the temperature difference between hot fluid inlet and cold fluid exit of the STHE is continuously decreasing with time from a maximum value of 27.6℃ at 17:48 hrs to a minimum value of 4.3℃ at 18:24 hrs. The exit temperature of cold fluid was found to be very close to the inlet temperature of hot fluid at the end of the experiment. The average heat transfer rate between the two fluids and *LMTD* was found to be decreasing with time as the exit temperature of cold fluid is increasing with time. The effectiveness of the STHE is found to be constant through the experiment and found to be an average value of 0.374.

Table 5.16: Fluid temperatures and performance parameters of heat exchanger on 13th May 2017

Conditions	$\dot{m}_h$ = 240 kg/hr			$\dot{m}_c$ = 180 kg/hr		(Re_t)=491.84		(Re_s)=131.24	
Time	T_{hi}	T_{ci}	T_{ho}	T_{co}	$\dot{Q}_c$	$\dot{Q}_h$	$\dot{Q}_{avg}$	*LMTD*	ε
	°C	°C	°C	°C	kW	kW	kW		
17:48	81.3	40.4	68.1	53.7	2.78	3.68	3.23	27.6	0.378
17:51	80.5	45.5	69.1	56.8	2.37	3.17	2.77	23.7	0.378
17:54	79.8	49.6	70.1	59.4	2.05	2.71	2.38	20.4	0.377
17:57	79.2	53.3	70.9	61.7	1.75	2.32	2.03	17.5	0.375
18:00	78.6	56.5	71.5	63.6	1.49	1.97	1.73	15	0.374
18:03	78.2	59.2	72.1	65.3	1.28	1.69	1.48	12.8	0.373
18:06	77.8	61.5	72.5	66.8	1.11	1.46	1.28	11	0.376
18:09	77.4	63.5	72.9	68	0.93	1.26	1.1	9.4	0.378
18:12	77.1	65.2	73.3	69	0.81	1.06	0.93	8.1	0.374
18:15	76.8	66.7	73.6	69.9	0.68	0.89	0.78	6.9	0.369
18:18	76.6	67.9	73.8	70.8	0.59	0.78	0.69	5.9	0.379
18:21	76.4	68.9	74.1	71.4	0.51	0.64	0.57	5.1	0.363
18:24	76.3	69.9	74.4	72	0.44	0.55	0.5	4.4	0.374
								Average	0.374

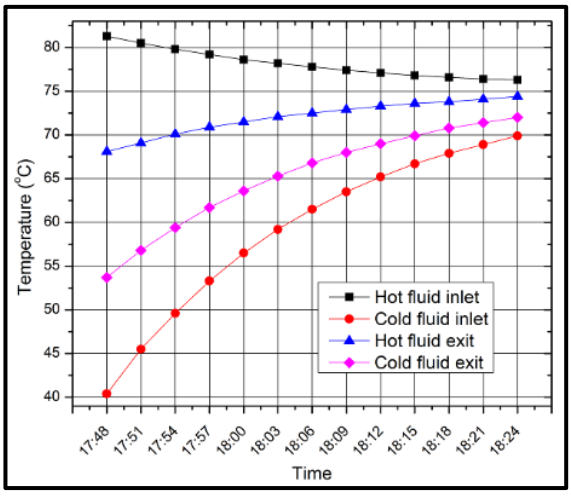

(a) *T* vs *t*

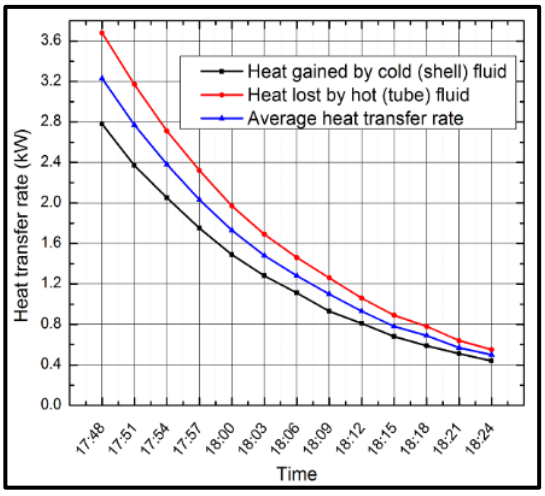

(b) *Q* vs *t*

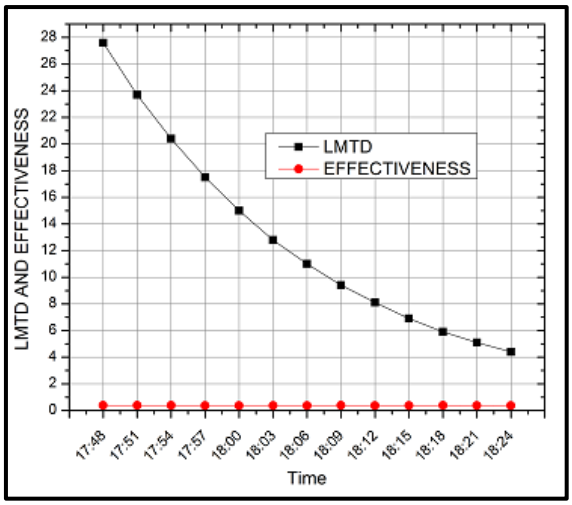

(c) *LMTD* vs *t* and ε vs *t*

Figure 5.16: Variation of different heat exchanger parameters with time based on the experimental results of 13th May 2017

5.3.16 Experiment on 14th May 2017:

The mass flow rate of hot fluid ($\dot{m}_h$) and cold fluid ($\dot{m}_c$) kept at 240 kg/hr and 240 kg/hr respectively. Variations of inlet and outlet temperatures of shell and tube side fluids with respect to the time are given in Figure 5.17 (a). Variations of $\dot{Q}_h$, $\dot{Q}_c$, $\dot{Q}_{avg}$ with respect to time and variations of *LMTD*, ε with respect to time are shown in Figure 5.17 (b) and (c) respectively. The hot fluid Reynold's number (Re_h) was found to be 491.84 and for cold fluid (Re_c) was found to be 174.99 with the set mass flow rates of the fluids. It was observed that the temperature difference between hot fluid inlet and cold fluid exit of the STHE is continuously decreasing with time from a maximum value of 28.4℃ at 18:03 hrs to a minimum value of 4.1℃ at 18:48 hrs. The exit temperature of cold fluid was found to be very close to the inlet temperature of hot fluid at the end of the experiment. The average heat transfer rate between the two fluids and *LMTD* was found to be decreasing with time as the exit temperature of cold fluid is increasing with time. The effectiveness of the STHE is found to be constant through the experiment and found to be an average value of 0.270.

Table 5.17: Fluid temperatures and performance parameters of heat exchanger on 14th May 2017

Conditions	$\dot{m}_h$ = 240 kg/hr			$\dot{m}_c$ = 240 kg/hr		(Re_t)=491.84		(Re_s)=174.99	
Time	T_{hi}	T_{ci}	T_{ho}	T_{co}	$\dot{Q}_c$	$\dot{Q}_h$	$\dot{Q}_{avg}$	*LMTD*	ε
	°C	°C	°C	°C	kW	kW	kW		
18:03	80	41.4	66.4	51.6	2.14	3.8	2.97	28.4	0.276
18:06	79.1	45.2	67.2	54.1	1.86	3.31	2.59	24.9	0.274
18:09	78.4	48.6	67.9	56.4	1.62	2.91	2.27	22	0.273
18:12	77.7	51.6	68.5	58.4	1.43	2.54	1.99	19.2	0.273
18:15	77	54.1	69	60.2	1.26	2.23	1.74	16.9	0.273
18:18	76.5	56.4	69.4	61.7	1.11	1.97	1.54	14.9	0.275
18:21	76.1	58.4	69.9	63	0.96	1.75	1.35	13.1	0.274
18:24	75.7	60.2	70.3	64.2	0.85	1.52	1.18	11.5	0.273
18:27	75.3	61.7	70.6	65.2	0.74	1.32	1.03	10.1	0.272
18:30	75	63.1	70.9	66.2	0.64	1.15	0.89	8.8	0.268
18:33	74.7	64.2	71.1	67	0.57	1.01	0.79	7.7	0.270
18:36	74.5	65.3	71.3	67.7	0.51	0.89	0.7	6.8	0.273
18:39	74.3	66.3	71.5	68.3	0.42	0.78	0.6	6	0.269
18:42	74.1	67	71.7	68.8	0.38	0.67	0.52	5.3	0.263
18:45	74	67.7	71.8	69.3	0.34	0.61	0.47	4.7	0.268
18:48	73.8	68.4	72	69.7	0.27	0.49	0.38	4	0.252
								Average	0.270

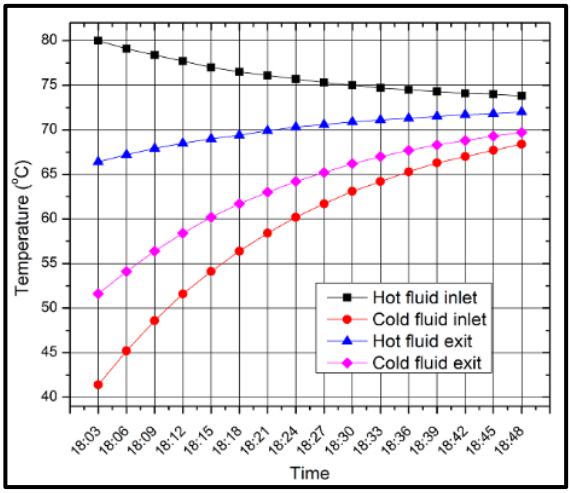

(a) *T* vs *t*

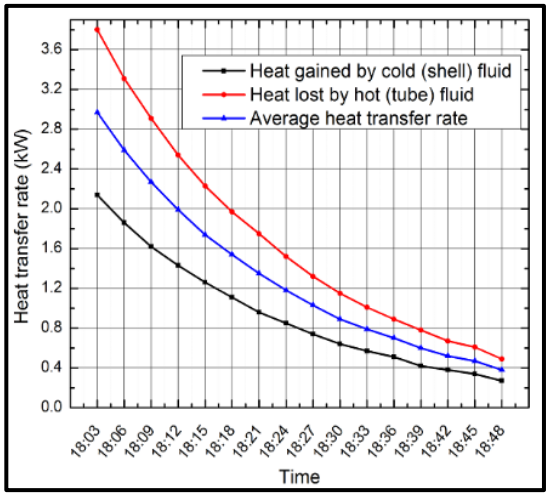

(b) *Q* vs *t*

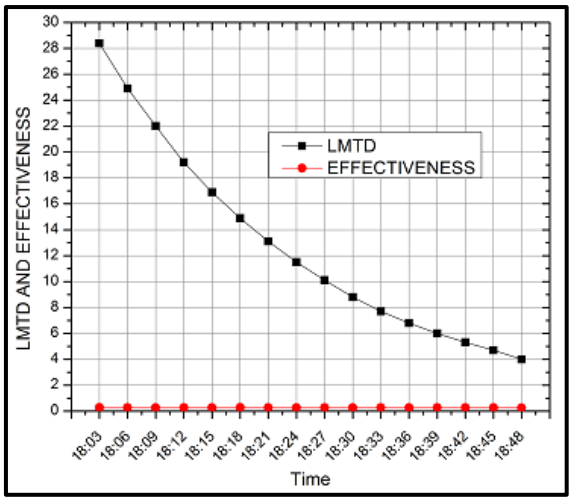

(c) *LMTD* vs *t* and ε vs *t*

Figure 5.17: Variation of different heat exchanger parameters with time based on the experimental results of 14th May 2017

5.3.17 Experiment on 3rd June 2017:

The mass flow rate of hot fluid ($\dot{m}_h$) and cold fluid ($\dot{m}_c$) kept at 60 kg/hr and 300 kg/hr respectively. Variations of inlet and outlet temperatures of shell and tube side fluids with respect to the time are given in Figure 5.18 (a). Variations of $\dot{Q}_h$, $\dot{Q}_c$, $\dot{Q}_{avg}$ with respect to time and variations of *LMTD*, ε with respect to time are shown in Figure 5.18 (b) and (c) respectively. The hot fluid Reynold's number (Re_h) was found to be 122.96 and for cold fluid (Re_c) was found to be 218.74 with the set mass flow rates of the fluids. It was observed that the temperature difference between hot fluid inlet and cold fluid exit of the STHE is continuously decreasing with time from a maximum value of 45.7℃ at 17:57 hrs to a minimum value of 7.2℃ at 18:48 hrs. The exit temperature of cold fluid was found to be very close to the inlet temperature of hot fluid at the end of the experiment. The average heat transfer rate between the two fluids and *LMTD* was found to be decreasing with time as the exit temperature of cold fluid is increasing with time. The effectiveness of the STHE is found to be constant through the experiment and found to be an average value of 0.739.

Table 5.18: Fluid temperatures and performance parameters of heat exchanger on 03rd June 2017

Conditions	$\dot{m}_h$ = 60 kg/hr		$\dot{m}_c$ = 300 kg/hr			(Re_t) = 122.96		(Re_s) = 218.74	
Time	T_{hi}	T_{ci}	T_{ho}	T_{co}	$\dot{Q}_c$	$\dot{Q}_h$	$\dot{Q}_{avg}$	*LMTD*	ε
	°C	°C	°C	°C	kW	kW	kW		
17:57	78.2	25.9	33.3	32.5	2.29	3.13	2.71	21	0.743
18:00	75.2	28.4	35.1	34.4	2.08	2.79	2.44	18.9	0.748
18:03	72.7	30.6	36.7	36	1.86	2.51	2.19	17	0.746
18:06	70.4	32.7	38.1	37.4	1.65	2.25	1.95	15.3	0.742
18:09	68.3	34.5	39.3	38.7	1.47	2.02	1.74	13.6	0.739
18:12	66.4	36.2	40.4	40	1.33	1.81	1.57	12.2	0.746
18:15	64.8	37.6	41.5	41	1.18	1.63	1.4	11	0.738
18:18	63.3	38.9	42.4	41.9	1.04	1.46	1.25	9.8	0.735
18:21	61.9	40	43.2	42.8	0.97	1.31	1.14	8.9	0.747
18:24	60.7	41.1	43.9	43.5	0.86	1.17	1.02	8	0.747
18:27	59.6	42.1	44.5	44.2	0.75	1.05	0.9	7	0.738
18:30	58.7	42.9	45.1	44.9	0.68	0.94	0.81	6.4	0.736
18:33	57.8	43.7	45.7	45.4	0.58	0.84	0.71	5.6	0.722
18:36	57	44.3	46.2	45.9	0.54	0.76	0.65	5.2	0.734
18:39	56.3	44.9	46.6	46.4	0.5	0.68	0.59	4.6	0.743
18:42	55.7	45.6	47	46.8	0.43	0.61	0.52	4.1	0.739
18:45	55.1	46	47.3	47.1	0.4	0.54	0.47	3.7	0.741
18:48	54.6	46.5	47.6	47.4	0.33	0.49	0.41	3.3	0.726
								Average	0.739

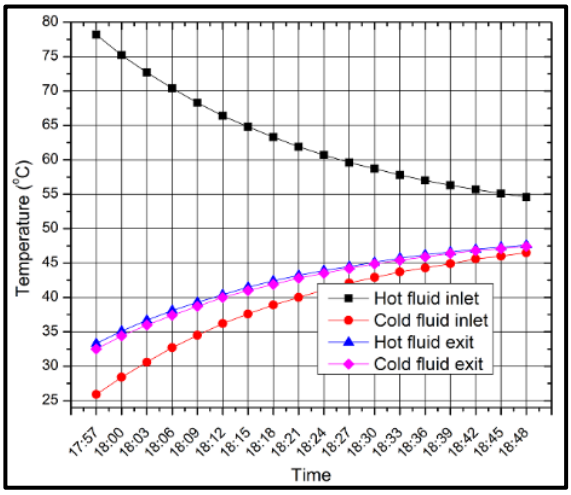

(a) *T* vs *t*

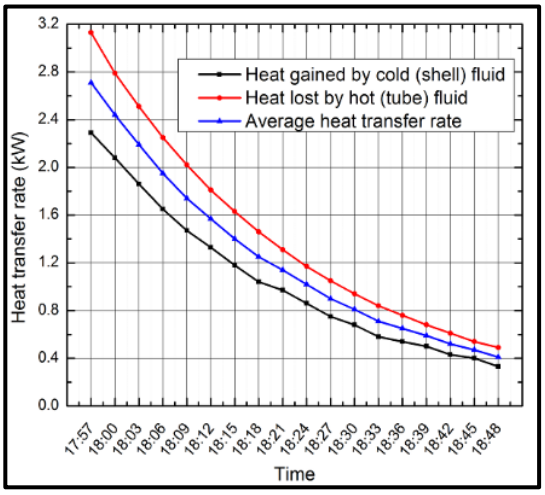

(b) *Q* vs *t*

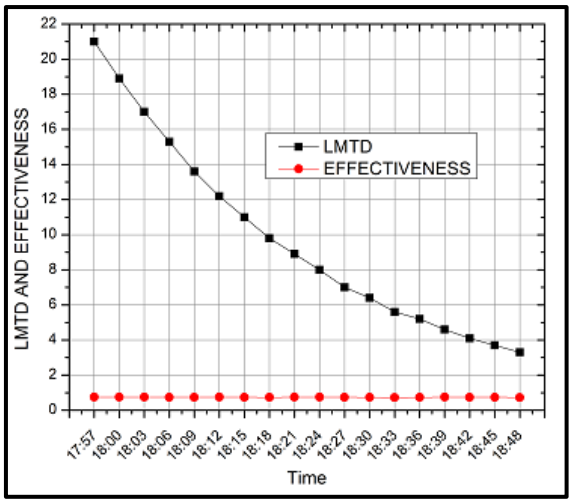

(c) *LMTD* vs *t* and ε vs *t*

Figure 5.18: Variation of different heat exchanger parameters with time based on the experimental results of 03rd June 2017

5.3.18 Experiment on 4th June 2017:

The mass flow rate of hot fluid ($\dot{m}_h$) and cold fluid ($\dot{m}_c$) kept at 120 kg/hr and 300 kg/hr respectively. Variations of inlet and outlet temperatures of shell and tube side fluids with respect to the time are given in Figure 5.19 (a). Variations of $\dot{Q}_h$, $\dot{Q}_c$, $\dot{Q}_{avg}$ with respect to time and variations of *LMTD*, ε with respect to time are shown in Figure 5.19 (b) and (c) respectively. The hot fluid Reynold's number (Re_h) was found to be 245.92 and for cold fluid (Re_c) was found to be 218.74 with the set mass flow rates of the fluids. It was observed that the temperature difference between hot fluid inlet and cold fluid exit of the STHE is continuously decreasing with time from a maximum value of 27.7℃ at 17:57 hrs to a minimum value of 6.7℃ at 18:36 hrs. The exit temperature of cold fluid was found to be very close to the inlet temperature of hot fluid at the end of the experiment. The average heat transfer rate between the two fluids and *LMTD* was found to be decreasing with time as the exit temperature of cold fluid is increasing with time. The effectiveness of the STHE is found to be constant through the experiment and found to be an average value of 0.604.

Table 5.19: Fluid temperatures and performance parameters of heat exchanger on 04th June 2017

Conditions	$\dot{m}_h$ =120 kg/hr		$\dot{m}_c$ =300 kg/hr			(Re_t) = 245.92		(Re_s) = 218.74	
Time	T_{hi}	T_{ci}	T_{ho}	T_{co}	$\dot{Q}_c$	$\dot{Q}_h$	$\dot{Q}_{avg}$	*LMTD*	ε
	°C	°C	°C	°C	kW	kW	kW		
17:57	73.5	39.9	53.7	45.8	2.63	3.54	3.08	26.7	0.658
18:00	72.2	42.2	54.4	47.4	2.34	3.12	2.73	23.6	0.653
18:03	71	44.1	55.2	48.8	2.05	2.77	2.41	20.8	0.643
18:06	70	46	55.9	50.2	1.83	2.45	2.14	18.5	0.640
18:09	69.1	47.5	56.4	51.3	1.62	2.17	1.9	16.3	0.631
18:12	68.3	48.9	56.9	52.3	1.4	1.91	1.65	14.4	0.610
18:15	67.6	50.3	57.4	53.2	1.22	1.69	1.46	12.8	0.605
18:18	66.9	51.4	57.8	54.1	1.11	1.49	1.3	11.3	0.602
18:21	66.3	52.4	58.1	54.8	0.97	1.32	1.14	10	0.588
18:24	65.8	53.3	58.5	55.5	0.85	1.17	1.01	8.8	0.580
18:27	65.3	54.2	58.8	56.1	0.74	1.02	0.88	7.8	0.569
18:30	64.9	55	59	56.7	0.65	0.92	0.78	6.9	0.565
18:33	64.5	55.6	59.3	57.1	0.6	0.8	0.7	6.1	0.564
18:36	64.2	56.2	59.5	57.5	0.51	0.7	0.61	5.4	0.547
								Average	0.604

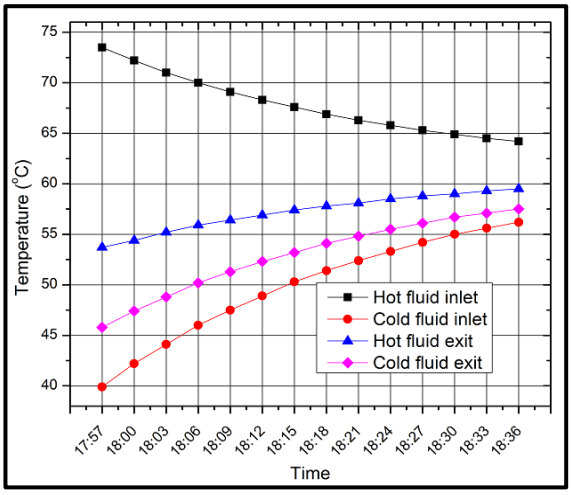

(a) *T* vs *t*

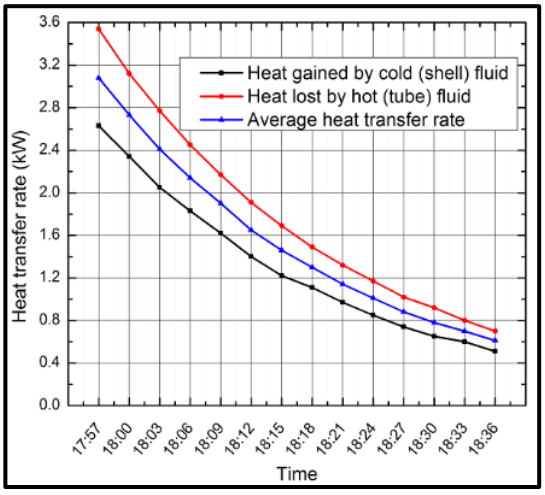

(b) *Q* vs *t*

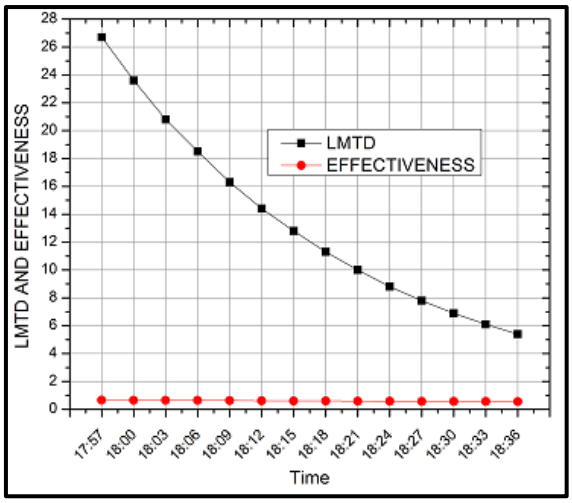

(c) *LMTD* vs *t* and ε vs *t*

Figure 5.19: Variation of different heat exchanger parameters with time based on the experimental results of 04th June 2017

5.3.19 Experiment on 5th June 2017:

The mass flow rate of hot fluid ($\dot{m}_h$) and cold fluid ($\dot{m}_c$) kept at 180 kg/hr and 300 kg/hr respectively. Variations of inlet and outlet temperatures of shell and tube side fluids with respect to the time are given in Figure 5.20 (a). Variations of $\dot{Q}_h$, $\dot{Q}_c$, $\dot{Q}_{avg}$ with respect to time and variations of *LMTD*, ε with respect to time are shown in Figure 5.20 (b) and (c) respectively. The hot fluid Reynold's number (Re_h) was found to be 368.88 and for cold fluid (Re_c) was found to be 218.74 with the set mass flow rates of the fluids. It was observed that the temperature difference between hot fluid inlet and cold fluid exit of the STHE is continuously decreasing with time from a maximum value of 41.3℃ at 17:57 hrs to a minimum value of 6.2℃ at 18:48 hrs. The exit temperature of cold fluid was found to be very close to the inlet temperature of hot fluid at the end of the experiment. The average heat transfer rate between the two fluids and *LMTD* was found to be decreasing with time as the exit temperature of cold fluid is increasing with time. The effectiveness of the STHE is found to be constant through the experiment and found to be an average value of 0.393.

Table 5.20: Fluid temperatures and performance parameters of heat exchanger on 05th June 2017

Conditions	$\dot{m}_h$ = 180 kg/hr		$\dot{m}_c$ = 300 kg/hr			(Re_t) = 368.88		(Re_s) = 218.74	
Time	T_{hi}	T_{ci}	T_{ho}	T_{co}	$\dot{Q}_c$	$\dot{Q}_h$	$\dot{Q}_{avg}$	*LMTD*	ε
	°C	°C	°C	°C	kW	kW	kW		
17:57	81.3	29.4	57.7	40	3.68	4.94	4.31	34.4	0.397
18:00	79.8	33.4	58.7	42.8	3.28	4.41	3.84	30.8	0.396
18:03	78.5	36.9	59.5	45.4	2.96	3.96	3.46	27.6	0.398
18:06	77.2	40	60.4	47.6	2.64	3.53	3.08	24.7	0.396
18:09	76.1	42.9	61.1	49.6	2.35	3.15	2.75	22.1	0.396
18:12	75.2	45.5	61.7	51.5	2.1	2.83	2.46	19.7	0.396
18:15	74.3	47.7	62.3	53.1	1.89	2.51	2.2	17.7	0.396
18:18	73.5	49.7	62.8	54.5	1.67	2.23	1.95	15.8	0.392
18:21	72.9	51.6	63.2	55.9	1.49	2.02	1.75	14.1	0.393
18:24	72.2	53.2	63.6	57	1.32	1.8	1.56	12.7	0.393
18:27	71.6	54.6	64	58.1	1.21	1.59	1.4	11.3	0.394
18:30	71.1	56	64.3	59	1.07	1.42	1.24	10.1	0.393
18:33	70.7	57.2	64.6	59.8	0.92	1.27	1.1	9.1	0.390
18:36	70.3	58.2	64.9	60.6	0.81	1.14	0.98	8.1	0.387
18:39	69.9	59.1	65.1	61.3	0.74	1.01	0.88	7.2	0.390
18:42	69.6	60	65.3	61.9	0.67	0.91	0.79	6.4	0.394
18:45	69.4	60.7	65.5	62.4	0.6	0.82	0.71	5.8	0.390
18:48	69.1	61.4	65.7	62.9	0.53	0.71	0.62	5.2	0.385
								Average	0.393

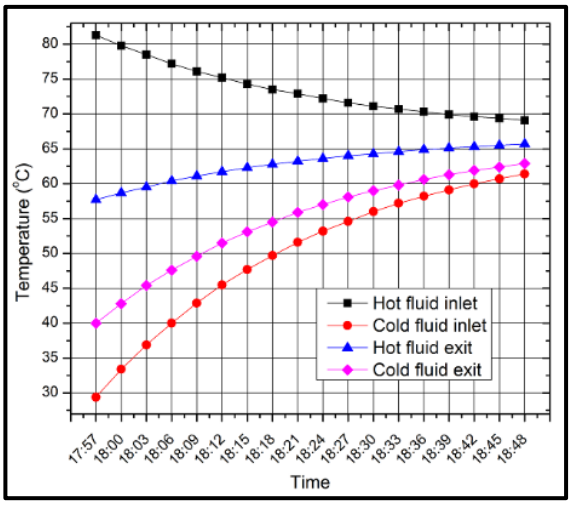

(a) *T* vs *t*

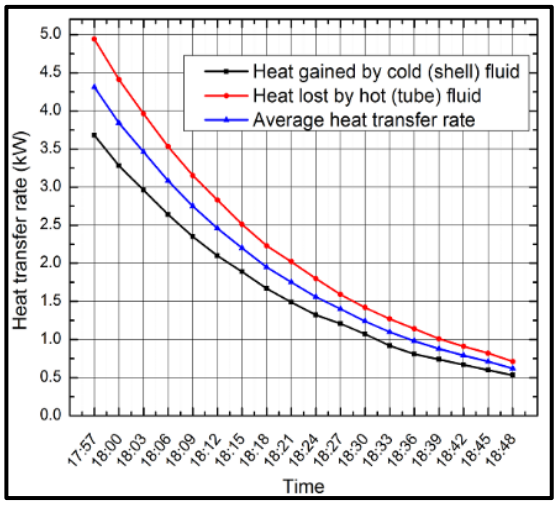

(b) *Q* vs *t*

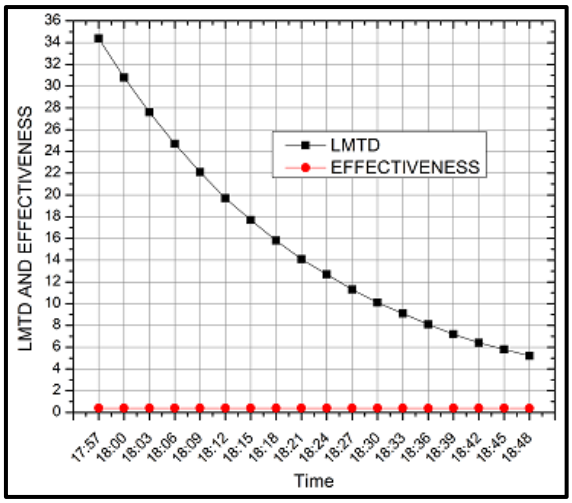

(c) LMTD vs *t* and ε vs *t*

Figure 5.20: Variation of different heat exchanger parameters with time based on the experimental results of 05th June 2017

5.3.20 Experiment on 6th June 2017:

The mass flow rate of hot fluid ($\dot{m}_h$) and cold fluid ($\dot{m}_c$) kept at 240 kg/hr and 300 kg/hr respectively. Variations of inlet and outlet temperatures of shell and tube side fluids with respect to the time are given in Figure 5.21 (a). Variations of $\dot{Q}_h$, $\dot{Q}_c$, $\dot{Q}_{avg}$ with respect to time and variations of *LMTD*, ε with respect to time are shown in Figure 5.21 (b) and (c) respectively. The hot fluid Reynold's number (Re_h) was found to be 491.84 and for cold fluid (Re_c) was found to be 218.74 with the set mass flow rates of the fluids. It was observed that the temperature difference between hot fluid inlet and cold fluid exit of the STHE is continuously decreasing with time from a maximum value of 35.8℃ at 17:57 hrs to a minimum value of 5.7℃ at 18:45 hrs. The exit temperature of cold fluid was found to be very close to the inlet temperature of hot fluid at the end of the experiment. The average heat transfer rate between the two fluids and *LMTD* was found to be decreasing with time as the exit temperature of cold fluid is increasing with time. The effectiveness of the STHE is found to be constant through the experiment and found to be an average value of 0.322.

Table 5.21: Fluid temperatures and performance parameters of heat exchanger on 06th June 2017

Conditions	$\dot{m}_h$ = 240 kg/hr		$\dot{m}_c$ = 300 kg/hr			(Re_t) = 491.84		(Re_s) = 218.74	
Time	T_{hi}	T_{ci}	T_{ho}	T_{co}	$\dot{Q}_c$	$\dot{Q}_h$	$\dot{Q}_{avg}$	*LMTD*	ε
	°C	°C	°C	°C	kW	kW	kW		
17:57	80.7	34.6	63.5	44.9	3.57	4.79	4.18	32.3	0.325
18:00	79.6	38.5	64.2	47.6	3.17	4.28	3.73	28.7	0.326
18:03	78.6	41.9	65	50.1	2.85	3.8	3.32	25.7	0.324
18:06	77.8	44.9	65.6	52.3	2.56	3.4	2.98	23	0.325
18:09	76.9	47.7	66.1	54.2	2.28	3.03	2.65	20.5	0.326
18:12	76.2	50.2	66.6	56	2.03	2.69	2.36	18.3	0.326
18:15	75.6	52.4	67	57.5	1.78	2.4	2.09	16.3	0.323
18:18	75.1	54.3	67.4	58.9	1.6	2.15	1.87	14.6	0.322
18:21	74.6	56.1	67.7	60.2	1.42	1.92	1.67	13	0.324
18:24	74.1	57.6	68	61.3	1.28	1.69	1.48	11.6	0.322
18:27	73.7	59	68.3	62.3	1.13	1.49	1.31	10.3	0.320
18:30	73.4	60.3	68.5	63.1	0.99	1.35	1.17	9.2	0.320
18:33	73.1	61.4	68.7	63.9	0.88	1.21	1.05	8.2	0.322
18:36	72.8	62.3	68.9	64.6	0.81	1.06	0.94	7.4	0.321
18:39	72.6	63.2	69.1	65.2	0.71	0.95	0.83	6.6	0.317
18:42	72.2	64	69.2	65.8	0.6	0.84	0.72	5.8	0.315
18:45	72	64.8	69.4	66.3	0.53	0.72	0.62	5.2	0.309
								Average	0.322

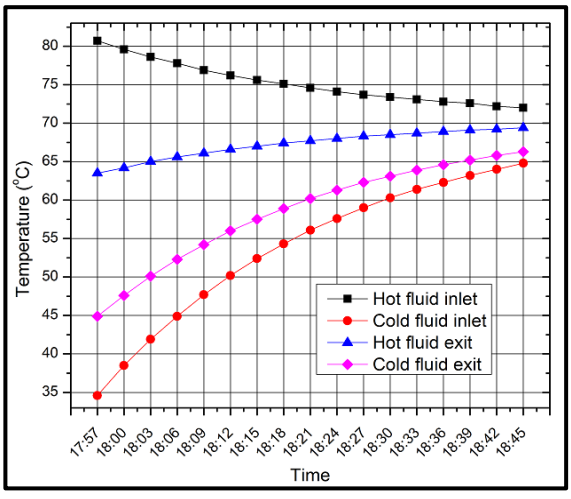

(a) *T* vs *t*

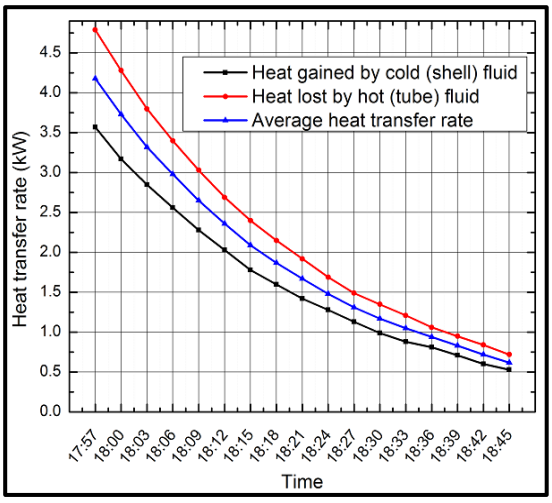

(b) *Q* vs *t*

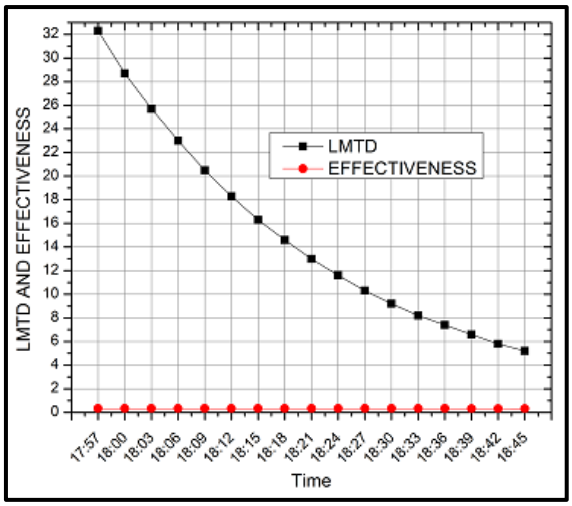

(c) *LMTD* vs *t* and ε vs *t*

Figure 5.21: Variation of different heat exchanger parameters with time based on the experimental results of 06th June 2017

5.3.21 Experiment on 7th June 2017:

The mass flow rate of hot fluid ($\dot{m}_h$) and cold fluid ($\dot{m}_c$) kept at 300 kg/hr and 60 kg/hr respectively. Variations of inlet and outlet temperatures of shell and tube side fluids with respect to the time are given in Figure 5.22 (a). Variations of $\dot{Q}_h$, $\dot{Q}_c$, $\dot{Q}_{avg}$ with respect to time and variations of *LMTD*, ε with respect to time are shown in Figure 5.22 (b) and (c) respectively. The hot fluid Reynold's number (Re_h) was found to be 614.8 and for cold fluid (Re_c) was found to be 43.75 with the set mass flow rates of the fluids. It was observed that the temperature difference between hot fluid inlet and cold fluid exit of the STHE is continuously decreasing with time from a maximum value of 18.9℃ at 17:57 hrs to a minimum value of 0.8℃ at 18:30 hrs. The exit temperature of cold fluid was found to be very close to the inlet temperature of hot fluid at the end of the experiment. The average heat transfer rate between the two fluids and *LMTD* was found to be decreasing with time as the exit temperature of cold fluid is increasing with time. The effectiveness of the STHE is found to be constant through the experiment and found to be an average value of 0.683.

Table 5.22: Fluid temperatures and performance parameters of heat exchanger on 07th June 2017

Conditions	$\dot{m}_h$ **= 300 kg/hr**		$\dot{m}_c$ **= 60 kg/hr**			(Re_t) **= 614.80**		(Re_s) **= 43.75**	
Time	T_{hi}	T_{ci}	T_{ho}	T_{co}	$\dot{Q}_c$	$\dot{Q}_h$	$\dot{Q}_{avg}$	*LMTD*	ε
	°C	**°C**	**°C**	**°C**	**kW**	**kW**	**kW**		
17:57	84.2	35	76.2	65.3	2.11	2.79	2.45	28.6	0.714
18:00	83.7	46.4	77.6	69.4	1.61	2.11	1.86	21.6	0.715
18:03	83.3	55.1	78.7	72.5	1.22	1.58	1.4	16.4	0.712
18:06	83	61.6	79.6	74.8	0.92	1.18	1.05	12.4	0.704
18:09	82.8	66.5	80.2	76.6	0.7	0.9	0.8	9.4	0.704
18:12	82.6	70.3	80.7	77.9	0.53	0.65	0.59	7.2	0.688
18:15	82.4	73.1	81	78.9	0.4	0.51	0.46	5.4	0.710
18:18	82.3	75.4	81.3	79.6	0.3	0.37	0.33	4.1	0.686
18:21	82.2	77	81.5	80.2	0.22	0.26	0.24	3.1	0.662
18:24	82.2	78.2	81.6	80.6	0.17	0.22	0.2	2.4	0.717
18:27	82.1	79.2	81.8	81.1	0.13	0.12	0.12	1.8	0.594
18:30	82.1	79.9	81.9	81.3	0.1	0.08	0.09	1.4	0.587
								Average	0.683

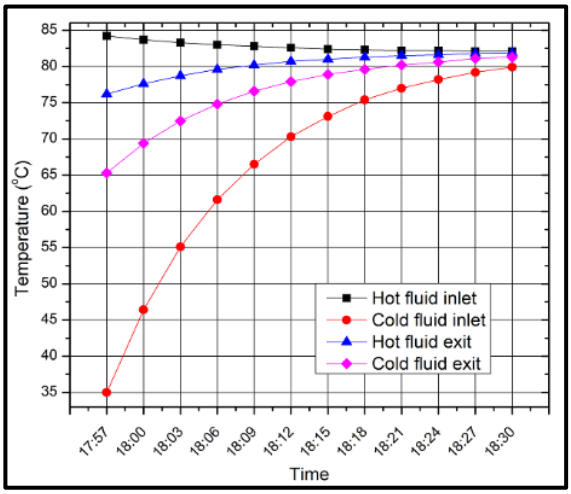

(a) *T* vs *t*

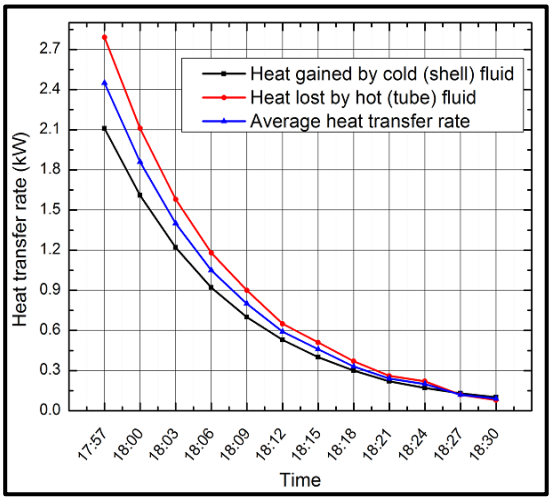

(b) *Q* vs *t*

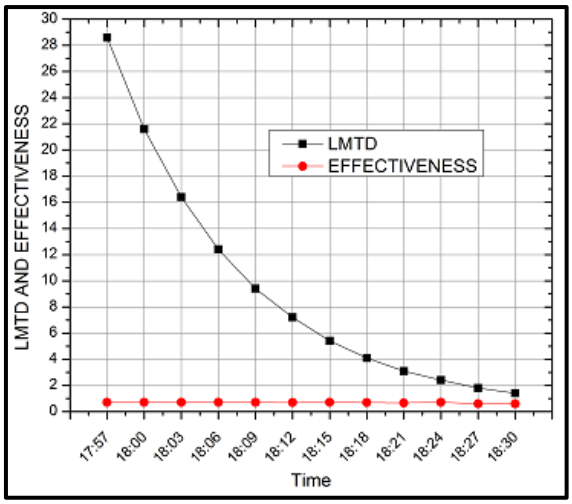

(c) *LMTD* vs *t* and ε vs *t*

Figure 5.22: Variation of different heat exchanger parameters with time based on the experimental results of 07th June 2017

5.3.22 Experiment on 8th June 2017:

The mass flow rate of hot fluid ($\dot{m}_h$) and cold fluid ($\dot{m}_c$) kept at 300 kg/hr and 120 kg/hr respectively. Variations of inlet and outlet temperatures of shell and tube side fluids with respect to the time are given in Figure 5.23 (a). Variations of $\dot{Q}_h$, $\dot{Q}_c$, $\dot{Q}_{avg}$ with respect to time and variations of *LMTD*, ε with respect to time are shown in Figure 5.23 (b) and (c) respectively. The hot fluid Reynold's number (Re_h) was found to be 614.8 and for cold fluid (Re_c) was found to be 87.5 with the set mass flow rates of the fluids. It was observed that the temperature difference between hot fluid inlet and cold fluid exit of the STHE is continuously decreasing with time from a maximum value of 24.4℃ at 18:12 hrs to a minimum value of 1.8℃ at 18:51 hrs. The exit temperature of cold fluid was found to be very close to the inlet temperature of hot fluid at the end of the experiment. The average heat transfer rate between the two fluids and *LMTD* was found to be decreasing with time as the exit temperature of cold fluid is increasing with time. The effectiveness of the STHE is found to be constant through the experiment and found to be an average value of 0.5.

Table 5.23: Fluid temperatures and performance parameters of heat exchanger on 08th June 2017

Conditions	$\dot{m}_h$ = 300 kg/hr		$\dot{m}_c$ = 120 kg/hr			(Re_t) = 614.80		(Re_s) = 87.50	
Time	T_{hi}	T_{ci}	T_{ho}	T_{co}	$\dot{Q}_c$	$\dot{Q}_h$	$\dot{Q}_{avg}$	*LMTD*	ε
	°C	°C	°C	°C	kW	kW	kW		
18:12	83.1	39.5	72.9	58.7	2.68	3.53	3.1	28.6	0.510
18:15	82.4	46.7	74	62.5	2.2	2.93	2.57	23.5	0.516
18:18	81.8	52.6	75.1	65.6	1.81	2.36	2.08	19.2	0.511
18:21	81.4	57.5	75.9	68	1.46	1.93	1.7	15.8	0.510
18:24	81.1	61.5	76.5	70.1	1.21	1.61	1.41	12.9	0.516
18:27	80.8	64.8	77.1	71.8	0.98	1.29	1.14	10.6	0.511
18:30	80.5	67.4	77.5	73.2	0.81	1.04	0.92	8.6	0.504
18:33	80.3	69.6	77.9	74.3	0.66	0.83	0.75	7.1	0.503
18:36	80.2	71.4	78.2	75.2	0.54	0.69	0.61	5.9	0.497
18:39	80	72.8	78.4	76	0.44	0.54	0.49	4.8	0.488
18:42	79.9	74.1	78.6	76.7	0.36	0.44	0.4	3.9	0.495
18:45	79.8	75.1	78.8	77.2	0.29	0.33	0.31	3.2	0.473
18:48	79.8	75.9	78.9	77.6	0.24	0.3	0.27	2.6	0.497
18:51	79.7	76.5	79	77.9	0.19	0.22	0.21	2.2	0.471
								Average	0.500

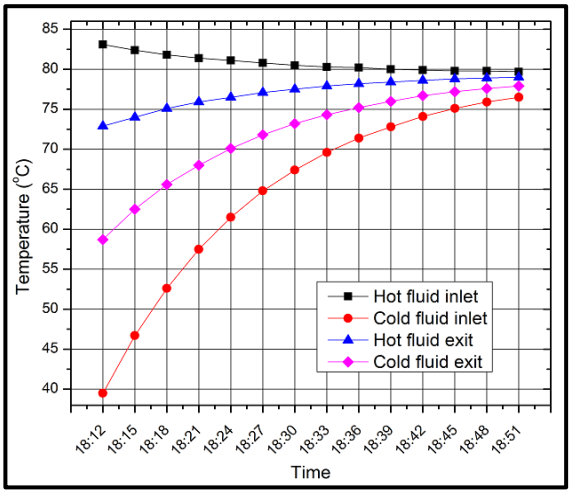

(a) *T* vs *t*

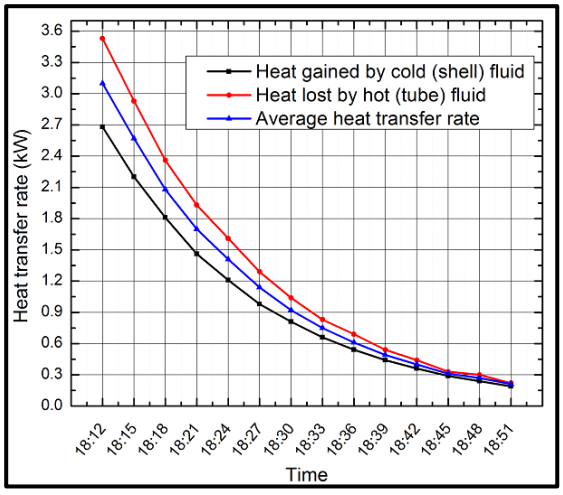

(b) *Q* vs *t*

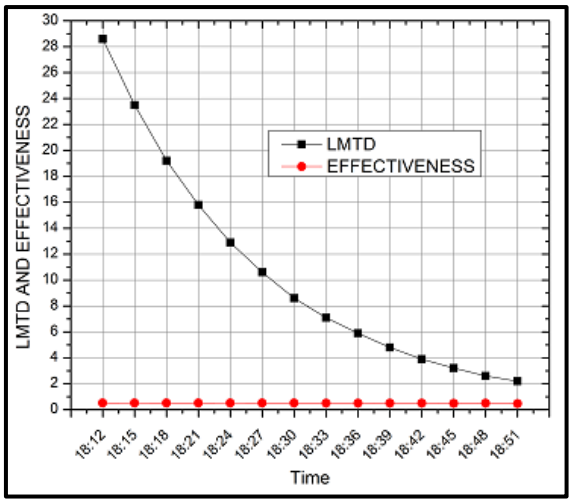

(c) *LMTD* vs *t* and ε vs *t*

Figure 5.23: Variation of different heat exchanger parameters with time based on the experimental results of 08th June 2017

5.3.23 Experiment on 9th June 2017:

The mass flow rate of hot fluid ($\dot{m}_h$) and cold fluid ($\dot{m}_c$) kept at 300 kg/hr and 180 kg/hr respectively. Variations of inlet and outlet temperatures of shell and tube side fluids with respect to the time are given in Figure 5.24 (a). Variations of $\dot{Q}_h$, $\dot{Q}_c$, $\dot{Q}_{avg}$ with respect to time and variations of *LMTD*, ε with respect to time are shown in Figure 5.24 (b) and (c) respectively. The hot fluid Reynold's number (Re_h) was found to be 614.8 and for cold fluid (Re_c) was found to be 131.4 with the set mass flow rates of the fluids. It was observed that the temperature difference between hot fluid inlet and cold fluid exit of the STHE is continuously decreasing with time from a maximum value of 26.5℃ at 18:39 hrs to a minimum value of 4.0℃ at 19:15 hrs. The exit temperature of cold fluid was found to be very close to the inlet temperature of hot fluid at the end of the experiment. The average heat transfer rate between the two fluids and *LMTD* was found to be decreasing with time as the exit temperature of cold fluid is increasing with time. The effectiveness of the STHE is found to be constant through the experiment and found to be an average value of 0.393.

Table 5.24: Fluid temperatures and performance parameters of heat exchanger on 09th June 2017

Conditions	$\dot{m}_h$ = 300 kg/hr		$\dot{m}_c$ = 180 kg/hr			(Re_t) = 614.80		(Re_s) = 131.24	
Time	T_{hi}	T_{ci}	T_{ho}	T_{co}	$\dot{Q}_c$	$\dot{Q}_h$	$\dot{Q}_{avg}$	*LMTD*	ε
	°C	°C	°C	°C	kW	kW	kW		
18:39	81.9	41.6	70.9	55.4	2.88	3.85	3.37	27.9	0.400
18:42	81.2	46.8	71.8	58.5	2.45	3.29	2.87	23.8	0.399
18:45	80.6	51.2	72.6	61.3	2.11	2.79	2.45	20.4	0.399
18:48	80.1	55	73.2	63.6	1.81	2.4	2.1	17.4	0.400
18:51	79.6	58.2	73.8	65.6	1.53	2	1.77	14.8	0.396
18:54	79.3	61	74.2	67.2	1.3	1.76	1.53	12.7	0.400
18:57	78.9	63.3	74.8	68.6	1.11	1.44	1.27	10.8	0.389
19:00	78.7	65.4	75.1	69.9	0.96	1.26	1.11	9.2	0.399
19:03	78.4	67.1	75.4	71	0.81	1.04	0.92	7.8	0.389
19:06	78.2	68.5	75.7	71.9	0.7	0.87	0.78	6.7	0.385
19:09	78.1	69.8	75.9	72.6	0.59	0.76	0.68	5.8	0.392
19:12	77.9	70.9	76.1	73.3	0.51	0.62	0.56	4.9	0.383
19:15	77.8	71.8	76.2	73.8	0.42	0.55	0.48	4.2	0.383
								Average	0.393

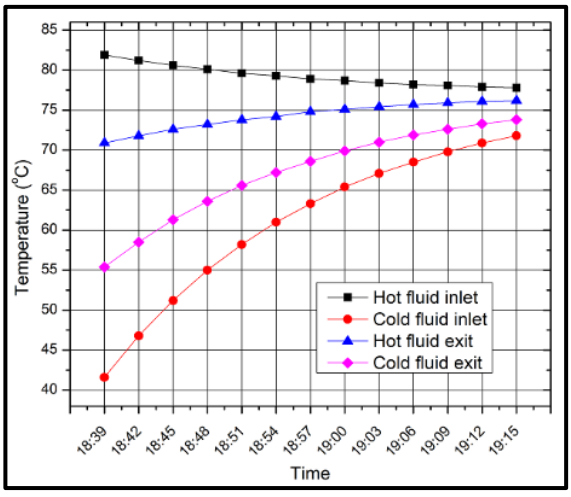

(a) *T* vs *t*

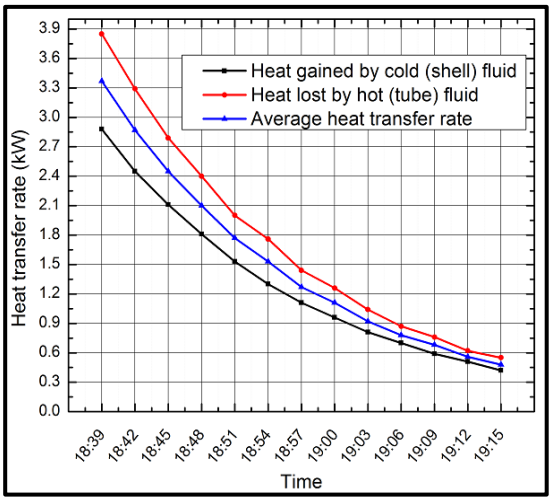

(b) *Q* vs *t*

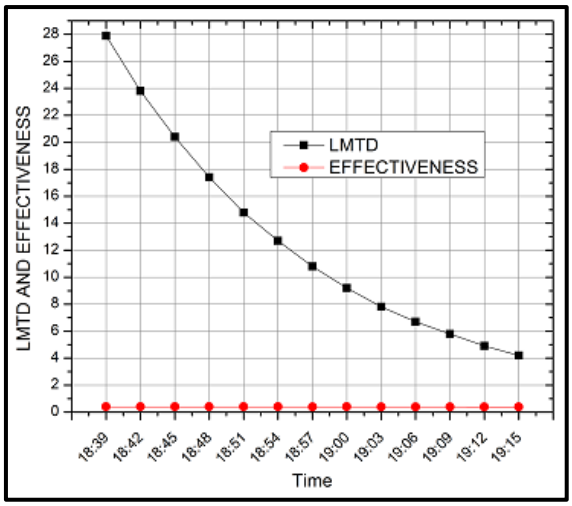

(c) *LMTD* vs *t* and ε vs *t*

Figure 5.24: Variation of different heat exchanger parameters with time based on the experimental results of 09th June 2017

5.3.24 Experiment on 10th June 2017:

The mass flow rate of hot fluid ($\dot{m}_h$) and cold fluid ($\dot{m}_c$) kept at 300 kg/hr and 240 kg/hr respectively. Variations of inlet and outlet temperatures of shell and tube side fluids with respect to the time are given in Figure 5.25 (a). Variations of $\dot{Q}_h$, $\dot{Q}_c$, $\dot{Q}_{avg}$ with respect to time and variations of *LMTD*, ε with respect to time are shown in Figure 5.25 (b) and (c) respectively. The hot fluid Reynold's number (Re_h) was found to be 614.8 and for cold fluid (Re_c) was found to be 174.99 with the set mass flow rates of the fluids. It was observed that the temperature difference between hot fluid inlet and cold fluid exit of the STHE is continuously decreasing with time from a maximum value of 35.8℃ at 18:18 hrs to a minimum value of 5.5℃ at 19:00 hrs. The exit temperature of cold fluid was found to be very close to the inlet temperature of hot fluid at the end of the experiment. The average heat transfer rate between the two fluids and *LMTD* was found to be decreasing with time as the exit temperature of cold fluid is increasing with time. The effectiveness of the STHE is found to be constant through the experiment and found to be an average value of 0.325.

Table 5.25: Fluid temperatures and performance parameters of heat exchanger on 10th June 2017

Conditions	$\dot{m}_h$ = 300 kg/hr		$\dot{m}_c$ = 240 kg/hr			(Re_t) = 614.80		(Re_s) = 174.99	
Time	T_{hi}	T_{ci}	T_{ho}	T_{co}	$\dot{Q}_c$	$\dot{Q}_h$	$\dot{Q}_{avg}$	*LMTD*	ε
	°C	°C	°C	°C	kW	kW	kW		
18:18	82.6	32.8	67.6	46.8	3.91	5.21	4.56	35.3	0.328
18:21	81.5	38.1	68.5	50.3	3.39	4.53	3.96	30.8	0.327
18:24	80.7	42.7	69.3	53.3	2.96	3.96	3.46	27	0.327
18:27	80	46.7	70.1	56.1	2.62	3.46	3.04	23.7	0.327
18:30	79.4	50.3	70.7	58.4	2.28	3.04	2.66	20.7	0.328
18:33	78.8	53.3	71.2	60.5	1.99	2.65	2.32	18.1	0.326
18:36	78.3	56	71.6	62.2	1.73	2.33	2.03	15.8	0.327
18:39	77.9	58.3	72	63.8	1.53	2.04	1.79	13.9	0.328
18:42	77.4	60.5	72.4	65.1	1.3	1.76	1.53	12.1	0.325
18:45	77.1	62.2	72.7	66.4	1.16	1.54	1.35	10.6	0.325
18:48	76.8	63.8	73	67.4	0.99	1.33	1.16	9.3	0.320
18:51	76.6	65.2	73.2	68.4	0.9	1.19	1.05	8.1	0.330
18:54	76.3	66.4	73.4	69.2	0.79	1.01	0.9	7.1	0.326
18:57	76.2	67.5	73.6	69.8	0.65	0.9	0.77	6.3	0.317
19:00	76	68.4	73.8	70.5	0.59	0.76	0.67	5.4	0.316
								Average	0.325

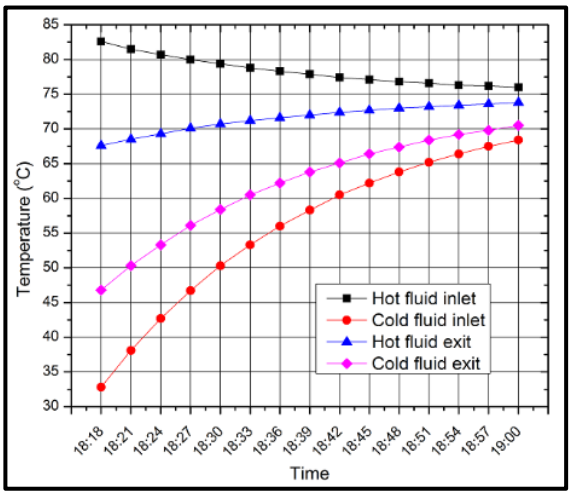

(a) *T* vs *t*

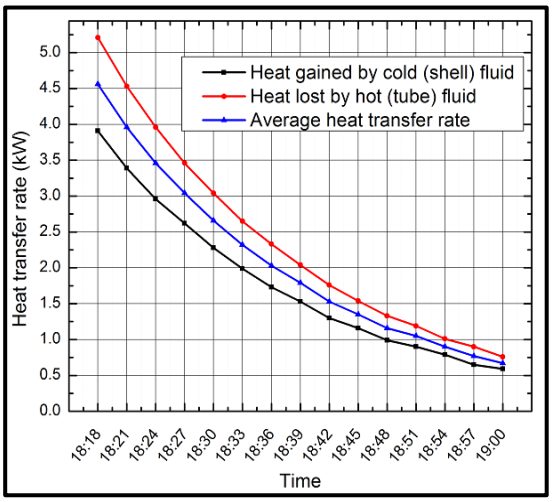

(b) *Q* vs *t*

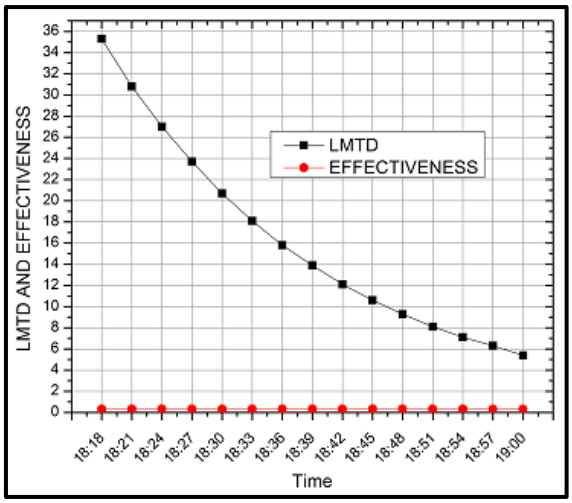

(c) *LMTD* vs *t* and ε vs *t*

Figure 5.25: Variation of different heat exchanger parameters with time based on the experimental results of 10th June 2017

5.3.25 Experiment on 11th June 2017:

The mass flow rate of hot fluid ($\dot{m}_h$) and cold fluid ($\dot{m}_c$) kept at 300 kg/hr and 300 kg/hr respectively. Variations of inlet and outlet temperatures of shell and tube side fluids with respect to the time are given in Figure 5.26 (a). Variations of $\dot{Q}_h$, $\dot{Q}_c$, $\dot{Q}_{avg}$ with respect to time and variations of *LMTD*, ε with respect to time are shown in Figure 5.26 (b) and (c) respectively. The hot fluid Reynold's number (Re_h) was found to be 614.8 and for cold fluid (Re_c) was found to be 218.74 with the set mass flow rates of the fluids. It was observed that the temperature difference between hot fluid inlet and cold fluid exit of the STHE is continuously decreasing with time from a maximum value of 34.8℃ at 18:15 hrs to a minimum value of 5.4℃ at 19:03 hrs. The exit temperature of cold fluid was found to be very close to the inlet temperature of hot fluid at the end of the experiment. The average heat transfer rate between the two fluids and *LMTD* was found to be decreasing with time as the exit temperature of cold fluid is increasing with time. The effectiveness of the STHE is found to be constant through the experiment and found to be an average value of 0.275.

Table 5.26: Fluid temperatures and performance parameters of heat exchanger on 11th June 2017

Conditions	$\dot{m}_h$ **= 300 kg/hr**		$\dot{m}_c$ **= 300 kg/hr**			(Re_t) **= 614.80**		(Re_s) **= 218.74**	
Time	T_{hi}	T_{ci}	T_{ho}	T_{co}	$\dot{Q}_c$	$\dot{Q}_h$	$\dot{Q}_{avg}$	*LMTD*	ε
	°C	**°C**	**°C**	**°C**	**kW**	**kW**	**kW**		
18:15	81.3	35.5	66.8	46.5	3.81	5.06	4.44	34.8	0.278
18:18	80.4	39.6	67.4	49.3	3.39	4.53	3.96	31.1	0.279
18:21	79.5	43.3	68	51.9	2.99	4	3.49	27.6	0.277
18:24	78.8	46.6	68.5	54.2	2.67	3.57	3.12	24.5	0.278
18:27	78.2	49.4	69	56.3	2.38	3.18	2.78	21.9	0.277
18:30	77.6	52	69.4	58.1	2.13	2.82	2.48	19.4	0.278
18:33	77	54.3	69.9	59.7	1.88	2.5	2.19	17.3	0.277
18:36	76.5	56.4	70.2	61.2	1.67	2.22	1.94	15.4	0.277
18:39	76.1	58.2	70.5	62.4	1.45	1.97	1.71	13.7	0.274
18:42	75.7	59.8	70.8	63.5	1.31	1.72	1.52	12.2	0.274
18:45	75.4	61.3	71	64.5	1.13	1.54	1.34	10.9	0.273
18:48	75.1	62.5	71.2	65.5	1.03	1.37	1.2	9.6	0.273
18:51	74.9	63.6	71.4	66.3	0.92	1.22	1.07	8.6	0.272
18:54	74.7	64.7	71.5	67	0.81	1.12	0.96	7.7	0.275
18:57	74.5	65.6	71.7	67.7	0.74	0.97	0.86	6.8	0.277
19:00	74.3	66.4	71.8	68.2	0.63	0.87	0.75	6.1	0.272
19:03	74.1	67.1	71.9	68.7	0.56	0.76	0.66	5.4	0.271
								Average	0.275

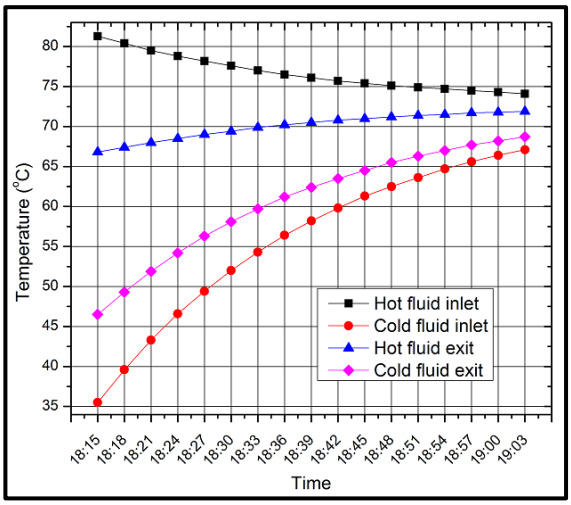

(a) *T* vs *t*

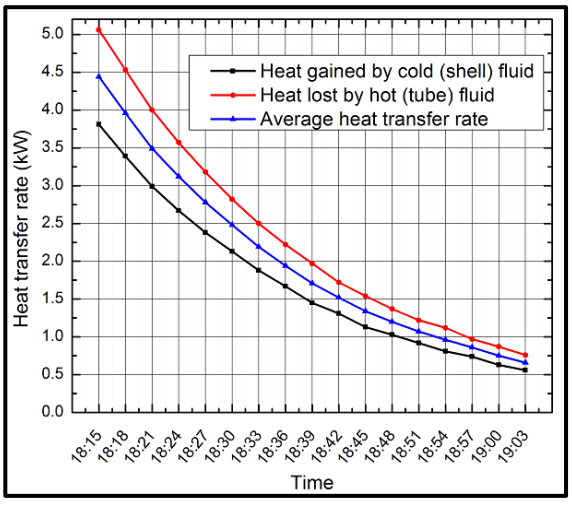

(b) *Q* vs *t*

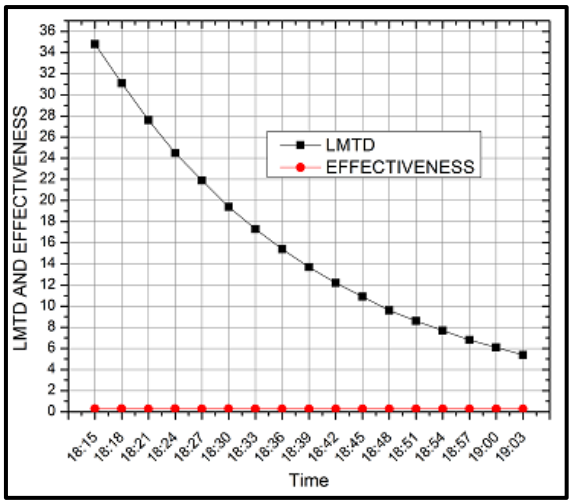

(c) *LMTD* vs *t* and ε vs *t*

Figure 5.26: Variation of different heat exchanger parameters with time based on the experimental results of 11th June 2017

5.4 Performance analysis of shell and tube heat exchanger

Variation of theoretical and experimental values of effectiveness of the STHE with mass flow rate of tube and shell side fluids is presented in Table 5.27. Similarly, variations of theoretical and experimental values of hot fluid shell side fluids Reynolds numbers with mass flow rate of hot fluid shell side fluids is also presented in Table 5.27. The theoretical and experimental values of effectiveness of STHE are in well agreement. It was observed that at lower value of mass flow rate of tube side fluid i.e. 60 kg/hr, the value of effectiveness of the STHE is increasing with increase in mass flow rate of shell side fluid from 120 kg/hr to 300 kg/hr. At higher values of mass flow rate of tube side fluid i.e. equal and above 120 kg/hr, the effectiveness of STHE is observed to be decreasing with the increase in shell side fluid from 120 kg/hr to 300 kg/hr. At higher values of mass flow rates the thermal stratification effects are more on cold fluid which tends to decrease the heat transfer coefficients and hence the effectiveness is observed to be decreased with the increase in mass flow rate of the shell side fluid. Lower values of effectiveness are obtained when both hot fluid and shell side fluids are allowed to flow at a lower mass flow rate of 60 kg/hr. The effectiveness is observed to be higher when mass flow rate of shell side fluid is kept lower i.e. 60 kg/hr and hot fluid mass flow rate is higher i.e. 120 kg/hr to 300 kg/hr.

Table 5.27: Variation of effectiveness of STHE, Reynold's number of tube and shell side with fluid mass flow rate

Hot fluid mass flow rate	Cold fluid mass flow rate	Calculated effectiveness	Experimental effectiveness	Tube side Reynold's no	Shell side Reynold's no
$\dot{m}_h$ (kg/hr)	$\dot{m}_c$ (kg/hr)	ε_{cal}	$\varepsilon_{\exp}$	$(\mathrm{Re}_t)_{cal}$	$(\mathrm{Re}_s)_{cal}$
60	60	0.50	0.514	122.96	43.75
	120	0.62	0.629	122.96	87.1
	180	0.68	0.691	122.96	130.61
	240	0.71	0.719	122.96	174.15
	300	0.73	0.739	122.96	217.7
120	60	0.60	0.604	245.92	43.75
	120	0.40	0.408	245.92	87.1
	180	0.45	0.459	245.92	130.61
	240	0.48	0.489	245.92	174.15
	300	0.50	0.604	245.92	217.7
180	60	0.65	0.651	368.88	43.75
	120	0.45	0.449	368.88	87.1
	180	0.34	0.493	368.88	130.61
	240	0.37	0.372	368.88	174.15
	300	0.39	0.393	368.88	217.7
240	60	0.68	0.665	491.84	43.75
	120	0.48	0.477	491.84	87.1
	180	0.37	0.374	491.84	130.61
	240	0.30	0.270	491.84	174.15
	300	0.32	0.322	491.84	217.7
300	60	0.70	0.683	614.8	43.75
	120	0.50	0.500	614.8	87.1
	180	0.39	0.393	614.8	130.61
	240	0.32	0.325	614.8	174.15
	300	0.27	0.275	614.8	217.7

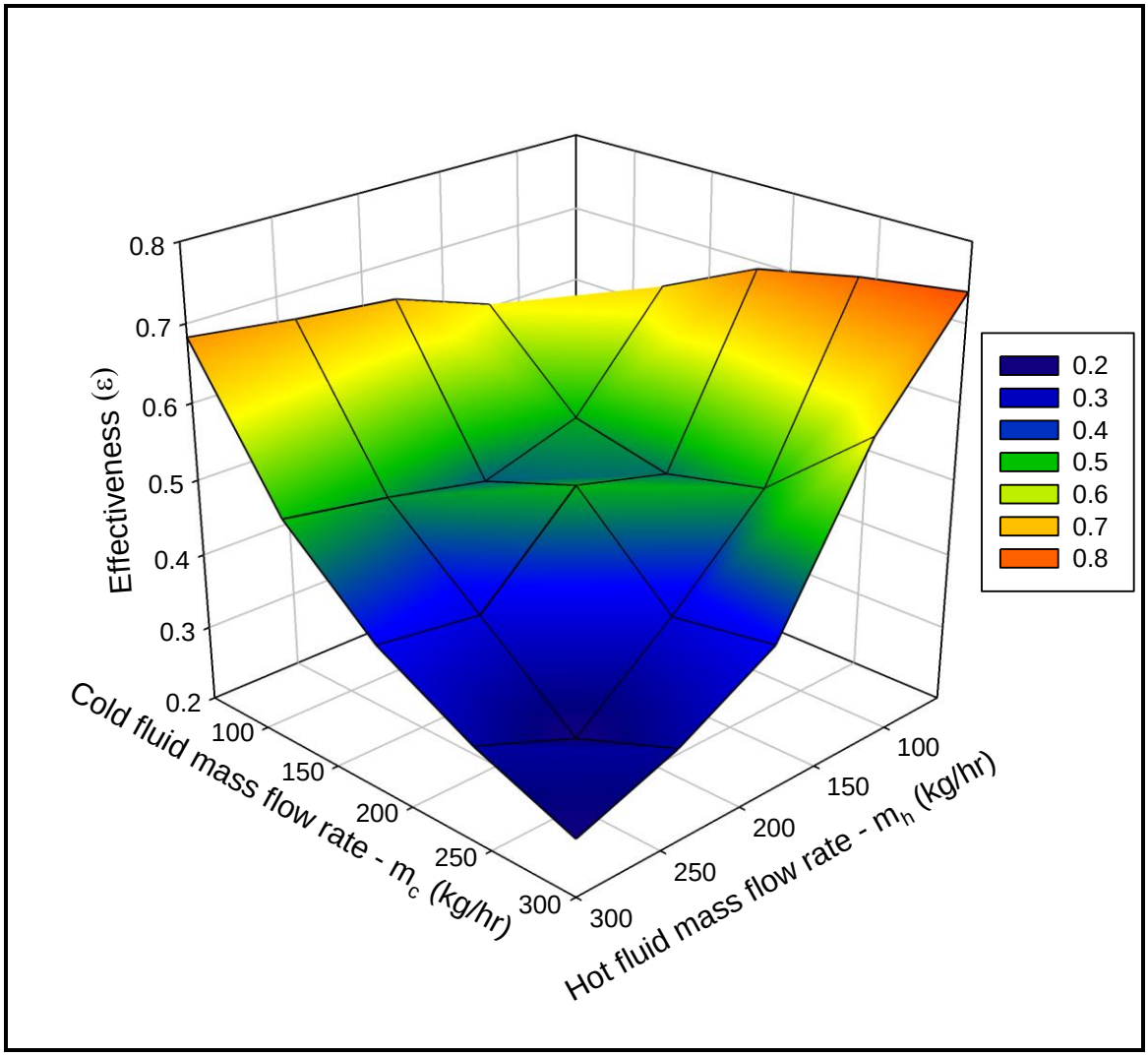

Figure 5.27: Variation of heat exchanger effectiveness w.r.t. fluid flow rate

It is concluded that to obtain higher values of effectiveness the shell side fluid mass flow rate should be lower with higher mass flow rates on tube side. A higher value of effectiveness of STHE can also be obtained with higher values of mass flow rate on shell side then the tube side mass flow rate should be lower.

5.5 Comparison between experimental and calculated fluid temperatures

In order to check the effectiveness of the method developed for STHE design, comparisons were done between the experimental outlet fluid temperatures and calculated

outlet fluid temperatures while keeping the inlet fluid temperatures same as that of the experimental results. One such comparison between experimental and calculated outlet fluid temperatures is indicated in Table 5.28. The percentage deviation as shown in Table 5.28 varied from -1.44 to 0.12 and -6.43 to -0.12 for hot and cold fluid outlet temperatures respectively. It concludes that the method developed to design STHE is very effective and should be used in STHE designing.

Table 5.28: Comparison between experimental and calculated fluid temperatures on 07th June 2017

Conditions	$\dot{m}_h$ = 300 kg/hr				$\dot{m}_c$ = 60 kg/hr			
Time	T_{hi}	T_{ci}	$(T_{ho})_{exp}$	$(T_{co})_{exp}$	$(T_{ho})_{cal}$	$(T_{co})_{cal}$	Percentage deviation from experimental results	
	°C	°C	°C	°C	°C	°C	$(T_{ho})_{percentage}$	$(T_{co})_{percentage}$
17:57	84.2	35	76.2	65.3	77.3	69.5	-1.44	-6.43
18:00	83.7	46.4	77.6	69.4	78.5	72.6	-1.16	-4.61
18:03	83.3	55.1	78.7	72.5	79.3	74.9	-0.76	-3.31
18:06	83	61.6	79.6	74.8	80.0	76.6	-0.50	-2.41
18:09	82.8	66.5	80.2	76.6	80.5	77.9	-0.37	-1.70
18:12	82.6	70.3	80.7	77.9	80.9	78.9	-0.25	-1.28
18:15	82.4	73.1	81	78.9	81.1	79.6	-0.12	-0.89
18:18	82.3	75.4	81.3	79.6	81.3	80.2	0.00	-0.75
18:21	82.2	77	81.5	80.2	81.5	80.6	0.00	-0.50
18:24	82.2	78.2	81.6	80.6	81.6	81	0.00	-0.50
18:27	82.1	79.2	81.8	81.1	81.7	81.2	0.12	-0.12
18:30	82.1	79.9	81.9	81.3	81.8	81.4	0.12	-0.12

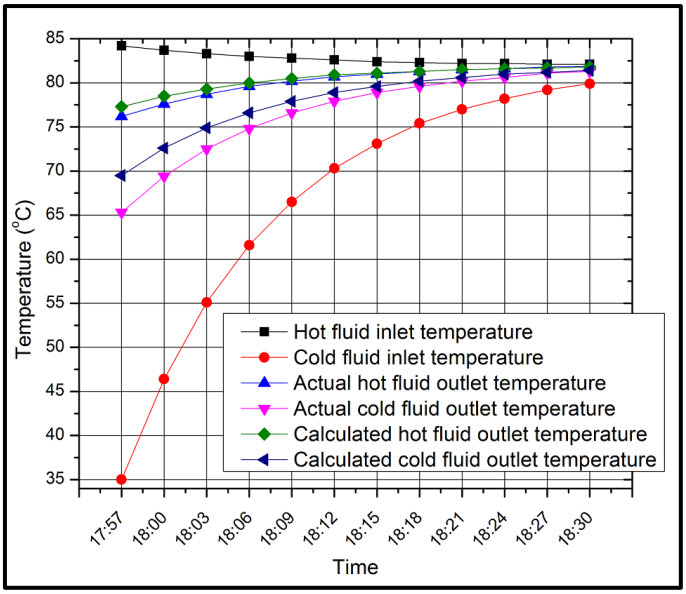

Figure 5.28: Comparison between experimental and calculated fluid temperatures on 07th June 2017

Chapter 6 CONCLUSIONS

Jaggery traditionally called as Gur in India, is prepared by using sugarcane juice and bagasse as raw materials. Dry Bagasse is used to produce the required amount of heat by combustion in an open earthen furnace. Heat produced is used to boil the sugarcane juice up to its striking point temperature to prepare jaggery. The energy loss due to inefficient combustion process, the energy loss through exhaust gases, conduction, convection and radiation energy losses from the furnace wall make the conventional open earthen pan furnace thermally inefficient unit. Bagasse can be saved either by making the process more efficient or using alternative sources of energy to produce heat required for the jaggery making process. The bagasse saved can be used as a raw material for paper and pulp industry and can also be used as a raw material to produce the industrial process heat, thereby generating additional money to the farmers.

In the present work, a modified process is proposed to substitute conventional jaggery making process. In the modified process, solar energy is proposed to use as a source of heat energy in place of bagasse to boil the sugarcane juice. As a part of the proposed process, a heat recovery unit comprising a heat exchanger and a solar collector is initially designed, fabricated and tested. An algorithm was developed for designing the shell and tube heat exchanger. Then using this algorithm, complete design of a shell and tube heat exchanger has been done using user defined program in M.S. Excel to optimise its geometric parameters. Heat exchanger integrated with a solar collector is being fabricated and tested to find its thermal performance.

The experimental results indicate that temperature of the liquid in the storage tank is steadily increasing and reaching to its maximum value by the evening time. The Evacuated Tube Solar Collector during its one day of operation is found to be achieving a maximum temperature of the liquid (water) nearly 85 ℃ from 60 ℃. The heated liquid from the ETSC is used to preheat the secondary liquid in the Shell and Tube Heat Exchanger. The effectiveness of STHE is reaching to a maximum value of 0.74 when hot fluid (flowing through the tube) mass flow rate is 60 kg/h and cold fluid (flowing through the shell) mass

flow rate is 300 kg/h. Similarly, it was reaching to an average maximum value of 0.6508 when the mass flow rate of cold fluid is 60 kg/h and mass flow rate of hot fluid is changing from 120 to 300 kg/h. Hence, it was concluded that the heat transfer coefficients and hence the effectiveness of the STHE would be maximum when either hot or cold fluid is set to be flowing at lower mass flow rate keeping the mass flow rate of other fluid at higher values.

6.1 Scope for future work

There is a lot of scope for future work. Following recommendations are proposed for future work in case of Evacuated tube solar collector:

- A comparison of Water in glass ETSC, U-tube ETSC and Heat pipe ETSC with and without reflector sheet can be carried out based on experimental results.
- CFD simulations can be carried out to optimise water in glass ETSC, U-tube ETSC and Heat pipe ETSC with and without reflector sheet.

Following recommendations are proposed for future work of the modified jaggery making system:

- A detailed parametric study can be carried out with different sizes of heat exchanger and multi-shell and tube pass heat exchanger.
- CFD simulations can be performed to optimise the present system.
- Other combinations of solar collector (like parabolic dish collector or parabolic trough collector) and heat exchanger (like multi shell and tube pass heat exchanger or open heat exchanger) may be investigated which could result in improved economics.
- Present work can be extended to calculate the cost of the life cycle, savings with the modified process and the payback period of the modified process.

References

Abubakar, G. B., & Egbo, G. (2014). Performance Evaluation of Flat Plate Solar Collector (Model Te39) In Bauchi. *3*(10), 34-40.

Agalave, G. B. (2015). Performance improvement of a single pan traditional jaggery making furnace by using fins and baffle. *4*(04), 85-89.

Allant. (2008, October 8). *Wikipedia*. (Wikimedia Foundation) Retrieved April 19, 2017, from https://commons.wikimedia.org/wiki/File:Centre_punch.JPG

Ambekar, A. S., Sivakumar, R., Anantharaman, N., & Vivekenandan, M. (2016). CFDSimulation study of shell and tube heat exchangers with different baffle segment configurations. *Applied Thermal Engineering, 108*, 999-1007.

Anwar, S. I. (2010). Fuel and energy saving in open pan furnace used in jaggery making through modified juice boiling/concentrating pans. *Energy Conversion and Management*, 360-364.

Arslan, M., & Igci, A. A. (2015). Thermal performance of a vertical solar hot water storage tank with a mantle heat exchanger depending on the discharging operation parameters. *Solar Energy, 116*, 184-204.

Arya, P. K., Kumar, S., & Jaiswal, U. K. (2013). Design Based Improvement in a Three Pan Jaggery Making Plant For Rural India. *International Journal of Engineering Research*, 264-268.

Beckwith, T. G., & Buck, N. L. (2006). *Mechanical Measurements* (Vol. 6). Pearson.

Budihardjo, I., Morrison, G. L., & Behnia, M. (2002). Performance of a Water-in-Glass Evacuated Tube Solar Water Heater. *Proceedings of Solar*, 1-6.

Caputo, A. C., Pelagagge, P. M., & Salini, P. (2008). Heat exchanger design based on economic optimisation. *Applied Thermal Engineering, 28*(10), 1151-1159.

D. T., T. P., & M. R. (2016). Gas tungsten arc welding of copper and mild steel. *Research and reviews: journal of engineering and technology, 5*(2), 12-17.

Edwards, J. E. (2008). *Design and Rating of Shell and Tube Heat Exchangers.* Teesside, UK: www.pidesign.co.uk.

Fanney, A. H., & Klein, S. A. (1988). Thermal performance comparisons for solar hot water systems subjected to various collector and heat exchanger flow rates. *Solar Energy, 40*(1), 1-11.

Gao, Y., Zhang, Q., Fan, R., Lin, X., & Yu, Y. (2009). Effects of thermal mass and flow rate on forced-circulation solar hot-water system : Comparison of water-in-glass and U-pipe evacuated-tube solar collectors. *Solar Energy, 98*, 290-301.

Garg, H. P., & Prakash, J. (2013). *Solar energy fundamentals and application.* New Delhi: Tata McGraw-Hill Publishing Company Limited.

Ghaderian, J., & Sidik, N. C. (2017). An experimental investigation on the effect of Al2O3/distilled water nanofluid on the energy efficiency of evacuated tube solar collector. *International Journal of Heat and Mass Transfer, 108*, 972–987.

GmbH, R. B. (n.d.). *Bosch India*. (The Bosch Group worldwide) Retrieved April 19, 2017, from http://www.bosch-pt.co.in/in/en/angle-grinder-gws-750-100-131459-06013940f0.html

Hamad Al-Khaffajy, M. A., & Mossad, R. (2013). Optimisation of the heat exchanger in a flat plate indirect heating integrated collector storage solar water heating system. *Renewable Energy, 57*, 413–421.

Hewitt, G. F. (1998). *Heat Exchanger Design Handbook.* New York: Begell House.

Hobbi, A., & Siddiqui, K. (2009). Experimental study on the effect of heat transfer enhancement devices in flat-plate solar collectors. *52*(19-20), 4435-4448.

ISHRAE. (2014). *Weather data.* Jaipur: ISHRAE.

Jakkamputi, L. P., & Mandapati, M. J. (2016). Improving the performance of jaggery making unit using solar energy. *Perspectives in Science*, 146-150.

Jayachandriah, D., & Kumar, V. V. (2015). Design of helical baffle in shell and tube heat exchanger and comparing with segmental baffle using kern. *International Journal of Emerging Technology in Computer Science & Electronics (IJETCSE), 13*(2), 157-162.

Kakac, S., & Liu, H. (2002). *Heat exchangers: selection, rating and thermal design.* CRC Press.

Kumar, D. S. (2015). *Heat and mass transfer* (Ninth ed.). S. K. Kataria & Sons.

Kumavat, P., & Manilal, M. (2016). Design, CFD analysis and Fabrication of solar flat plate. *International Research Journal of Engineering and Technology (IRJET), 3*(1), 1000-1004.

Mahendran, M., Ali, T. S., Shahrani, A., & Bakar, R. A. (2013). The Efficiency Enhancement on the Direct Flow Evacuated Tube Solar Collector Using Water-Based Titanium Oxide Nanofluids. *Applied Mechanics and Materials, 465-466*, 308-315.

Mahendran, M., Lee, G. C., Sharma, K. V., Shahrani, A., & Bakar, R. A. (2012). Performance of evacuated tube solar collector using water-based titanium oxide nanofluid. *Journal of Mechanical Engineering and Sciences (JMES), 3*, 301-310.

Manjare, A., & Hole, J. (2016). Exhaust heat recovery of Jaggery making furnace. *5*(4).

Mishra, D. (2015). Experimental analysis of thermal performance of evacuated U-tube solar collector. *Advance Physics Letter*, *2*(3), 1-7.

Mossad, R., & -Khaffajy, M. A. (2012). Investigating two configurations of a heat exchanger in an indirect heating integrated collector storage solar water heating system (IHICSSWHS). *International Conference on Renewable Energies and Power Quality - ICREPQ, 1*, pp. 1404-1409. Santiago de Compostela (Spain).

Munsamy, S. S. (2008). Optimising bagasse dewatering in a cane diffuser at sezela sugar factory. *Proceedings of the Annual Congress - South African Sugar Technologists' Association. 81*, pp. 154-159. Mount Edgecombe, South Africa: South African Sugar Technologists' Association.

Naik, B. K., Varshney, A., Muthukumar, P., & Somayaji, C. (2016). Modelling and Performance Analysis of U Type Evacuated Tube Solar Collector Using Different Working Fluids. *5th International Conference on Advances in Energy Research, ICAER. 90*, pp. 227-237. Energy Procedia.

Patel, V. K., & Rao, R. V. (2010). Design optimisation of shell-and-tube heat exchanger using particle swarm optimisation technique. *Applied Thermal Engineering*, *30*(11-12), 1417-1425.

Primo, J. (2012). *Shell and Tube Heat Exchangers Basic Calculation.* Meadow Estates Drive: PDH Online.

Rao, P. J., Das, M., & Das, S. K. (2006, September 14). Jaggery - ATraditional Indian Sweetner. *Indian Journal of Traditional Knowledge*, *6*(1), 95-102.

Rohsenow, W. M., & Hartnett, J. P. (1973). *Handbook of Heat Transfer*. New York: McGraw-Hill.

Sabiha, M. A., Saidur, R., & Mekhilef, S. (2015). An experimental study on Evacuated tube solar collector using nanofluids. *Transactions on Science and Technology*, *2*(1), 42-49.

Sardeshpande, V. R., Shendage, D. J., & Pillai, I. R. (2010). Thermal performance evaluation of a four pan jaggery processing furnace for improvement in energy utilisation. *Energy*, 4740-4747.

Selbas, R., Kizilkan, O., & Reppich, M. (2006). A new design approach for shell and tube heat exchangers using genetic algorithms from economic point of view. *Chemical Engineering and Processing, 45*, 268-275.

Sharon, M. E., Abirami, C. K., & Alagusundaram, K. (2013). Energy Losses in Traditional Jaggery Processing. *Indian Food Industry Magazine*, 22-25.

Shiralkar, K. Y., Kancharla, S. K., Shah, N. G., & Mahajani, S. M. (2014). Energy Improvements in Jaggery Making Process. *Energy for Sustainable Development, 18*(1), 36-48.

Singh, S., Saini, P., & Kumar, M. (2016). Performance evaluation of parabolic solar water heater. *2*(6), 1-5.

Solomon, S. (2011). Sugarcane by-products based industries in India. *Sugar tech*, 408-416.

Status Paper on Sugarcane. (2016-17). *Status Paper on Sugarcane.*

Struckmann, F. (2008). *Analysis of a Flat-plate Solar Collector.* Lund (Sweden).

Wikipedia oganization. (2017, june 01). *Geography of India*. Retrieved from Wikipedia, the free encyclopedia: https://en.wikipedia.org/wiki/Geography_of_India

Winter, F. d. (1975). Heat exchanger penalties in double-loop solar water heating systems. *Solar Energy, 17*(6), 335-337.

Appendix-A.1 Costing of the experimental setup

Table A.1.1: Costing of all the items used in the experimental setup

S. No.	Name of item/ equipment	Quantity	Name of firm.	Rate (₹)	Amount (₹)
1	Thermocol Sheet	4	Chitranshu Stationers	25	100
2	Cello Tape	1		50	50
3	Nitrile insulation tube 3/4"	5	Jaipur Refrigeration Centre	40	200
4	1 ¼“ Socket	1	Jhalani Traders	53	53
5	1 ¼” Pluck	1		21	21
6	¾ * 1” Socket	2		42	84
7	¾ * 1” MT	2		116	232
8	¾ * 1/2” MT	4		95	380
9	Teflon Tape	2		32	64
10	1” FAPT	1		53	53
11	1*3/4” Brass Elbow	1		21	21
12	¾ * ½“ FABT	8		63.5	508
13	½“ Nozzle	8		31.5	252
14	Saw Blade double side	2	Jitendra Hardware Store	10	20
15	Saw Blade single side	2		5	10
16	Evacuated Tube Solar Water Heater 100LPD and 190D	1	Kayam Solar	12500	12500
17	Solar water heater installation charge			500	500
18	Fabrication of Heat Exchanger	1	Meera Electronic’s	8800	8800
19	Fevikwick	1	Nikki Stationary Store	10	10
20	Dori	1		20	20
21	Threaded Pipe	24 feet	Prakashchand Dharmchand Jain	8	192
22	Pipe clips	20		5	100
23	Flexible Wire	7	Rajdeep Colours & Light Fittings	6	42
24	Al Foil	3	Ravi Traders	220	660
25	M-seal	5		10	50

26	F.A.B.T. ¾”	4	Saraswati Traders	150	600
27	Teflon Tape	5		15	75
28	T joint 3/4"	4		40	160
29	Pipe 3/4"	3		290	870
30	Elbow 3/4"	10		20	200
31	T 3/4"	4		40	160
32	Valve 3/4"	8		150	1200
33	Solvent	1		150	150
34	Pressure gauge	4	Steel Tube Traders	458	1832
35	ms socket 3/8"	4		11.5	46
36	ms round socket 3/8"*3/8"	4		25.5	106
37	T type Thermocouple Cable wire	150 m	Surya Pyro Electric Co.	Rs31.5/m	4725
38	Glass wool	2kg	S. Kalra Refrigeration and Air conditioner	105.5	211
39	Sleeves	3		42.2	127
				Total (₹)	**35384**

Appendix-A.2 Calibration of the temperature sensors

Table A.2.1: Calibration of temperature sensors from 1 to 19

Readings	1	2	3	4	5	6	7	8	9	10	11	12
RTD (°C)	91.9	91.9	76.6	76.6	61.3	61.3	46.0	46.0	30.8	30.8	15.8	15.7
1 (°C)	89.9	89.9	74.9	74.9	60.0	60.0	45.1	45.1	30.2	30.2	15.4	15.4
2 (°C)	89.9	89.9	75.0	75.0	60.0	60.0	45.1	45.1	30.2	30.2	15.4	15.4
3 (°C)	89.9	89.9	75.0	75.0	60.1	60.1	45.1	45.1	30.2	30.2	15.5	15.4
4 (°C)	89.9	89.9	74.9	74.9	60.0	60.0	45.1	45.1	30.2	30.2	15.4	15.4
5 (°C)	89.9	89.9	75.0	75.0	60.1	60.1	45.1	45.1	30.2	30.2	15.4	15.4
6 (°C)	89.9	89.9	75.0	75.0	60.1	60.1	45.1	45.1	30.2	30.2	15.4	15.4
7 (°C)	89.9	89.9	74.9	74.9	60.0	60.0	45.0	45.0	30.1	30.0	15.3	15.2
8 (°C)	89.9	89.9	74.9	74.9	60.0	60.0	45.0	45.0	30.2	30.1	15.4	15.3
9 (°C)	89.9	89.9	74.9	74.9	60.0	60.0	45.0	45.0	30.2	30.1	15.3	15.3
10 (°C)	89.9	89.9	74.9	74.9	60.0	60.0	45.0	45.0	30.1	30.1	15.3	15.3
11 (°C)	89.9	89.9	74.9	74.9	60.0	60.0	45.0	45.0	30.2	30.1	15.4	15.3
12 (°C)	89.8	89.8	74.9	74.9	60.0	60.0	45.0	45.1	30.2	30.2	15.4	15.4
13 (°C)	89.9	89.9	75.0	75.0	60.0	60.1	45.1	45.1	30.2	30.2	15.4	15.3
14 (°C)	89.9	89.9	74.9	74.9	60.0	60.0	45.0	45.0	30.2	30.1	15.3	15.3
15 (°C)	89.9	89.9	75.0	75.0	60.0	60.0	45.1	45.0	30.2	30.1	15.3	15.3
16 (°C)	90.0	90.0	75.0	75.0	60.1	60.1	45.1	45.1	30.2	30.2	15.4	15.4
17 (°C)	89.8	89.9	74.9	74.9	60.0	60.0	45.0	45.0	30.1	30.1	15.3	15.3
18 (°C)	90.0	90.0	75.0	75.0	60.1	60.1	45.1	45.1	30.2	30.1	15.3	15.3
19 (°C)	89.9	89.9	75.0	75.0	60.1	60.1	45.1	45.1	30.2	30.1	15.3	15.3

Table A.2.2: Calibration of temperature sensors from 20 to 30

Readings	1	2	3	4	5	6	7	8	9	10	11	12
RTD (°C)	15.8	15.8	30.7	30.7	45.9	46.0	61.2	61.2	76.5	76.5	91.8	91.8
20 (°C)	15.4	15.3	30.1	30.1	45.0	45.1	60.0	60.0	75.0	75.0	89.9	89.9
21 (°C)	15.4	15.4	30.1	30.1	45.0	45.0	60.0	60.0	74.9	74.9	89.8	89.9
22 (°C)	15.4	15.4	30.1	30.2	45.1	45.1	60.1	60.1	75.0	75.0	89.9	89.9
23 (°C)	15.4	15.4	30.2	30.2	45.1	45.1	60.1	60.1	75.0	75.0	89.9	90.0
24 (°C)	15.4	15.4	30.1	30.1	45.0	45.1	60.0	60.0	75.0	75.0	89.9	89.9
25 (°C)	15.5	15.4	30.2	30.2	45.1	45.1	60.1	60.1	75.0	75.0	89.9	89.9

26 (°C)	15.4	15.4	30.1	30.2	45.1	45.1	60.1	60.1	75.0	75.0	89.9	89.9
27 (°C)	15.3	15.3	30.0	30.0	45.0	45.0	60.0	60.0	74.9	74.9	89.8	89.8
28 (°C)	15.4	15.4	30.1	30.1	45.1	45.1	60.0	60.0	75.0	75.0	89.9	89.9
29 (°C)	15.4	15.4	30.1	30.1	45.0	45.1	60.0	60.0	74.9	74.9	89.9	89.9
30 (°C)	15.4	15.4	30.1	30.1	45.0	45.0	60.0	60.0	74.9	74.9	89.8	89.8